Offshore Load and Discharge of a turret moored FPSO

Max Dumans

Technische Universiteit Delft

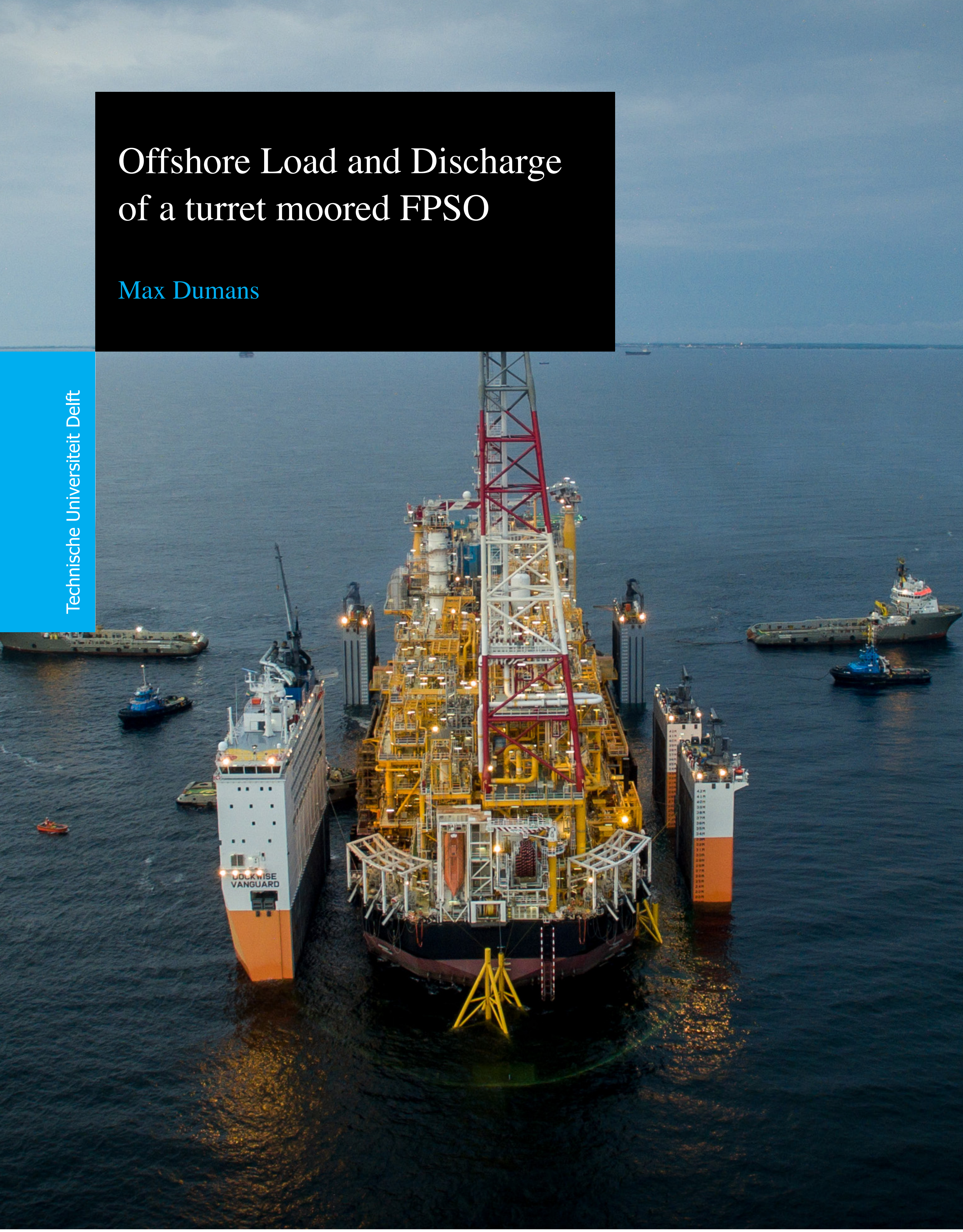

Delft University of Technology

Challenge the future

Front cover: Float-off operation of the Likouf FSU for the Moho Nord project, offshore Port-Gentil, Gabon. Float-off supported by AHTs Union Bear, Union Lynx, Union Boxer, Union Manta and Smit Lamnalco Weaver and Rima. November 16, 2016. https://brandcenter.boskalis.com/media. Changes made: picture was resized

TU DELFT

Offshore Load and Discharge of a turret moored FPSO

by

Max Dumans

In partial fulfillment of the requirements
for the degree of Master of Science

in

Offshore and Dredging Engineering

Student number	4016440	
date	*October* 19, 2017	
Thesis committee	Prof.dr. A.Metrikine	TU Delft - Chairman
	Dr.ir. A. Jarquín Laguna	TU Delft
	Dr.ir. F. Pisanò	TU Delft
	Ir. O. Sáinz Avila	Boskalis

Preface

This report presents the study that I have done as a part of my thesis for the finalisation of my master study in Offshore and Dredging Engineering at the Delft University of Technology. The research has been conducted at the R&D department of Royal Boskalis Westminster and covers the topic "Offshore Load and Discharge of a turret moored FPSO". It is a topic that has become very dear to me and has challenged me over the past months.

I would like to take the opportunity to thank all of those who contributed to this work. First, I would like to thank Oscar for his unrelenting assistance to the realisation of this master thesis. Secondly, I would like to thank Antonio for always being available for questions and explanations. Thirdly, I would like to thank Andrei for his inexhaustive knowledge and the "I do not understand" questions which motivated me over the past months.

Finally, I would like to thank my parents and family for supporting me during my studies and many thanks to my friends and girl-friend for supporting me throughout.

Max Dumans, October 2017

TU DELFT

Abstract

Offshore and Dredging Engineering

Master of Science

by Max Dumans

Boskalis subsidiary Dockwise is the global market leader in heavy marine transport. Their fleet of over 20 semi-Submersible Heavy Transport Vessels (SHTV) is capable to carry the heaviest and largest structures. Until today the load or discharge operation of a floating body has only been performed in sheltered waters. Here, the influences of the environmental loading (wind, waves and current) are limited. Floating Production Storage and Offloading vessels (FPSO) are subjected to hull maintenance and repairs in the near future, which causes a major downtime due to transportation. If the maintenance of FPSOs could be performed offshore, it could reduce this downtime significantly.

Due to the environmental loading the SHTV and FPSO move separately. In order to perform a safe offshore load/discharge operation their relative motion should be within the width of the cribbing. The aim of this thesis is to analyse the influence of the location of the connections between the two vessels on the relative transverse motion at keel level of the FPSO. Sway, roll and yaw are considered as the main degrees of freedom (DOF) that have influence on the transverse motion.

A numerical model is built to solve the equations of motion in the frequency domain for a 3DOF system. This system consists of a rigid body which represents the FPSO. The rigid body is connected to a set of springs and dashpots which influence its behaviour. For every combination of location and parameters of the spring/dashpot system the numerical model calculates the response. The outcome of all these runs are brought together in contour graphs that give insight to a possible optimal location for the connections and their corresponding parameters.

It is found possible to get the transverse motions at keel level within the limits of the cribbing. By positioning the spring/dashpot systems in the corresponding optimal location the minimum required stiffness can be reduced. A fraction of the critical damping at each spring location appears to be adequate in reducing the motions during resonance. The significant forces in both spring/dashpot locations are very high but workable.

Contents

Preface **i**

Abstract **ii**

List of Figures **v**

List of Tables **vi**

Abbreviations **vii**

Symbols **viii**

1 Introduction **1**
- 1.1 Background . . . 1
- 1.2 Objective . . . 2
- 1.3 Approach . . . 3
- 1.4 Research question . . . 3
- 1.5 Structure of the report . . . 4

2 Environmental and system conditions **5**
- 2.1 System description . . . 5
- 2.2 Connection complexity reduction . . . 6
- 2.3 Load & Discharge operation . . . 7
  - 2.3.1 Step by step . . . 7
  - 2.3.2 Duration . . . 9
- 2.4 Influences of the environment to the offshore load/discharge operation . . . 10
- 2.5 Vessel specifications . . . 11
- 2.6 West Africa region, South America region and the rest of the world . . . 12
- 2.7 Waves and water depth in the West-African region . . . 12
- 2.8 Assumptions summery . . . 14

3 Frequency analysis **15**
- 3.1 The numerical model . . . 15
- 3.2 Characteristics of the numerical model . . . 16
  - 3.2.1 Python script . . . 16
  - 3.2.2 Parameters and components . . . 17
  - 3.2.3 Mooring system . . . 18

3.2.4 Viscous roll damping . . . 18
3.3 Frequency domain analysis in Python . . . 19
3.4 Wave spectrum . . . 23
3.5 Natural frequency calculation . . . 24

4 Validation of the numerical model **26**
4.1 Octopus seaway vs Python script . . . 26
4.2 Ansys AQWA vs Python script . . . 29
4.3 Conclusion . . . 30

5 Results of the numerical model **32**
5.1 Natural frequencies . . . 32
5.2 Significant motion in the contact points . . . 34
5.2.1 Vertical position vs stiffness . . . 34
5.2.2 Vertical position vs longitudinal position . . . 37
5.2.3 Spring 3 at different longitudinal positions . . . 40
5.2.4 Minimum stiffness . . . 42
5.3 Damping . . . 43

6 Discussion **46**

7 Conclusion **48**
7.1 Conclusion . . . 48
7.2 Future research . . . 50

A Vanguard specifications **52**

B Environmental data **54**
B.1 Wave roses for the coast of Brazil . . . 55
B.2 Wave roses for the coast of West-Africa . . . 56
B.3 Wind roses for the coast of West-Africa . . . 57
B.4 Workability West Africa in January . . . 58

C Minimal required stiffness **59**
C.1 Minimum stiffness for different spring heights . . . 60
C.2 Minimum stiffness including damping . . . 61

D Hydrodynamic data from Octopus Seaway **62**

E Hydrodynamic from data Ansys AQWA **69**

Bibliography **73**

List of Figures

1.1 Vanguard with an FPSO loaded on deck[1] 2

2.1 Vessel motions 6
2.2 Load/Discharge operation step by step 8
2.3 FPSO and SHTV used 11
2.4 The orbital motion of the water particles[2]. 13

3.1 Reference system 18
3.2 Modified Pierson Moskowitz wave spectrum $H_s = 1[m], t_p = 14[s]$ 24

4.1 RAOs of Seaway-Python coupled 28
4.2 RAOs of Seaway-Python uncoupled 29
4.3 RAOs of AQWA-Python 30

5.1 Sway natural frequency of different locations vs stiffness ($x_3 = 200[m]$) . . 33
5.2 Roll natural frequency of different locations vs stiffness ($x_3 = 200[m]$) . . 34
5.3 Yaw natural frequency of different locations vs stiffness ($x_3 = 200[m]$) . . 34
5.4 Significant motion in point 2 at multiple locations of x_4 36
5.5 Significant motion point in 4 at multiple locations of x_4 36
5.6 Significant motion in point 2 for different spring stiffnesses 38
5.7 Significant motion in point 4 for different spring stiffnesses 38
5.8 Significant roll motion for different spring stiffnesses 39
5.9 Significant motion in point 2 at different locations of x_3 41
5.10 Significant transverse motion in point 4 at different locations of x_3 41
5.11 Minimal required stiffness at $z = 9$[m](C=0[kNs/m]) 42
5.12 Combined spring/dashpot forces in [kN] x_3=240[m], x_4=30[m], z=9[m] . . 44
5.13 Motion in the outer contact points in [m](x_3=240[m], x_4=30[m], z=9[m]) 45

B.1 Workability West Africa January 58

C.1 Minimum stiffness for different spring height in [kN/m] 60
C.2 Minimum stiffness including damping at z=9[m] 61

List of Tables

2.1 Vessel specifications . . . 11
2.2 Location of FPSO's around the world[3] . . . 12
2.3 Workability West-Africa January . . . 13

3.1 Parameters used . . . 17
3.2 Mooring system stiffness . . . 18

4.1 Testcase parameters . . . 26
4.2 Natural frequencies Python vs seaway . . . 27

Abbreviations

COG	Centre Of Gravity
DOF	Degree Of Freedom
ET	External Turret
FPSO	Floating Production Storage and Offloading vessel
IT	Internal Turret
MPM	Most Probable Maximum
MSL	Mean Seal Level
OL&D	Offshore Load and/or Discharge
RAO	Response Amplitude Operator
SHTV	Semi submersible Heavy Transport Vessel
SM	Spread Moored

Symbols

x_g	longitudinal distance of COG	m
x_1	longitudinal distance of spring 1	m
x_2	longitudinal distance of spring 2	m
x_3	longitudinal distance of spring 3	m
x_4	longitudinal distance of spring 4	m
z_g	vertical distance of COG	m
z_1	vertical distance of spring 1	m
z_2	vertical distance of spring 2	m
z_3	vertical distance of spring 3	m
z_4	vertical distance of spring 4	m
K_1	stiffness of spring 1	kNm^{-1}
K_2	stiffness of spring 2	kNm^{-1}
K_3	stiffness of spring 3	kNm^{-1}
K_4	stiffness of spring 4	kNm^{-1}
C_3	structural damping at spring 3	kNsm^{-1}
C_4	structural damping at spring 4	kNsm^{-1}
k_{xx}	radius of gyration along the longitudinal	m
k_{zz}	radius of gyration along the vertical	m
D	duration	hr
t	time	s
t_p	peak period	s
t_z	zero upcrossing period	s
H_s	significant wave height	m
H_m	most probable maximum wave height	m
N	number of waves	

M	Mass matrix of the FPSO	ton
$M_{Jasmine}$	Mass of the FPSO Jasmine	ton
A	added mass	ton
C	viscous damping	kNsm^{-1}
C_{hydro}	wave radiation damping	kNsm^{-1}
K	structural stiffness	kNm^{-1}
K_{hydro}	hydro static stiffness	kNm^{-1}
F	wave loads	kN
y_p	transverse motion	m
y_a	amplitude of sway RAO	m
V_{FPSO}	submerged volume of FPSO Jasmine	m^3
V_{SHTV}	submerged volume of SHTV Vanguard	m^3
Q	volumetric flow rate	$\mathrm{m}^3\mathrm{hr}^{-1}$
GM	metacentric height	m
$S(\omega)$	wave spectrum	$\mathrm{m}^2\mathrm{s}^{-1}$
$S_y(\omega)$	response spectrum in transverse direction	$^2\mathrm{s}^{-1}$
m_0	zero order moment	m^2
$f(\omega)$	natural frequency function	rads^{-1}
ω	frequency	rads^{-1}
ω_w	wave frequency vector	rads^{-1}
ω_n	natural frequency	rads^{-1}
ω_p	peak frequency	rads^{-1}
ω_v	natural frequency vector	rads^{-1}
ϕ_a	amplitude of roll RAO	rad
ψ_a	amplitude of yaw RAO	rad
ϵ_y	phase of the sway RAO	rad
ϵ_ϕ	phase of the roll RAO	rad
ϵ_ψ	phase of the yaw RAO	rad
g	Gravitational acceleration	$9.81\mathrm{ms}^{-2}$
ρ_w	density of seawater	$1025\mathrm{tonm}^{-3}$

Chapter 1

Introduction

1.1 Background

Boskalis is one of the largest dredging and marine companies worldwide in which it is a successful subcontractor for the oil and gas companies. The oil and gas market has been expanding and predictable for many years. When the oil price dropped dramatically in 2014/2015 oil and gas companies put a hold to most of their investments in new explorations. As a consequence there are less tenders on the market which causes a fierce competition. Subcontractors like Boskalis have difficulties to find enough work for their fleet of offshore vessels. Therefore subcontractors that used to focus mainly on the offshore oil and gas sector have been exploring new markets [4].

In 2013, as part of the expansion of its offshore activities, Boskalis acquired Dockwise, the global market leader in heavy marine transport. The Dockwise fleet of over 20 semi submersible heavy transport vessels (SHTV) is unique world wide: most vessels are able to carry the heaviest and largest structures. By submerging the SHTV it is able to place itself under a floating body (a structure or a vessel) and by discharging ballast water it can lift the entire floating body. Subsequently the SHTV can transport and discharge the cargo at the new location. Until today this load/discharge operation can only take place in a sheltered area like a harbour, a fjord or a bay.

In the last couple of years more than 150 Floating Production Storage and Offloading vessels (FPSO) found their way to an offshore location. In the near future these vessels are most likely subjected to hull maintenance and repairs. To execute maintenance and

FIGURE 1.1: Vanguard with an FPSO loaded on deck[1]

repairs the FPSO must now be disconnected and towed to a shipyard with dry-docking capabilities. The number of lost production days for the FPSO depends on the time it takes to connect/disconnect to the turret mooring system but mostly on the towing distance. Since most FPSOs are in remote areas this downtime is very substantial[3]. If Dockwise is able to perform an offshore load/discharge operation of an FPSO, it could reduce the downtime by performing the maintenance offshore see figure 1.1.

This offshore operation is difficult due to the environmental loading factors which include waves, wind and current. These environmental loading factors causes the floating body and SHTV to move separately which could lead to collisions and misalignment. In order to load/discharge in a safe manner the vessels should move synchronously. If the Dockwise vessels are able to load and discharge outside sheltered places (offshore), then a new market can be created for Dockwise.

1.2 Objective

Dockwise has been devoting research in the field of the offshore load/discharge operation of a turret moored FPSO. In order to perform a safe operation the relative motions should be reduced. Therefore the interaction between the vessels should be investigated and well understood before a relative motion reduction system can be designed. This relative motion reduction system is the connection between the two vessels with the purpose to reduce their relative motions. In order to design this system research is done to the interaction between the vessels. This interaction consists of small gap influence, wave reflections in shallow water and the connections between the FPSO and SHTV.

The key area of this research is to gain insight in the influence of the location of the connections between the FPSO and SHTV on the relative motions in order to control them.

1.3 Approach

In order to achieve the objective several steps have been taken to understand the system's behaviour. The two vessel system shall be described in components and their interdependence. Then this system is simplified to its most essential components. These most essential components are brought together in a numerical model. In this model a vessel is represented by a mass and the connections between the vessels are represented by a spring/dashpot system. Multiple calculation runs are performed for different parameters of the spring/dashpot location and characteristics to see if there is an optimal combination to reduce the transverse motion.

1.4 Research question

In this section the research question is presented. In order to find an answer to this question three sub questions are defined.

What is the influence of the location of the connections on the relative motions between an FPSO and an SHTV to enable a safe offshore load/discharge operation? Sub questions:

1. What are the influences of sway, roll and yaw on the transverse motion in the outer contact points to the cribbing?
2. What is the minimum amount of stiffness required to reduce the transverse motion in the outer contact points within limits?
3. What is the influence of adding structural damping to the system on the spring/-dashpot forces and motion in the outer contact points to the cribbing?

1.5 Structure of the report

Chapter 2, Environmental and system conditions, gives a detailed description of the system's components and interactions, followed by a step by step analysis of the offshore load/discharge operation. Multiple assumptions are introduced and explained about the vessel specifications, the environment and the location.

Chapter 3, Frequency analysis describes the method of this research. It shows how the different components have been modelled and why these are modelled in the python programming language. The chosen wave spectrum is described and the equations are introduced in order to predict the significant transverse motion.

Chapter 4, Validation of the numerical model describes a reference case calculated with Octopus Seaway. The results obtained from the reference case are compared to the results obtained by the python script. Results include the natural frequencies, the uncoupled system and the coupled system.

Chapter 5, Results of the numerical model shows the results from the python script. First, the natural frequency changes due to the location and stiffness of the springs shall be discussed. Secondly the significant motions in the outer contact points to the cribbing and finally the influence of the damping on the spring/dashpot forces.

Chapter 6, Discussion describes the impact of the assumptions about the viscous roll damping, the West-African environment and the used vessels. The impact of the enabled roll motion on the heave motion and if the approach would work for the surge and pitch motion.

Chapter 7, Conclusion describes the conclusions and future research. Answers to the sub questions and the research question are given. The optimal point based on this parametric research is presented and the relevant significant forces are shown.

Chapter 2

Environmental and system conditions

2.1 System description

During the offshore load/discharge operation there are two components that interact with each other. The SHTV which is able to lift an entire FPSO off the water and the FPSO that is usually moored somewhere in a remote area. The motions of these two components are influenced by environmental loading. They have a different motion due to their difference in properties like mass, draft and shape. Therefore a system is needed to connect both vessels and influence their relative motion.

Each vessel is assumed to be a rigid body and is able to move in six degrees of freedom as showed in figure 2.1. It can move in longitudinal- (surge), transfers- (sway), vertical-direction (heave) and it can rotate around these axes (roll, pitch and yaw). Since this system consists of two vessels there are 12 motions to account for. The interaction between the vessels is mainly caused by three phenomena which are elaborated below:

Small gap influences: During the operation there is gap between the bottom of the FPSO and the deck of the SHTV. This gap is continuously made smaller as the SHTV de-ballast itself. At a certain moment this gap becomes so small that the in and outflow of water influences the behaviour of the vessels. This phenomena causes damping and added mass effects. The alignment of the two vessels might be difficult due to the small layer of water. Ongoing research on this topic is performed at Boskalis[5].

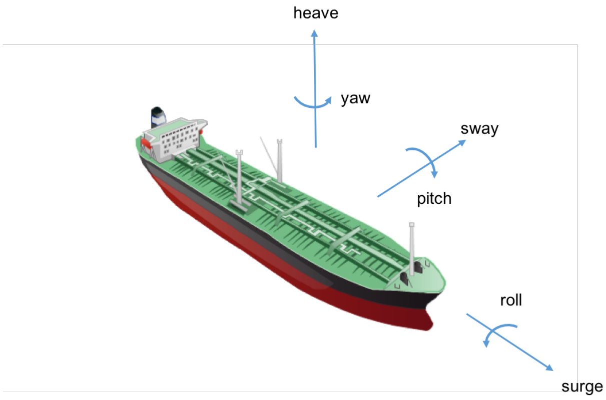

FIGURE 2.1: Vessel motions

Wave radiation and reflection: In the case of the offshore load/discharge operation the SHTV and FPSO float close together and therefore the radiated and reflected waves from one vessel could be the excitation to the other vessel. Commercial software like Ansys AQWA are able to solve these wave interactions between the vessels although a highly computational demanding model is to be solved.

Connections: The FPSO and SHTV have connections in between and they will interact through them. These connections could be anything that connects the vessels, e.g. ropes, springs, cylinders, etc. The impact of the location of these connections on the transverse motion has not been investigated yet. This thesis is focusing on the impact of and the interaction through these connections.

2.2 Connection complexity reduction

Previous research done by J.W van Beelen [6] focused on the design of these connections between the two vessels. In search of a relative motion reduction system multiple designs were compared in a multi-criteria analysis. Two of these designs were worked out in detail: The first system is a passive stiff system that can be best explained as a vice that clamps the FPSO to the Vanguard. Although the system was designed in some depth, it was only developed for one degree of freedom (DOF). The second system is an actively controlled soft system. The vessel is connected to lines and an actuator. By changing the properties of this actuator the system is controlled in time. More research to this system was done by P.C Lee [7]. This system proofed to be rather ineffective in swell conditions.

This research shall focus on the connection characteristics and their locations to better understand the interaction between the two vessels. In order to understand the system the 12 DOF are brought back to 3. This is done under the assumptions described below:

Since this research is about the best location to position the connections at the FPSO, the motions of the SHTV are assumed to be zero and therefore only the motions of the FPSO are studied. This assumption eliminates 6 of the 12 DOF. Section 2.4 and 2.7 elaborate more on the influences from the wind and waves on the SHTV motions.

As described in section 2.1 a vessel has 6 DOF. Some of these DOF are coupled, for example the yaw motion has a coupling to the sway motion. When the vessel rotates around the z-axis the bow of the vessel moves to the left and the stern moves to the right in transverse direction. There are more DOF that influence the transverse motion those are sway, roll and yaw [8]. For more information about the numerical model see chapter 3.Since sway, roll and yaw are the only DOF that have influence on the transverse motion these are the motions that are studied.

The motion compensation system will only be built if it is economically feasible. Therefore it is good to keep in mind that the costs of the final system are highly related to the amount of stiffness and damping required and the forces that act through them on the hull of the FPSO. The more stiffness is needed the larger, heavier and more complex the spring system will be. If extra mechanical damping is necessary this is an extra component to the system and that will bring extra costs. The hull of the FPSO was never designed to withstand large compressive forces. Therefore it is most likely that the hull of the FPSO needs to be reinforced at particular locations. The higher the forces the more steel and offshore man hours are needed. Taking this into consideration it is preferable that the system has a relatively small stiffness, small forces and without an extra viscous damping system.

2.3 Load & Discharge operation

2.3.1 Step by step

The load operation covers several steps, see figure 2.2. The discharge operation is mainly the reverse load operation. Since the two operations contain the same steps only the

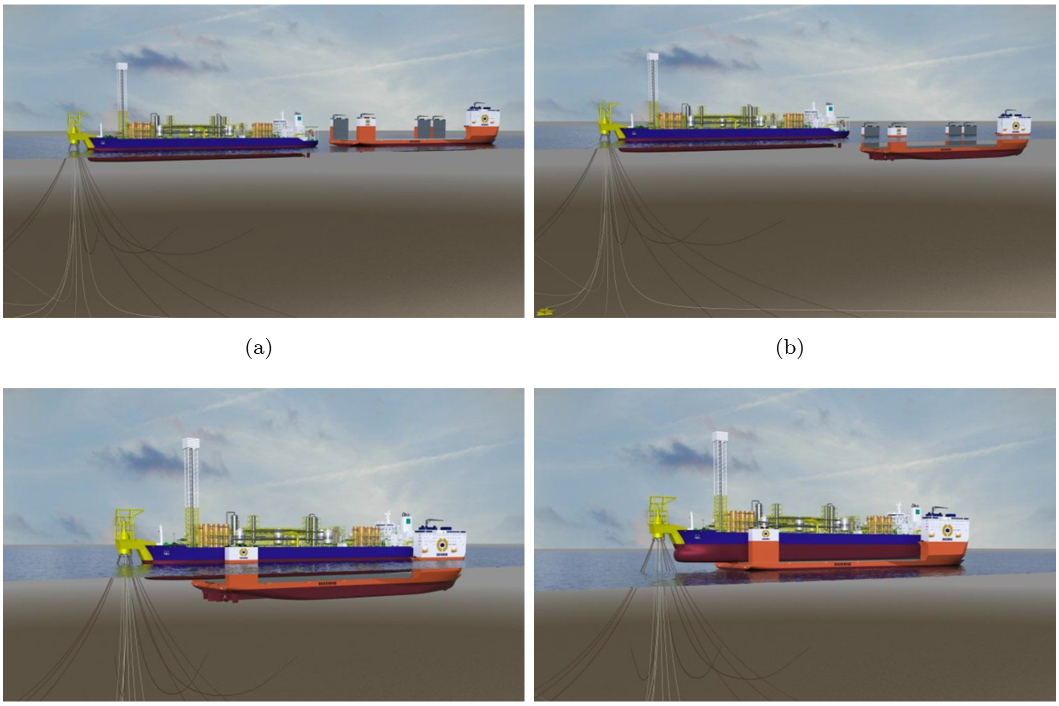

(a) (b) (c) (d)

FIGURE 2.2: Load/Discharge operation step by step

load operation is described below.

Figure 2.2(a) shows the first step of the load operation. The SHTV Vanguard positions itself right behind the FPSO and preparations are made to the cribbing and connection systems. The cribbing system exists of large wooden blocks that are attached to the Vanguard's deck. The wooden blocks are structured so that the FPSO can stand on its hull strong-points. Figure 2.2(b) shows the second step in which the SHTV is ballasted. The mooring lines of the SHTV are connected to the FPSO. Then the SHTV is ballasted at a certain depth so that the vessels are not able to make contact between the keel and the deck during the next phase. Figure 2.2(c) shows the third step of the load operation. The SHTV moves itself right under the FPSO. The two vessels are aligned and the relative motion reduction system is attached. The final step is shown in figure 2.2(d). The Vanguard starts discharging ballast water and lifts the FPSO out of the water. During this phase the relative motion reduction system is active to synchronise the motions between the vessels as much as possible to get the alignment right. Sea fastening is installed and the FPSO is ready for the required maintenance, work-over or sailing.

To completely counteract the relative motions a set of huge spring stiffnesses is required. Therefore it is most important to understand the limits. A ship consist of a skeleton to which the hull plates are welded. The vessel hull is at its strongest at the ribs of this skeleton. Both the Vanguard as the FPSO have strong points in their ship hull. During a dry dock operation it is important that the strong-points of the FPSO are right above the strong-points of the Vanguard. In reality this means that the alignment between these vessels should be within $+/-0.1$[m] in both longitudinal and transverse direction. This means that the maximum allowed relative motion is 0.1[m]. A relative motion reduction system should minimise these motions. It is worth noticing that this maximum allowed motion is at the location of the strong-points. At the FPSO these are located at keel level and it is assumed that the outer points are located at 40m from both bow and stern.

2.3.2 Duration

In order to understand the environmental limits it is important to have a rough estimate of the duration of the load operation. The ballast pumps of the Dockwise Vanguard have a total flow rate of 24100[m3/hr] (see appendix A). The total submerged volume of the Vanguard is estimated by the total area of the caissons (610[m^2]) times the depth of the deck (12[m]). The load operation is assumed to be completed as soon as the SHTV's deck equals mean sea level (MSL). When the SHTV's deck is at MSL waves are still rolling over the deck but it is expected that the waves do not have enough energy to lift the FPSO from the cribbing. The submerged volume of the FPSO is equal to the estimated area of 10.000[m2] times the draft of 6[m] considering the FPSO as box shaped.

To investigate if the system can withstand the environmental loading during the operation the most probable maximum wave height is calculated. This is the single highest wave expected during the operation. Forces are calculated and compared to the material specifications. During the load operation H_m is equal to 1.81 times H_s using the equations 2.1-2.2. Where T_z is the zero upcrossing period of the waves. The total load operation is estimated as 2.8[h].

$$D = \frac{V_{SHTV} + V_{FPSO}}{Q} \tag{2.1}$$

$$N = 3600\frac{D}{t_z} \tag{2.2}$$

$$H_m = H_s\sqrt{\frac{\ln N}{2}} \tag{2.3}$$

2.4 Influences of the environment to the offshore load/discharge operation

A load/discharge operation normally takes place in a sheltered area such as a harbour, a fjord or in a bay. AIn a sheltered area the environmental loads are low that it can be assumed that it has no influence on the SHTV and it's cargo. By performing the operation offshore this environmental loading may be significant and therefore it is necessary to take into account. Environmental loading is a combination of the loads due to nature such as wind, current and waves.

The wind has the main effect on the FPSO since it has a large area above water. The SHTV's caissons and bridge are the only parts above water and so the wind has a relatively small area to act on. The current is a relatively stable load that act on both vessels, since the SHTV has a larger area under MSL the influence of the current might be higher on the SHTV. The waves act on both vessels. The combination of local wind generated and swell waves have the most influence on the behaviour of the vessels. The much longer infra-gravity waves are assumed to be slow enough that both vessels move synchronously on them.

The water depth has influence on both the waves as well as the operation. During a load/discharge operation in a sheltered area it could be difficult to find a place that is deep enough to allow the SHTV to float under the FPSO. Offshore this is not an issue. For the offshore load/discharge operation of an FPSO it is expected that at least a 100[m] of water depth is required to have enough slack in the FPSO's mooring system[3].

2.5 Vessel specifications

In this thesis there are two commercial vessels selected: the SHTV; Dockwise Vanguard and the FPSO; Jasmine (see figure 2.3). The specifications and data of these two vessels have been used for the calculations and optimisation.

The Dockwise Vanguard is the largest SHTV ever built and is therefore the most suitable vessel of the Dockwise fleet. Already during the built of this vessel the engineers accounted for the possibility of lifting an FPSO. In 2015 it transported the Armada Intrepid FPSO (245[m]) from the Netherlands to Indonesia. These capabilities make the Vanguard the ideal SHTV to use in the offshore dry-dock operation of an FPSO.

FPSO: Jasmine			HTV: Dockwise Vanguard		
Length	248.4	[m]	Length overall	275	[m]
Width	38.9	[m]	Width moulded	70	[m]
Draft	6.04	[m]	Draft submerged	31.5	[m]
Mass	41241	[ton]	Mass	116,175	[ton]
			Max water depth above deck	16	[m]

TABLE 2.1: Vessel specifications

The average length of an FPSO moored in West Africa is 316 [m][9]. FPSOs of such a size are close to the limits of the Vanguard. Therefore a smaller FPSO is chosen so that the size and weight wont bring any extra design limitations. Boskalis has the hydro dynamic data available of the Jasmine. This is a relatively small external turret moored FPSO which is currently located in the gulf of Thailand. A number of similar FPSOs can be found in the West Africa region. The Jasmine data is available and has been used for this study. The vessel specifications are listed in table 2.1.

(a) Dockwise Vanguard (b) Jasmine

FIGURE 2.3: FPSO and SHTV used

2.6 West Africa region, South America region and the rest of the world

The location of the moored FPSO is important for the financial aspect of the operation. Table 2.2 lists the mooring types (IT=internal turret, ET=external turret, SM=spread moored) per region. These four regions make up 81% of the total amount of moored FPSO vessels. To make offshore dry-docking beneficial it is important to do the operation in a remote area. It is assumed that in Europe and Asia repair yards with dry dock facilities are within a relatively short distance. From a financial point of view the FPSOs moored in South America and West Africa are most interesting. Figure B.1 and B.2 show multiple wave roses of both South-America and West-Africa regions. It can be noticed that the waves in South-America are higher and that the waves in the West-African region are more unidirectional. For these reasons this research has been focusing on the FPSOs moored in the West-Africa region. Wind, wind-waves, current and swell have their influence on the load and discharge operations. Since the current is a relatively constant factor which influences both vessels equally it is assumed that it will not influence the relative motion. Furthermore it is assumed that there will be an operational window in which the wind and wind-wave loads are small compared to the swell waves. Figure B.3 shows the wind roses of a typical location in West-African waters. It can be noticed that more than 60% of the time the wind velocity is less than 5m/s which can be compared to a summer breeze. As a result in this research the main issues to be tackled are due to the swell conditions in West-Africa.

REGION	#	IT	ET	SM	OTHER
West Africa	41	2	9	29	1
South America	39	17	3	17	2
Europe	25	20	0	4	1
Asia/Far East	42	8	12	6	16
TOTAL	147	47	24	56	20

TABLE 2.2: Location of FPSO's around the world[3]

2.7 Waves and water depth in the West-African region

Deep water linear wave theory describes the motion of the independent particles as orbital motions see figure 2.4. The water particles move in circles over and over again.

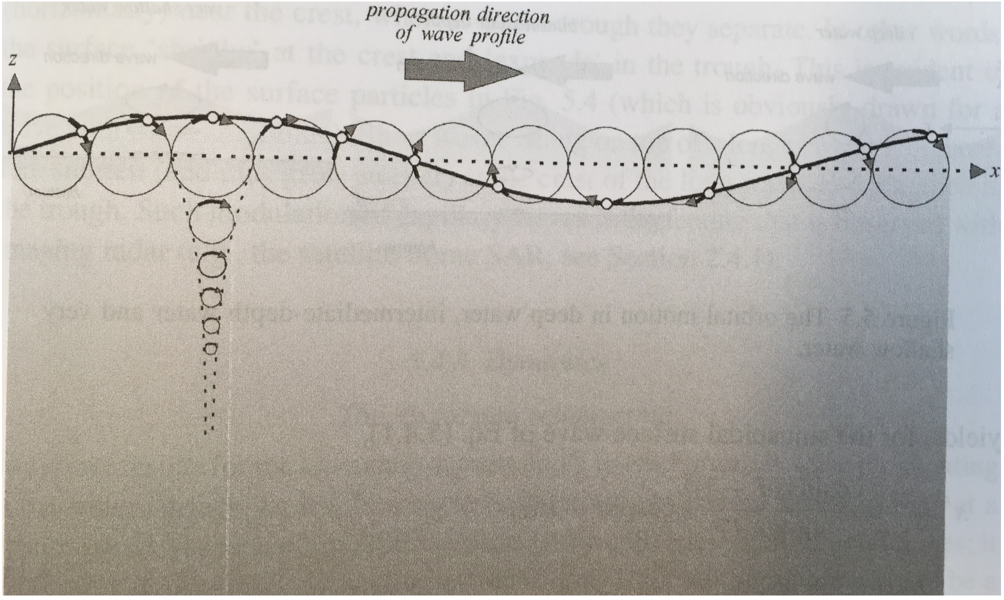

FIGURE 2.4: The orbital motion of the water particles[2].

As can be noticed the particle motions get smaller as the water depth increases. This is why the ballasted SHTV experiences way less wave loads than the FPSO and therefore moves less. In this thesis it is assumed that the motions of the SHTV are so small compared to the motions of the FPSO that the wave loads have no influence on the SHTV. The waves loads will only act on the FPSO in the numerical model.

Appendix B.2 shows the wave roses of a typical offshore location off the coast in West-Africa. During the months December till march the weather is relatively calm. The workability in January is showed in Appendix B.4 for multiple combinations of H_s and T_p. The range of workability is estimated and summarised in table 2.3 for each combination of H_s and T_p within 300 [km] from shore. At a peak period of 14[s] and a significant wave height of 1[m] there is a minimum of 20% workability. Therefore the aim of this thesis is to reduce the relative motions in these conditions.

T_p	$_s$	Workability [%] (January)
10	1.0	4-24
10	1.25	8-35
10	1.5	8-38
14	1.0	20-60
14	1.25	30-85
14	1.5	70-90

TABLE 2.3: Workability West-Africa January

The water depth is an important limitation to the offshore dry-docking concept. The water depth should be sufficient to provide enough slack in the mooring lines to the increase in height. Depths less than 100[m] are expected to require a lengthening of the mooring system [3]. Since the FPSOs in West-Africa region lay in deep water, the water depth in this research is taken as 1000[m].

2.8 Assumptions summery

This section summarises the key assumptions of this chapter. For the environmental conditions the West-African region is used because it is a remote area and compared to the South American's east coast the environment is relatively calm. Wave loads are calculated with a significant wave height of 1[m] and a peak period of 14[s]. Wind and current effects are assumed to be minimal and therefore neglected. Since the FPSO is able to weathervane and the waves are unidirectional the maximum wave angle is set to 30[deg].

The system consists of two floating bodies. For the SHTV the properties and dimensions of the Dockwise Vanguard have been used and for the FPSO the properties and dimensions of the Jasmine. Since the SHTV is far less subjected to the waves it is assumed that it doesn't move at all. The non-linear behaviour like the small-gap effects and wave reflection have not been considered. The system is modelled as a rigid body with a 3 DOF mass spring dashpot system to better understand the transverse motion of the FPSO. Sway, Roll and Yaw and their coupling terms have been considered.

Chapter 3

Frequency analysis

3.1 The numerical model

A variety of computer simulation programs are being used for the calculation of the hydrodynamic data of a vessel in waves. At Boskalis there are two programs available: Octopus Seaway, which is a linear strip theory program and Ansys Aqwa, which is based on the panel method.

In this research Octopus Seaway is used[10] as it is a practical tool in an early stage of design since the calculation time is short. Seaway makes use of the assumption that the vessel motions are small relative to the dimensions of the vessel. As a result of this, the motions of a floating body in waves is linear or can be linearised. Only the hydrodynamic effects of the hull bellow still water level are accounted for and the above part is neglected. Therefore, inaccuracies can be expected when large parts of the vessel go in or out of the water. The strip theory works best on a slender body and is based on potential flow theory. This holds that viscous effects are neglected, this can deliver serious problems when predicting the roll motion around the resonance frequencies. Although the strip theory has some limitations it is most practical for the calculation of the wave induced motions of the vessel, at least in an early design stage since the calculation time is short.

For the validation of the numerical model both Octopus Seaway and Ansys AQWA are used. AQWA is based on the same linear theory as Seaway. The main difference is the way it solves the potential flow equations. The panel method is much more precise than the strip theory. For slender bodies like the FPSO the solutions of both programs should give the solution in the same order of magnitude. The panel methods main disadvantage is that it is computational demanding software. The calculation time of Ansys AQWA could take minutes up to an hour compared to seconds with Octopus Seaway.

The Octopus Seaway program has two downsides: First it is not able to include dampers in the system. Secondly it is only capable of running one calculation at a time. For each different set of conditions the user has to run a new calculation. For the final results of this thesis 208.000 calculations were made. It was too cumbersome to run these one by one. The practical solution found is to develop a script using the Python programming language. The script imports the hydrodynamic data from Seaway and solves the frequency domain problem.

During the load/discharge operation the FPSO's draft changes over time due to the upward forces of the water discharging SHTV. By the time the draft of the FPSO changes the SHTV and FPSO make contact. In this research only interactions through the spring/dashpot systems are studied and therefore this change in draft is left out of scope. The hydrodynamic properties of the FPSO will not change and are calculated using Seaway. The same hydrodynamic data is used in the Python script for each run. The math and equations used in the script are explained in section 3.3.

3.2 Characteristics of the numerical model

3.2.1 Python script

The Python script is build to solve the equations of motion in the frequency domain of a 3DOF system. This system consists of a single mass with hydrodynamic properties. These properties are derived from a calculation done in Octopus Seaway. This mass is connected to a set of spring/dashpot systems which influence the behaviour of the mass.

The spring/dashpot systems are always connected to the longitudinal centre plane area of the vessel. In other words their y coordinate is always equal to zero. Since the model is based on linear theory, small angles are assumed. Therefore it shouldn't make any difference for the transverse motion if the spring/dashpot systems are connected outside the centre plane area. Their longitudinal and vertical location is varied over different runs. The Python script calculates the motion behaviour of every combination of x,z location and properties (K,C) of the spring/dashpot system. The outcome of all these runs are brought together in different contour graphs to show the behaviour. This give insight to the question if there is an optimal location for the connections.

3.2.2 Parameters and components

This section describes the parameters shown in figure 3.1 which are used throughout this research. As shown in table 3.1 some parameters are constant while others are varied with a certain step. Spring 1&2 represents the mooring system and are located at the bow at keel level, shown in green in the figure. Spring/dashpot 3&4 are shown in red in the figure. The stiffness, damping and vertical location (z3&z4) of spring/dashpot system 3&4 are kept equal throughout the calculations.

Point 1 to 5 are the contact points. In these points the significant transverse motion is calculated. Point 1 and 5 are located at the outer most part of the FPSO where the largest motions can be expected. At keel level the sway and roll component of the transverse motion are equal in any of the 5 motion points. However the yaw component increases the further the contact points move towards the bow or stern of the vessel. As discussed in the Background section 1.1; the outer points of the FPSO that make contact with the SHTV's cribbing are the points at which the largest transverse motions can be expected. The outer contact points to the cribbing are shown in figure 3.1 as points 2&4.

parameter	minimum	maximum	step	unit
x_1 & x_2	248.4	[-]	[-]	[m]
x_3	200	240	[10]	[m]
x_4	0	90	10	[m]
z_1 & z_2	0	[-]	[-]	[m]
z_3 & z_4	0	9	1	[m]
K_2	125	[-]	[-]	[kN/m]
K_3 & K_4	1000	32000	1000	[kN/m]
C_3 & C_4	0	6000	500	[kNs/m]

TABLE 3.1: Parameters used

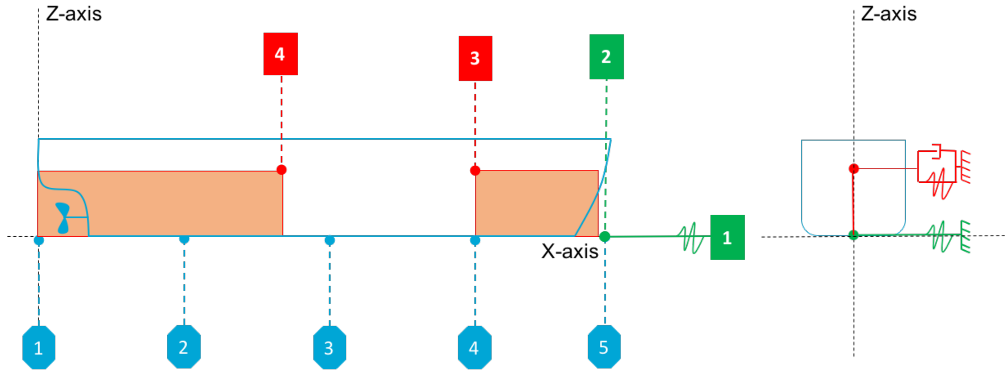

FIGURE 3.1: Reference system

3.2.3 Mooring system

The Jasmine is an external turret moored FPSO. This mooring system is simplified into two springs (K1&K2) which represent the mooring lines of the real system. K1 is the longitudinal spring and K2 is the transverse spring. Together they can simulate the mooring system in all directions. Since the stiffness of the mooring system is unknown it has been estimated. A typical mooring system of a turret moored FPSO at a depth of 1000[m] has a natural frequency between 120-150 seconds [11]. Multiple runs in Seaway are executed with different values for K1 and K2 to find the corresponding natural frequency. These results are summarised in table 3.2. K1 is equal to K2 because the FPSO is able to weathervane and therefore has the same properties after a rotation of 90 degrees. As showed in table 3.2 a stiffness value between 100 and 150[kN/m] should be used. For the Python model the stiffness of both K1 and K2 were set to 125[kN/m].

Stiffness [kN/m]	Natural surge period [s]	Natural sway period [s]
100	144	152
125	128	136
150	117	124
250	91	96
500	65	68

TABLE 3.2: Mooring system stiffness

3.2.4 Viscous roll damping

The hydrodynamic data from Octopus Seaway is based on potential flow theory. This means that the viscous effects are generally neglected. There is however an option in the seaway program to account for this viscous roll damping. To be able to compare the results from the Python script with the Seaway results both programs should perform the same calculation. Therefore the viscous roll damping is not accounted for in the hydrodynamic data from seaway.

Neglecting the viscous roll damping can cause serious problems in predicting the roll motion around the resonance frequencies. It is expected that the natural roll frequency shifts away from the wave frequency as the location and stiffness of the springs move towards the optimum. Results show that the roll natural frequency is around 0.7[rad/s] and higher as showed in figure 5.2. The wave frequency studied is around 0.45[rad/s] and therefore it is assumed to be far enough from the resonance frequency. For this reason the viscous roll damping is not included in the Python script.

3.3 Frequency domain analysis in Python

This section describes the Calculation of the transverse motion in the outer contact points that make contact to the cribbing at keel level of the FPSO. First the hydrodynamic data is imported in the equation of motion [12] [13] [14]. Then for sway, roll and yaw the RAO is calculated for every frequency between 0 and 2.5 in steps of 0.05[rad/s]. These RAOs are used to calculate the overall transverse motion in the points of interest at keel level. Finally, the wave spectrum is added to calculate the significant transverse motion in points 2&4. In the matrices to follow sway, roll and yaw are indicated with underscore 22, 44, 66 respectively. Combinations such as 24 stand for a coupling term, in this case the coupling between the sway and roll motion.

The equation of motion 3.1 is written in matrices notated between brackets and vectors notated bold. The force vector and added mass, wave radiation damping and hydrostatic stiffness matrices are derived from the hydrodynamic data. Also the mass, viscous damping and structural stiffness matrices are known.

$$[M + A(\omega)]\ddot{\mathbf{x}} + [C + C_{hydro}(\omega)]\dot{\mathbf{x}} + [K + K_{hydro}]\mathbf{x} = \mathbf{f} \tag{3.1}$$

The complex valued wave load RAO is imported from Seaway and implemented in the Python model as a force vector.

$$\mathbf{f} = \mathbf{F}e^{-i\omega t} = \begin{bmatrix} F_2(\omega) \\ F_4(\omega) \\ F_6(\omega) \end{bmatrix} e^{-i\omega t} \tag{3.2}$$

The motion, velocity and acceleration vectors are unknown. In order to solve the equation of motion a solution for $\mathbf{x}$ is suggested as equation 3.3 shows. This suggested solution is differentiated as showed in equations 3.4 and 3.5. y_a, ϕ_a and ψ_a are the amplitudes in sway, roll and yaw respectively.

$$\mathbf{x} = \mathbf{X}e^{-i\omega t} = \begin{bmatrix} y_a e^{i\epsilon_y} \\ \phi_a e^{i\epsilon_\phi} \\ \psi_a e^{i\epsilon_\psi} \end{bmatrix} e^{-i\omega t} \tag{3.3}$$

$$\dot{\mathbf{x}} = -i\omega\mathbf{X}e^{-i\omega t} \tag{3.4}$$

$$\ddot{\mathbf{x}} = -\omega^2\mathbf{X}e^{-i\omega t} \tag{3.5}$$

These solutions are substituted in the equation of motion. Due to this substitution the time related part can be eliminated from both sides of the equation. The equation of motion is reorganised and showed in equation 3.6. $\mathbf{X}$ is a complex valued vector and equal to the motion RAO around the COG.

$$\mathbf{X} = (-\omega^2[M + A(\omega)] - i\omega[C + C_{hydro}(\omega)] + [K + K_{hydro}])^{-1}\mathbf{F} \tag{3.6}$$

With equation 3.7 the transverse motion RAO can be calculated in point $P(x_b, y_b, z_b)$. By taking the absolute value of y_p the amplitude is gained and the phase angle is equal to the angle of the complex argument[8]. The motion in points 2&4 described in section 3.2.2 are calculated this way. The calculation is written in a loop in order to deliver the results for every combination of the parameters described in section 3.2.2.

$$y_p = \mathbf{X}(1) - \mathbf{X}(2)(z_b - z_g) + \mathbf{X}(3)(x_b - x_g) \tag{3.7}$$

The structural mass Eq3.8 is constant and is calculated with Eq3.9-Eq3.11. $M_{Jasmine}$ is the mass of the vessel and $k_{xx}\&k_{zz}$ are the radius of gyration along the longitudinal and vertical axis of the Jasmine.

$$M = \begin{bmatrix} M_{22} & 0 & 0 \\ 0 & M_{44} & 0 \\ 0 & 0 & M_{66} \end{bmatrix} \tag{3.8}$$

$$M_{22} = M_{Jasmine} \tag{3.9}$$

$$M_{44} = M_{Jasmine} k_{xx}^2 \tag{3.10}$$

$$M_{66} = M_{Jasmine} k_{zz}^2 \tag{3.11}$$

The added mass 3.12 is calculated with Octopus Seaway and imported into the Python script. The added mass is frequency dependent and symmetric.

$$A(\omega) = \begin{bmatrix} A_{22} & A_{24} & A_{26} \\ A_{42} & A_{44} & A_{46} \\ A_{62} & A_{64} & A_{66} \end{bmatrix} \tag{3.12}$$

The structural damping Eq3.13 is a symmetric matrix. The equations 3.14-Eq3.19 are used to calculate the structural damping matrix.

$$C = \begin{bmatrix} C_{22} & C_{24} & C_{26} \\ C_{42} & C_{44} & C_{46} \\ C_{62} & C_{64} & C_{66} \end{bmatrix} \tag{3.13}$$

$$C_{22} = C_3 + C_4 \tag{3.14}$$

$$C_{24} = C_3(z_g - z_3) + C_4(z_g - z_4) \tag{3.15}$$

$$C_{26} = C_3(x_3 - x_g) + C_4(x_4 - x_g) \tag{3.16}$$

$$C_{44} = C_3(z_g - z_3)^2 + C_4(z_g - z_4)^2 \tag{3.17}$$

$$C_{46} = C_3(x_3 - x_g)(z_g - z_3) + C_4(x_4 - x_g)(z_g - z_4) \tag{3.18}$$

$$C_{66} = C_3(x_3 - x_g)^2 + C_4(x_4 - x_g)^2 \tag{3.19}$$

$$\tag{3.20}$$

The wave radiation damping is calculated with Octopus Seaway and imported into the Python script. The wave radiation damping is frequency dependent and symmetric.

$$C_{hydro}(\omega) = \begin{bmatrix} C_{hydro22} & C_{hydro24} & C_{hydro26} \\ C_{hydro42} & C_{hydro44} & C_{hydro46} \\ C_{hydro62} & C_{hydro64} & C_{hydro66} \end{bmatrix} \tag{3.21}$$

The structural stiffness matrix, equation3.22, is symmetric. The equations 3.23-3.28 are used to calculate the structural stiffness matrix.

$$K = \begin{bmatrix} K_{22} & K_{24} & K_{26} \\ K_{42} & K_{44} & K_{46} \\ K_{62} & K_{64} & K_{66} \end{bmatrix} \tag{3.22}$$

$$K_{22} = K_2 + K_3 + K_4 \tag{3.23}$$

$$K_{24} = K_2(z_g - z_2) + K_3(z_g - z_3) + K_4(z_g - z_4) \tag{3.24}$$

$$K_{26} = K_2(x_2 - x_g) + K_3(x_3 - x_g) + K_4(x_4 - x_g) \tag{3.25}$$

$$K_{44} = K_2(z_g - z_2)^2 + K_3(z_g - z_3)^2 + K_4(z_g - z_4)^2 \tag{3.26}$$

$$K_{46} = K_2(x_2 - x_g)(z_g - z_2) + K_3(x_3 - x_g)(z_g - z_3) + K_4(x_4 - x_g)(z_g - z_4) \tag{3.27}$$

$$K_{66} = K_2(x_2 - x_g)^2 + K_3(x_3 - x_g)^2 + K_4(x_4 - x_g)^2 \tag{3.28}$$

The hydrostatic stiffness has influence on the vertical motions which are; heave, roll and pitch. This matrix consist of sway, roll and yaw and therefore only one term has a value higher than zero.

The hydrostatic stiffness:

$$K_{hydro} = \begin{bmatrix} 0 & 0 & 0 \\ 0 & \rho_w V_J g GM & 0 \\ 0 & 0 & 0 \end{bmatrix} \tag{3.29}$$

3.4 Wave spectrum

Nowadays a double peaked spectrum is often used in order to describe both the wind and swell waves in one spectrum. Since this research's focus is on the swell conditions in the West-African region a single wave spectrum is considered (see section 2.7). The Bretschneider or modified Pierson-Moskowitz wave spectrum [15] is formulated by equation 3.30. The spectrum describes the concept of a fully developed sea. Figure 3.2 shows the spectrum for a significant wave height of 1[m] and a peak period of 14[s] or 0.45[rad/s]. The response spectrum for the transverse direction is calculated with equation 3.31 then the zero order moment is calculated with equation 3.32 in order to find the significant amplitude in transverse direction of the FPSO with equation 3.33.

$$S(\omega) = \frac{5}{16}\frac{\omega_p^4}{\omega^5} H_s^2 \exp(\frac{-5}{4}(\frac{\omega_p}{\omega})^4) \tag{3.30}$$

$$S_y(\omega) = y_p^2 S(\omega) \tag{3.31}$$

$$m_0 = \int_0^\infty S_y(\omega) d\omega \tag{3.32}$$

$$\zeta_{a1/3} = 2\sqrt{m_0} \tag{3.33}$$

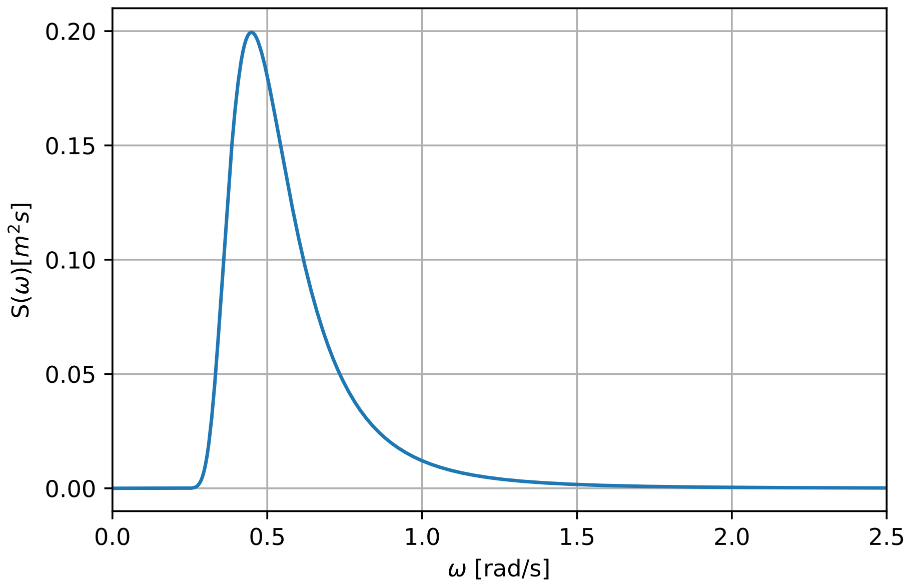

FIGURE 3.2: Modified Pierson Moskowitz wave spectrum $H_s = 1[m], t_p = 14[s]$

3.5 Natural frequency calculation

As discussed before the natural frequencies of the system are an important characteristic. To find the natural frequencies of the system, the following determinant should be set to zero[12]:

$$det[K - \omega^2 M] = 0 \tag{3.34}$$

Which is equivalent to finding the eigenvalues of the matrix KM^1. The natural frequencies can be obtained in both ways. The normal modes of the free vibrations can be found by searching for the eigenvectors of the matrix KM^1. In this research the natural frequencies of the uncoupled system are calculated. This is done for two reasons: First, to be able to validate the numerical model to the commercial software Octopus Seaway and Ansys AQWA as described in chapter 4. These two programs calculate the natural frequencies of the uncoupled system. The second reason is that the uncoupled natural frequencies each directly refer to a single DOF. This is use full to gain insight in the influence of the locations of the spring/dashpot systems.

The K-matrix in equation 3.34 represents both the stiffness and the hydrostatic stiffness matrices. The M-matrix represents both the mass and the added mass matrices. In order to calculate the uncoupled natural frequencies the coupling terms of the added mass and stiffness matrices are set to zero. All the matrices used in equation 3.34 are now considered to have diagonal terms only and so for each DOF the natural frequency is calculated. However, the added mass matrix is frequency dependent. The hydrodynamic data used in the numerical model contains 50 wave frequencies ranging from 0.05 to 2.5[rad/s] and therefore 50 different natural frequencies are calculated for each DOF. The systems true natural frequencies are the ones that are equal to the wave frequency. The calculated natural frequencies are interpolated to find the systems true natural frequencies.

Chapter 4

Validation of the numerical model

To make sure that the Python script runs correctly and provides reliable results, it is validated to Octopus seaway. With this program the hydrodynamic data input determined and therefore this program is used to validate the numerical model. In order to compare both systems testcase parameters are determined which can be found in table 4.1. The damping is set to zero since Octopus seaway is not able to account for structural damping. For the testcase, all the matrices in the equation of motion are exactly the same in both programs, therefore the results should match. The validation to Octopus Seaway is done in two steps. First, the natural frequencies in sway, roll and yaw are compared and secondly the RAOs in the 3DOF are compared.

quantity	value	unit	quantity	value	unit
K_1	125	[kN/m]	x_2	248.4	[m]
K_2	125	[kN/m]	x_3	200	[m]
K_3	16000	[kN/m]	x_4	0	[m]
K_4	16000	[kN/m]	z_1	0	[m]
C_3	0	[kNs/m]	z_2	0	[m]
C_4	0	[kNs/m]	z_3	0	[m]
x_1	248.4	[m]	z_4	0	[m]

Table 4.1: Testcase parameters

4.1 Octopus seaway vs Python script

The natural frequencies in sway, roll and yaw are important characteristics of the system. The idea is to reduce the relative motions and therefore move away from the resonance frequencies. In table 4.2 the natural frequencies of Seaway and python script are compared. It shows that both programs determined exactly the same results except for the yaw natural frequency. The yaw natural frequency shows a minor difference which is most likely related to a rounding error. The validation test indicates that the results from our Python model are reliable for the purpose of this study.

	Python		**Seaway**	
	freq [rad/s]	period [s]	freq [rad/s]	period [s]
Sway	0.756	8.32	0.756	8.32
Roll	0.932	6.74	0.932	6.74
Yaw	1.391	4.52	1.392	4.52

Table 4.2: Natural frequencies Python vs seaway

The second validation step is comparing the RAOs of both systems. Since the two systems should run the same calculation and their input matrices and parameters to the equation of motion (see section 3.3) are equal, similar results are expected. Figure 4.1 shows the results of the amplitudes and phasing of both systems for each DOF. It shows that both the sway and roll amplitude are almost equal however between 0.5 and 1 rad/s there is a small difference. The yaw amplitude has the correct curvature, but the values around 0.5 [rad/s] do not match. The phase angles in all DOF show differences.

In order to find where these differences come from, all the used matrices and parameters were compared to make sure that the differences do not come from an input difference. To investigate if this problem is in one DOF or in all of them, the two programs are uncoupled. This should again show results of the amplitude and phase of the 3DOF. However the coupling terms are set to zero. In order to do this a Seaway run was executed for each degree of freedom on its own. In the Python script the coupling terms of the added mass, wave radiation damping, structural damping and structural stiffness were set to zero. Figure 4.2 shows six graphs of the decoupled systems. It can be noticed that the amplitude of the three motions are exactly the same.

The phase graphs might give a distorted picture of the differences between the two lines. For example, the roll phase angle at 1.6 [rad/s] is 359.9[deg] in the python script and 1.5[deg] in Seaway. Since a circle consists of 360 degrees this is only 1.6 degrees off nevertheless this is shown as a huge difference in the graph. The sway and yaw phase angels are more off than the roll phase angle. Overall, the lines have a similar shape while the peak values do not exactly match.

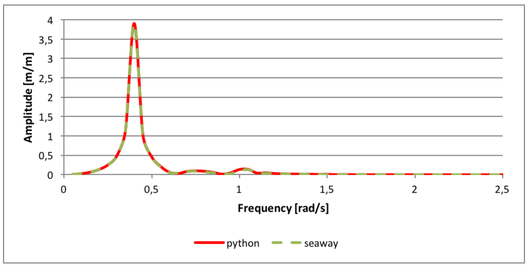

(a) RAO - sway - amplitude

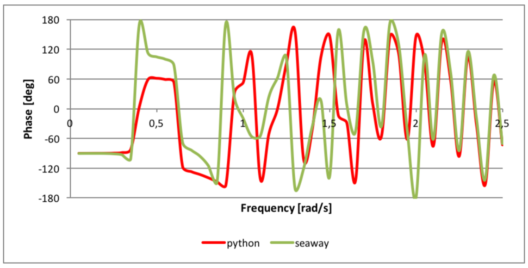

(b) RAO - sway - phase

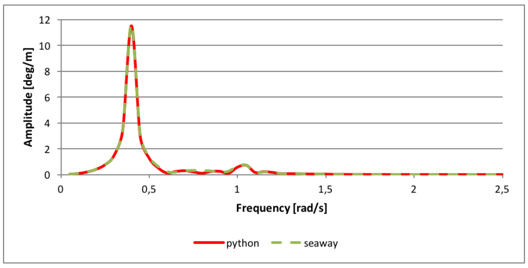

(c) RAO - roll - amplitude

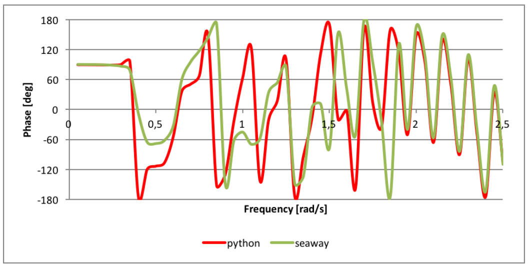

(d) RAO - roll - phase

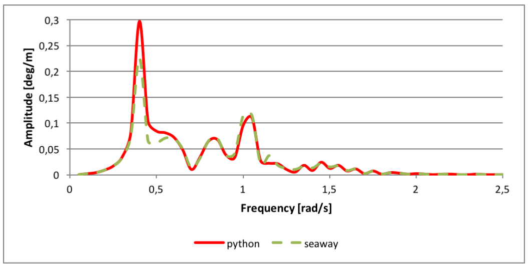

(e) RAO - yaw - amplitude

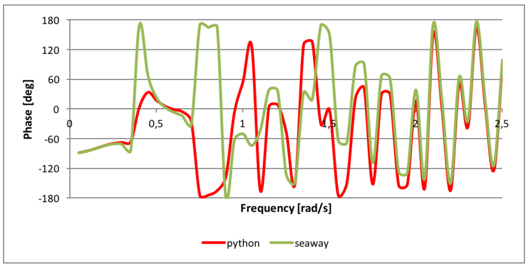

(f) RAO - yaw - phase

FIGURE 4.1: RAOs of Seaway-Python coupled

Through uncoupling the system it is learned that the differences in amplitude in the coupled system come from the coupling terms. These coupling terms might be distorted by the phasing. For the purpose of this study the outcome might be acceptable but to make sure that there are no mistakes in the python script it will be further validated to the commercial program Ansys AQWA.

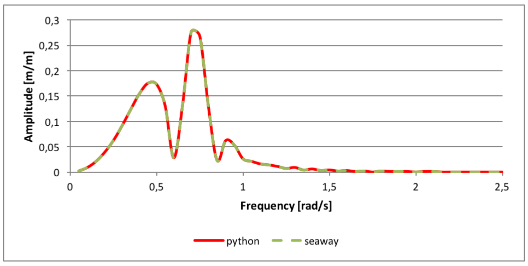

(a) RAO - sway - amplitude

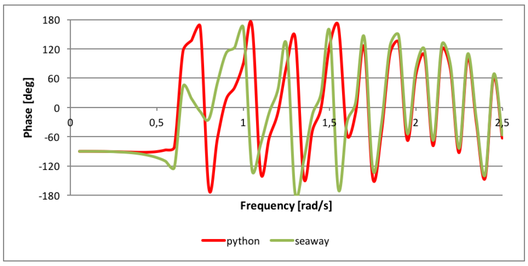

(b) RAO - sway - phase

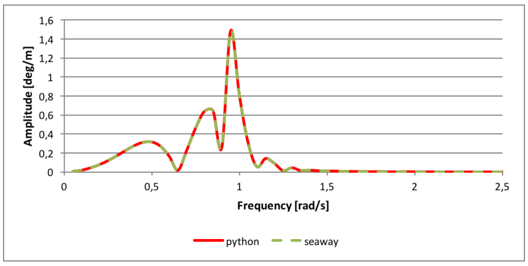

(c) RAO - roll - amplitude

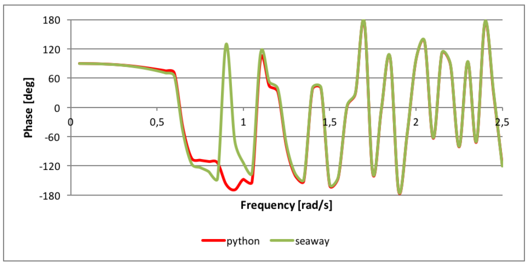

(d) RAO - roll - phase

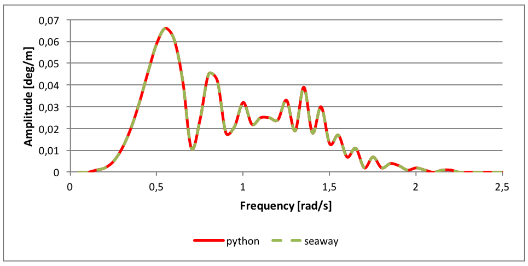

(e) RAO - yaw - amplitude

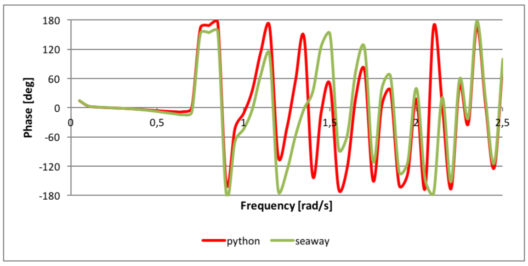

(f) RAO - yaw - phase

FIGURE 4.2: RAOs of Seaway-Python uncoupled

4.2 Ansys AQWA vs Python script

To make sure that the python script's results are correct it is further validated to the commercial program Ansys AQWA. In order to validate the program a new model of the jasmine FPSO is build that runs in AQWA. This model has the same dimensions but there could be minor differences to the model used in Seaway. Hydrodynamic data is calculated with AQWA and this data is imported into the python script to make the right comparison. The testcase parameters (table 4.1) are used again. The validation is done by comparing the amplitudes and phase of the RAOs in each degree of freedom calculated separately by both programs. The results are shown in figure 4.3. Both the amplitudes and the phases correspond correctly as the lines lay on top of each other. Therefore it can be stated that the python script generates reliable results.

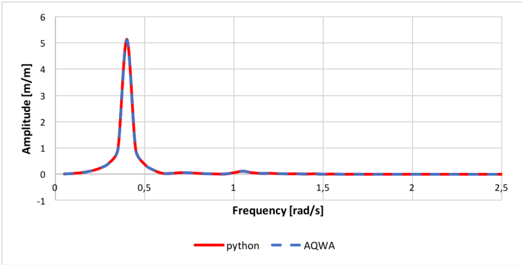

(a) RAO - sway - amplitude

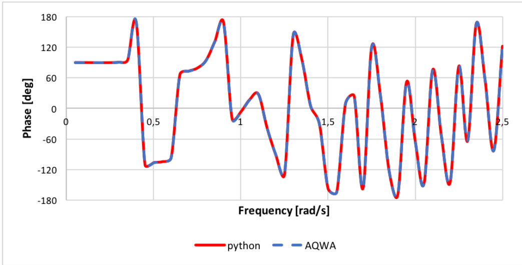

(b) RAO - sway - phase

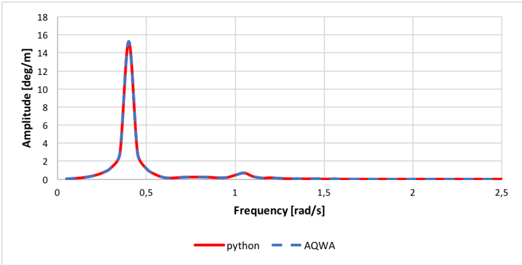

(c) RAO - roll - amplitude

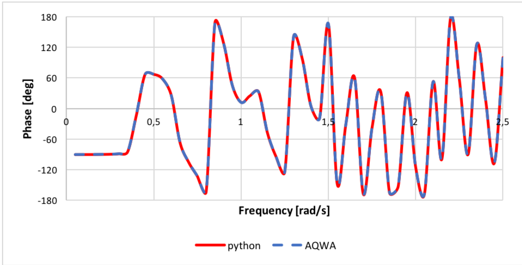

(d) RAO - roll - phase

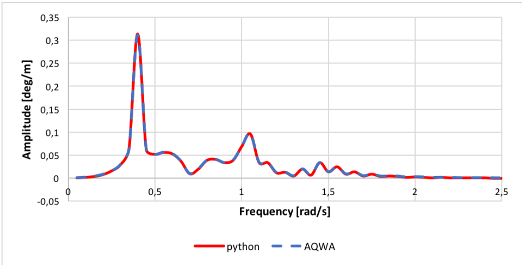

(e) RAO - yaw - amplitude

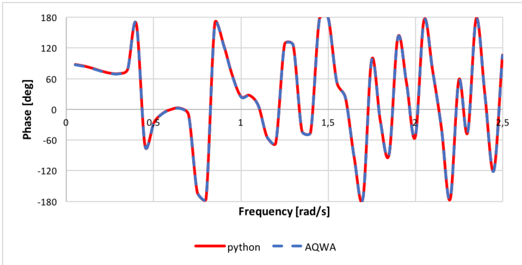

(f) RAO - yaw - phase

FIGURE 4.3: RAOs of AQWA-Python

4.3 Conclusion

The python script is validated to the commercial programs Octopus Seaway and Ansys AQWA. By using a testcase, the same hydrodynamic data and the same potential theory were used, therefore similar results were expected. Since the hydrodynamic data used throughout this thesis is obtained with Seaway it would be logical to validate to this software. The validation to Seaway of the RAOs resulted in a difference in both amplitude and phasing. For the uncoupled system the amplitudes showed to be similar and the phasing showed a similar shape. However the peak amplitudes are different. To understand if this difference comes from the python script or from Octopus Seaway, the python script is validated to Ansys AQWA. A new model is build to run in AQWA and the newly obtained hydrodynamic data is used for this validation. The validation resulted in a positive result. The RAO's amplitudes and phasing in all 3DOF are similar and therefore the python script is validated.

Chapter 5

Results of the numerical model

This chapter shows the results from the Python script calculations. 208.000 runs have been done to investigate multiple combinations of parameters. The environmental conditions were kept constant at 1[m] significant wave height, 14[s] peak period and a wave angle of 30[deg] off stern. The modified Pierson-Moskowitz wave spectrum has been used to take irregular waves into account.

5.1 Natural frequencies

This section describes the change of the natural frequencies of the 3DOF system due to changes in stiffness, vertical and longitudinal position of the springs. The resonance behaviour occur when natural frequencies are close to the wave frequency.

Figures 5.1-5.3 show the sway, roll and yaw natural frequencies each represented in two graphs per figure. The first graph (a) shows the longitudinal location of spring 4 (x_4) plotted against the stiffness of the springs and the second graph (b) shows the vertical location of spring 3 and spring 4 plotted against the stiffness. Spring 3 and spring 4 are varied in stiffness between 1000 and 32000 [kN/m] in steps of 1000. The vertical positions of spring 3&4 are always equal and varied from 0 to 9 [m] in steps of 1[m]. The longitudinal location of spring 4 (x_4) is varied from 0 to 90 [m] in steps of 10[m]. The longitudinal position of spring 3 (x_3) is kept constant at 200[m]. Vertical contour lines suggests that only the stiffness has influence on the natural frequency while horizontal contour lines would suggest that only the location has influence.

From figure 5.1 can be observed that the contour lines in both graphs are vertical. This indicates that the sway natural frequency is not influenced by a change in location of the springs in longitudinal or vertical direction. It is only influenced by the stiffness of the springs. It can be stated that; the stiffer the system, the higher the natural frequency and the further the natural frequency lies from the wave frequency, the smaller the expected motions.

From the roll natural frequency showed in figure 5.2 can be observed that both the stiffness and the vertical location of the springs have their influence. Again, the stiffer the system the higher the natural frequency and therefore the further the natural frequency lies from the wave frequency. The influence of the vertical location is clearly shown in figure 5.2(b). The closer the springs are located to keel level (z=0[m]), the higher the natural frequency and therefore less roll motion is expected.

From the yaw natural frequency showed in figure 5.3 can be observed that both the stiffness and longitudinal location of the springs have their influence. The influence of the longitudinal location of spring 4 is clearly shown in figure 5.3(a). At a stiffness of 5000 [kN/m] the natural frequency is equal to the wave frequency when spring 4 is located 90[m] off stern. However the natural frequency is almost double when spring 4 is located at the stern (x_4=0[m]). This indicates that the longitudinal position has a high influence on the yaw motion and therefore it seems optimal to locate the spring at the stern. The explanation for this is that the yaw moment created depends on the length of the arm. The further the spring is located from the centre of the vessel the larger is the moment it creates.

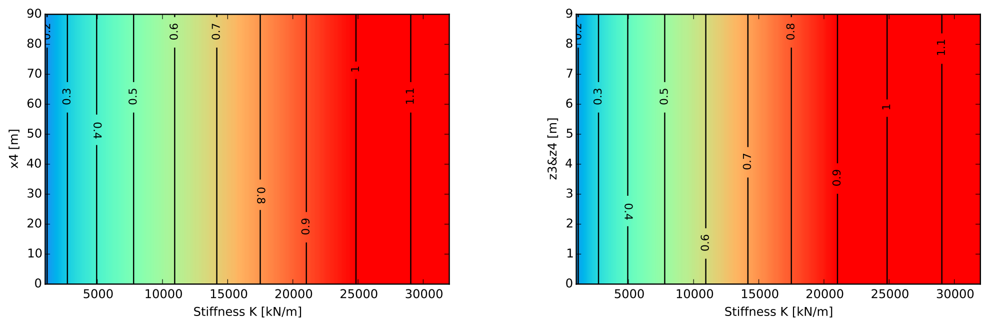

(a) z=0[m] (b) x_4=0[m]

FIGURE 5.1: Sway natural frequency of different locations vs stiffness ($x_3 = 200[m]$)

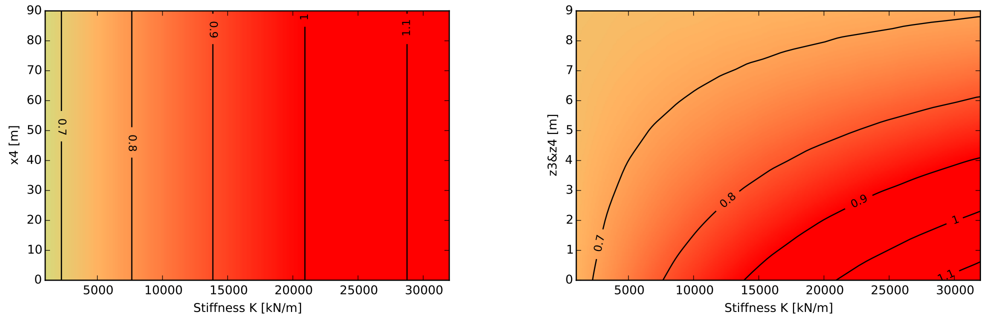

(a) z=0[m]

(b) x_4=0[m]

FIGURE 5.2: Roll natural frequency of different locations vs stiffness ($x_3 = 200[m]$)

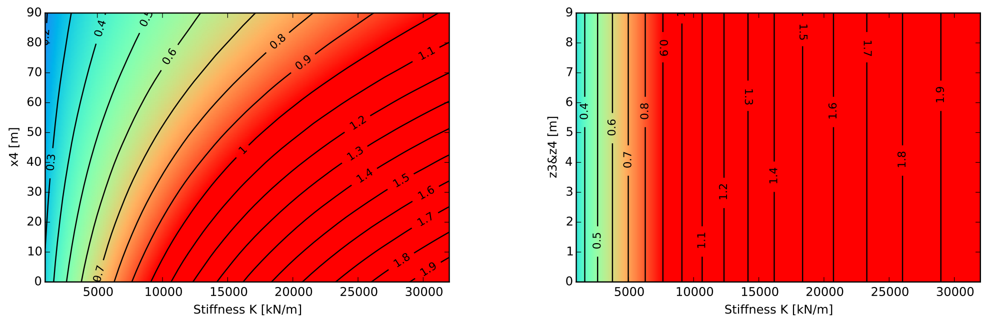

(a) z=0[m]

(b) x_4=0[m]

FIGURE 5.3: Yaw natural frequency of different locations vs stiffness ($x_3 = 200[m]$)

5.2 Significant motion in the contact points

This section describes the motion behaviour of the vessel in the outer contact points to the cribbing. In these points the largest motions are expected and therefore they are most important. Figure 3.1 shows the reference system of the numerical model with the outer contact points as point 2 and point 4.

5.2.1 Vertical position vs stiffness

Figure 5.4 shows four contour graphs of the significant motion in point 2. Each graph represents a different longitudinal position of spring 4. The vertical axis represents the vertical location of the springs 3&4 and the horizontal axis represents the stiffness. For each combination of stiffness and location of the springs, the significant motion is calculated and plotted in the graph. The influence of the natural frequencies in each degree of freedom can clearly be noticed. The progression of the sway natural frequency causes large motions for small stiffness and less motions when the stiffness increases. The yaw natural frequency influence is shown over the four graphs of figure 5.4 as the red area gets wider as spring 4 moves towards the centre of gravity.

The roll natural frequency moves away from the wave frequency as the springs are positioned closer to the keel, as discussed in section 5.1. Therefore, it is expected that the springs attached at keel level (z=0[m]) would give the best results. However figure 5.4 shows that at 12000[kN/m] the optimal height seems to be 9[m] and as the stiffness increases the optimal height decreases to 2.5[m] at 32000[kN/m]. The way it decreases suggests that there is a value to which it converges for an infinite stiff value of the springs. The value to which it converges seem to be at the same location as the resultant wave force is expected to be.

Figure 5.5 shows four contour graphs of the significant motion in point 4. Again the progression of the sway natural frequency graphs explains the large motions for small stiffness and smaller motions for a stiffer system. The four contour graphs show relatively small differences. This means that changing the position of spring 4 has minor impact on motion in point 2. Furthermore, it may also be noticed that a higher stiffness is needed compared to point 2 to meet the target of maximum 0.1[m] of significant motion.

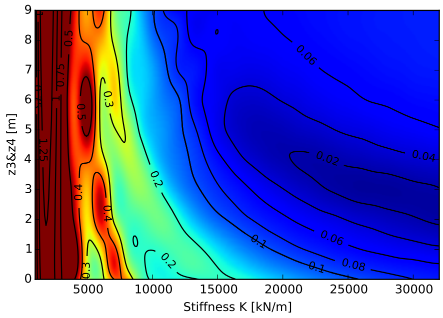

(a) x_4=0[m]

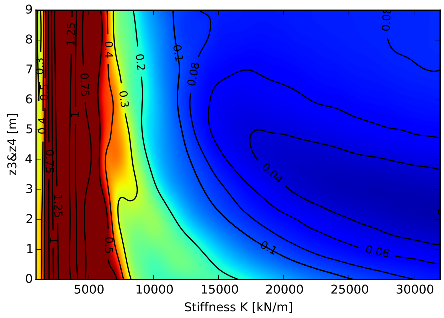

(b) x_4=30[m]

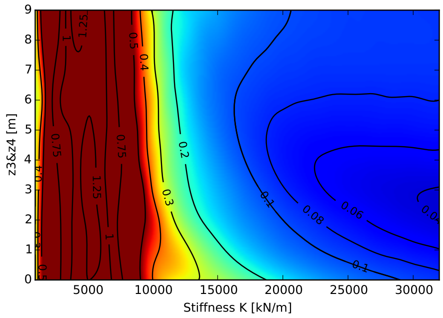

(c) x_4=60[m]

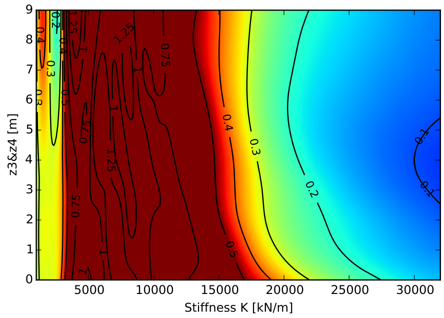

(d) x_4=90[m]

FIGURE 5.4: Significant motion in point 2 at multiple locations of x_4

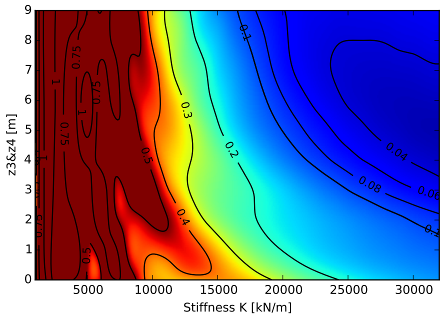

(a) x_4=0[m]

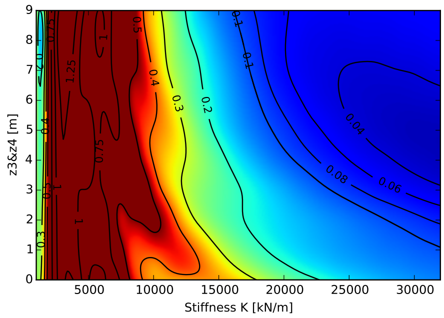

(b) x_4=30[m]

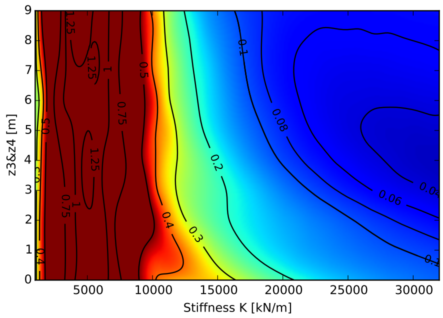

(c) x_4=60[m]

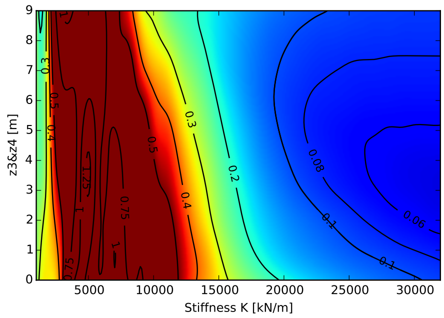

(d) x_4=90[m]

FIGURE 5.5: Significant motion point in 4 at multiple locations of x_4

5.2.2 Vertical position vs longitudinal position

Figure 5.6 shows four contour graphs of the significant motion in point2. Figure 5.7 shows four contour graphs of the significant motion in point 4. Each graph represents a different stiffness for spring 3 and spring 4. The horizontal axis represents the longitudinal position of spring 4 and the vertical axis represents the vertical position of the two springs. The system is in resonance for both points at 8000[kN/m].This indicates that the motions are too large and therefore the graphs coloured red. At a stiffness of 12000[kN/m] graph 5.6(b) shows an area for which the motion is less than 0.1[m]. In this case, the optimal location for point 2 is at x_4=0[m] and z=9[m]. Point 4 is for a stiffness of 12000[kN/m] still close to resonance and large motions occur as shown in figure 5.7(b). In this graph best location for the springs to minimise the motion in point 4 seems to be x=40[m] and z=9[m]. At 16000[kN/m] a larger area of graph 5.6(c) is now within 0.1[m] for point 2. A shift of the optimum can be noticed and spring location x_4=0[m] and z=5.5[m] experiences the least amount of motion. Point 4 in graph 5.7(c) there is still no area within the 0.1[m]. The optimal location is still at x_4=40[m] and z=9[m]. At 20000[kN/m] point 2 in graph 5.6(d) shows an even larger area within 0.1[m]. Again the optimal location has shifted and is now at x_4=0[m] and z=4.5[m]. Point 4 in graph 5.7(d) shows an area that is within 0.1[m] motion.

It can be stated that the springs connected at 9[m] enable more significant roll motion than when they are located at a lower position. Yet the overall motion is less. This is because the roll motion is in phase with sway. Whenever sway pushes the vessel to the right, the roll rotates so that the points at keel level moves to the left and vice versa. In figure 5.8 the significant roll motion of the coupled system at keel level is shown. It can be observed that the roll motions decrease as the vertical position of the springs move down towards the keel of the vessel.

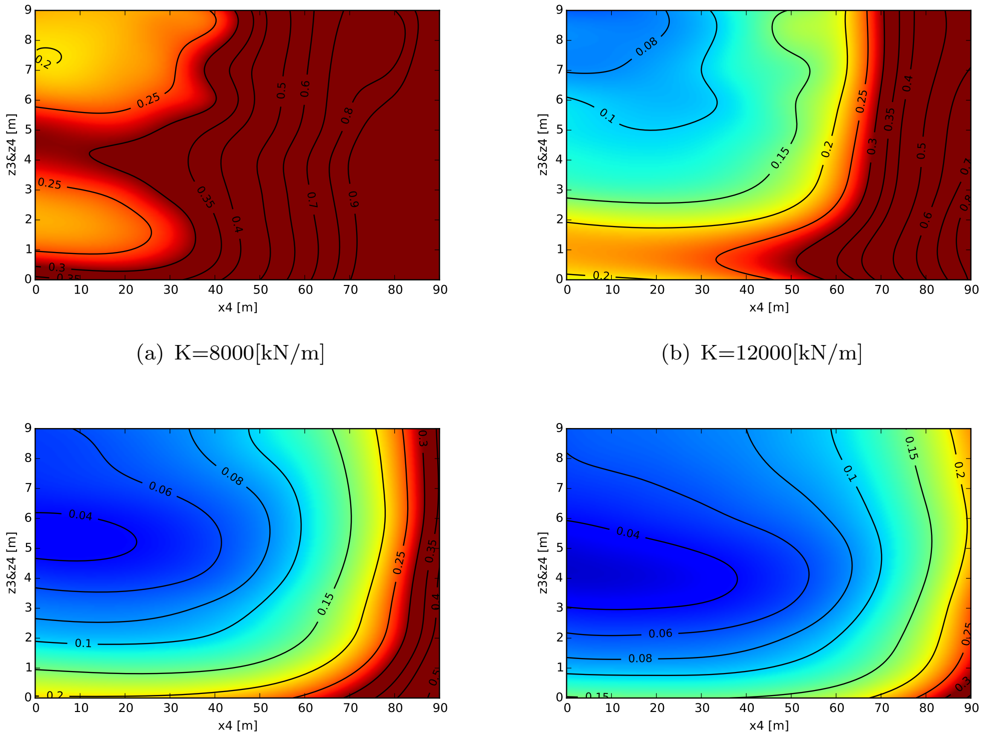

(a) K=8000[kN/m]

(b) K=12000[kN/m]

(c) K=16000[kN/m]

(d) K=20000[kN/m]

FIGURE 5.6: Significant motion in point 2 for different spring stiffnesses

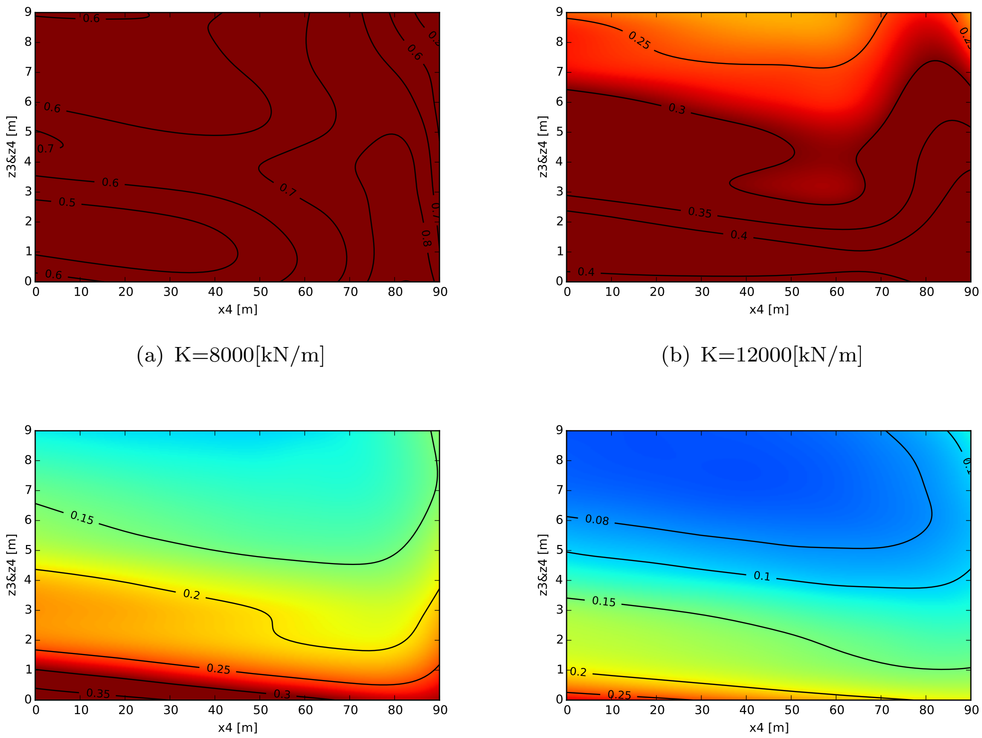

(a) K=8000[kN/m]

(b) K=12000[kN/m]

(c) K=16000[kN/m]

(d) K=20000[kN/m]

FIGURE 5.7: Significant motion in point 4 for different spring stiffnesses

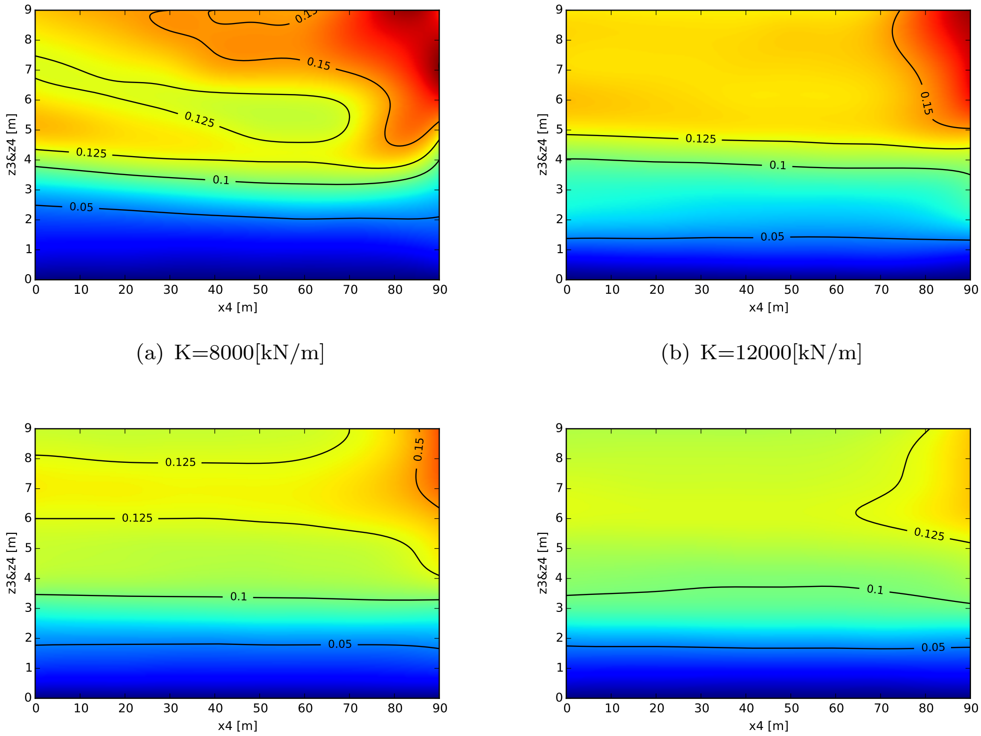

(a) K=8000[kN/m]

(b) K=12000[kN/m]

(c) K=16000[kN/m]

(d) K=20000[kN/m]

FIGURE 5.8: Significant roll motion for different spring stiffnesses

5.2.3 Spring 3 at different longitudinal positions

In the previous section it was shown that the motions in point 2 are overall less than the motions in point 4. This could be because spring 3 has been fixed so far at 200[m]. Additional runs have been created and executed using the numerical model to understand how much the system could be improved by varying the longitudinal position of spring 3 between 200[m] and 240[m] in steps of 10[m].

Figures 5.9 and 5.10 both consist of contour four graphs. For each graph the vertical axis represents the vertical position of spring 3 and spring 4. The horizontal axis represents the longitudinal position of spring 4. In all of these graphs the the significant motion is shown. The stiffness of spring 3 and spring 4 are kept constant at 12000[kN/m] to gain insight in the influence of a different longitudinal location of spring 3.

The graphs of point 2, figure 5.9 show that the area within 0.1[m] decreases as spring 3 moves towards the bow. But even in graph 5.9(d), when the spring is at 240[m] there is an area in which the significant motion is smaller than 0.1[m]. The figures of point 4 5.10 show an impressive improvement. When spring 3 is at 210[m] (graph 5.10(a)) there is no area within 0.1[m]. At 240[m] (graph 5.10(d)) there is a larger area within this 0.1[m].

Both point 2 and point 4 show the least amount of motion when the springs are attached at 9[m]. For point 2 spring 4 is best attached at 0[m] while for point 4 90[m] seems optimal. To optimise the overall behaviour the independent points are compromised. It can be concluded that the optimal spring locations for a stiffness of 12000[kN/m] is $x_3 = 240[m], x_4 = 30[m], z = 9[m]$ to decrease the motions in point 2 and point 4.

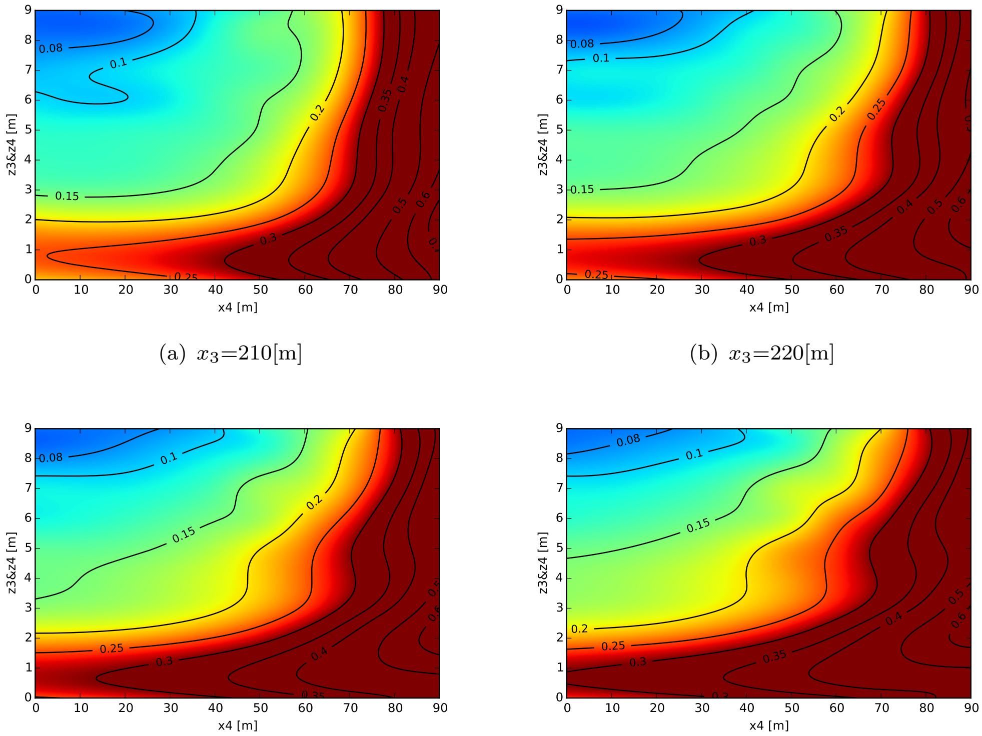

(a) x_3=210[m] (b) x_3=220[m]

(c) x_3=230[m] (d) x_3=240[m]

FIGURE 5.9: Significant motion in point 2 at different locations of x_3

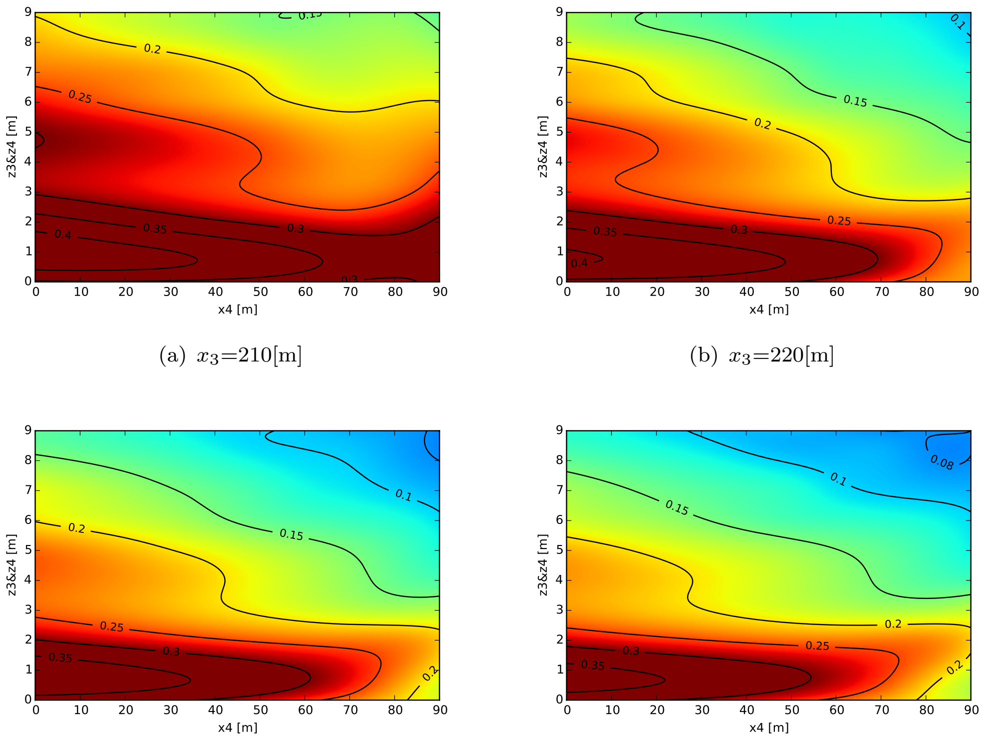

(a) x_3=210[m] (b) x_3=220[m]

(c) x_3=230[m] (d) x_3=240[m]

FIGURE 5.10: Significant transverse motion in point 4 at different locations of x_3

5.2.4 Minimum stiffness

In section 5.2.3 an optimal point has been found for a spring stiffness of 12000[kN/m] for both spring 3 and spring 4. In this section the minimum required spring stiffness to get both contact points within 0.1[m] significant motion is further investigated.

Figure 5.11 shows a contour graph of the minimum amount of stiffness required in both spring 3 and spring 4 to have a significant motion in both contact points 2 and 4 smaller or equal to 0.1[m]. For each combination of the locations of spring 3 and spring 4 the significant motion is calculated in the contact points 2 and 4. This calculation is repeated for all the stiffnesses ranging from 1000 to 32000[Kn/m] in steps of 1000[kN/m] in order to find the minimal stiffness where the motions of both contact points are smaller or equal to the motion limit of 0.1[m]. The results are plotted in figure 5.11 where the vertical axis represents the longitudinal position of spring/dashpot3 and the horizontal axis represents the longitudinal position of spring/dashpot 4. The height of the springs for this figure is kept constant at 9[m]. Appendix C.1 shows six of the same figures, each for a different height of the springs. These figures show that 9[m] is the height to which the stiffnesses are smallest.

In figure5.11 there is only one position calculated in this parametric study that has a minimum stiffness of 12000[kN/m] and still reduces the transverse motion of the outer contact points to the cribbing within 0.1[m]. Therefore position $x_3 = 240[m], x_4 = 30[m], z = 9[m]$ is the best location to position the springs.

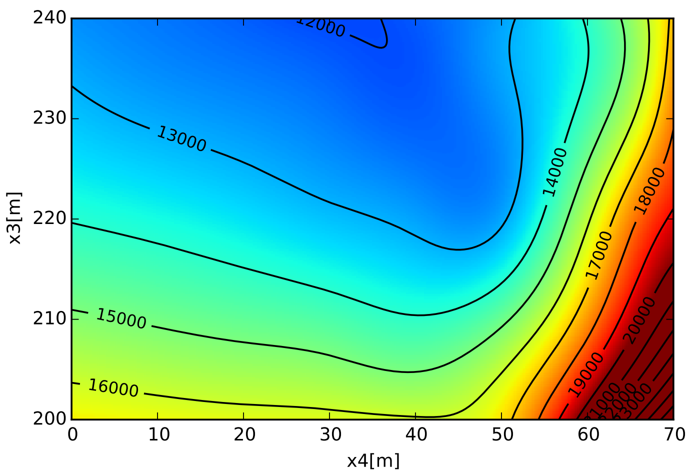

FIGURE 5.11: Minimal required stiffness at $z = 9$[m](C=0[kNs/m])

5.3 Damping

Until this section the analysis and all the shown figures were done without structural damping. In this section the structural damping is investigated. To build an extra system that adds structural damping to the system might bring extra costs with it. However there are two reasons to add structural damping to the system.

The first reason is to get through the resonance frequencies safely. Imagine the spring system without damping. During installation it might not be at full stiffness at once. It could take some time to build up this amount of stiffness. This means that at some point the stiffness causes the total system to have a natural frequency around the wave frequency. The system will be in resonance. Structural damping is most effective around the resonance frequencies and is therefore a good solution to keep the operation safe during the installation phase of the system.

The second reason is to flatten the force curves. By adding structural damping to the system energy is taken from the system. As a result of adding damping the motion reduces and therefore the spring forces. The spring and damper forces act at a different time moment. Think of the system as an oscillating system in waves. The spring forces will be maximum at the maximum displacement of the vessel and the spring forces are zero when the system passes its equilibrium point. The damper forces will be maximum at the maximum velocity of the vessel. So the damper forces are maximum when the spring forces are zero and vice versa. The spring and damper forces together will be smaller than the case when only springs are used. A more flattened force curve can be achieved in stead of the high peaks from a system with only springs. This might help to not exceed the maximum force allowed on the hull.

Figure 5.12 shows the combined spring/dashpot force in the location they are positioned. Spring/dashpot 3 is positioned at 240[m] longitudinal and 9[m] vertical and spring/dashpot 4 is located at 30[m] longitudinal and 9[m] vertical. The horizontal axis represents the stiffness in [kN/m] and he vertical axis represents the damping in [kNs/m]. In the graphs several characteristics are noticed and explained below.

When the structural damping is equal to zero, the forces of both spring/dashpot systems go up to 5500 [kN] for a stiffness around 4000[kN/m]. By adding structural damping

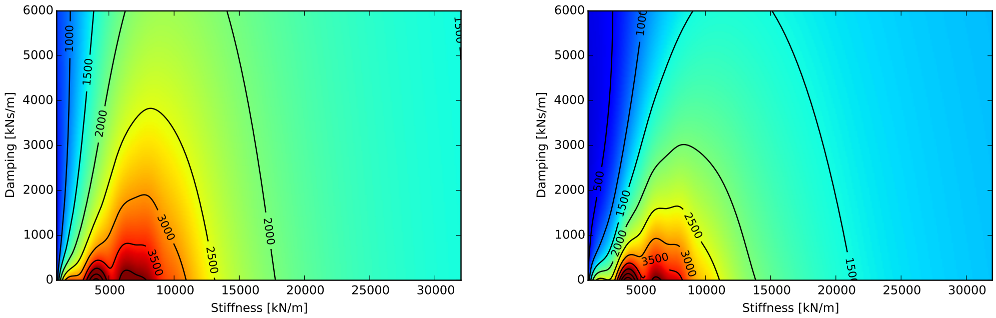

(a) Force spring/dashpot 3 [kN] (b) Force spring/dashpot 4 [kN]

FIGURE 5.12: Combined spring/dashpot forces in [kN] x_3=240[m], x_4=30[m], z=9[m]

these combined forces drop. For example, at a damping 2000[kNs/m] the peak forces drop from 5000[kN] to 2500 [kN] for spring/dashpot 4.

The natural frequency of the system shifts to the right when applying more damping. This can be noticed in figure 5.12. The peaks of the contour lines tend to move to the right. This phenomena is explained by the fact that the damped natural frequency is slightly different from the natural frequency and changes with the amount of damping. The higher the damping the smaller the damped natural frequency and so it shifts away from the resonance frequency. Damping takes energy out of the system, that is why forces and motion become lower around the natural frequency when more damping is applied.

In order to gain insight about the amount of damping used it is compared to the critical damping. Critical damping provides the quickest approach to zero amplitude for a damped oscillator. The theory of critical damping only holds for a single degree of freedom system and therefore the critical damping is calculated only for sway this is done using equation 5.1. The added mass term is frequency dependent and therefore changes for every frequency. To get an estimation of the critical damping the average of all the sway added mass terms is taken from appendix D. The average sway added mass for a wave height of 1[m] is equal to 50500[ton]. The mass of the vessel is known and equal to 41241[ton]. For the stiffness two springs of 12000[kN/m] are used and so together there is a stiffness of 24000[kN/m]. This estimation leads to a critical damping of 93846[kNs/m]. However this is an estimation it is clear that the damping considered (2500[kN/m]) in this research is only a fraction of the critical damping of the system.

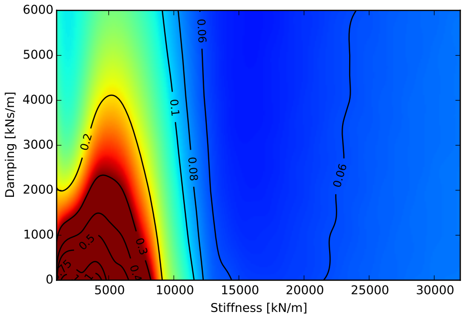

(a) Motion in point 2[m]

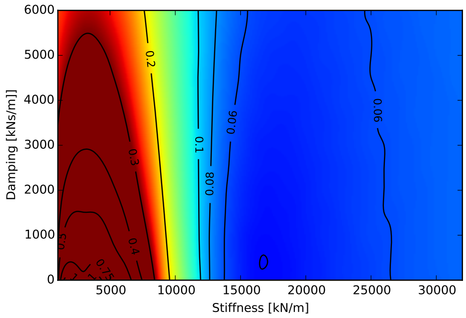

(b) Motion in point 4[m]

FIGURE 5.13: Motion in the outer contact points in [m](x_3=240[m], x_4=30[m], z=9[m])

Since the amount of damping used is smaller than the critical damping the system is under damped.

$$C_{critical} = 2\sqrt{(M_{Jasmine} + A)K} \tag{5.1}$$

The influence of damping to the system's behaviour is huge. During the resonance frequencies the combined spring/damper force drops almost half by only adding 2500[kN-s/m] of damping see figure 5.13. The motion in the outer contact points drop from 1[m] to 0.43[m]for point 4 and 0.30[m] for point 2. Therefore this research suggests to include structural damping in the relative motion reduction system. By adding damping to the system the optimal location of the spring damper system changes. This behaviour can be observed from the graphs in appendix C.2. The amount of stiffness necessary doesn't change significantly, but the optimal longitudinal location of spring/damper 4 moves towards the COG. This is not further studied in this research because the damping would mainly be used in order to reduce the motions during the installation of the connections.

Chapter 6

Discussion

In this chapter the results are discussed as the numerical model is based on assumptions. These assumptions were necessary to come up with a system that would be able to run thousands of calculations in a relatively short amount of time. Effort is taken to make these assumptions explicit throughout this report. The achieved output of the numerical model is discussed at the end of this chapter.

The choice for the West-African region and the combination of the Jasmine and Vanguard vessels provides this research to be relevant to the smaller FPSO vessels and relatively calm swell conditions. Since there is no room for trial and error in the offshore industry, the design approach is to find a system that works on a smaller FPSO in these relatively calm swell conditions. With the lessons learned from the first real offshore load/discharge operation it might be scaled up to the larger FPSO vessels.

Based on the results it can be stated that if the roll motion is in phase with the sway motion their combined transverse motion is less in the points at keel level. Therefore a lower spring stiffness might be applicable. However this might give a distorted picture as the vertical motions will also play a roll in the overall behaviour of the vessels. The allowed roll motion compensating the sway motion could have a bad influence on the vertical motion at the side of the vessel.

The coupling between roll and sway allows the system to use less stiffness. This raises the question if this would be applicable to surge and pitch coupling? Surge and pitch are the same way related as sway and roll, however the length/width ratio makes it different. Pitch and roll are both coupled to the heave motion and therefore have influence on the vertical motion of the vessel. Since pitch has influence over the length of the vessel, even a small angle will cause a noticeable vertical displacement at the stern or bow of the vessel.

The mooring system has been taken into account in this research but less attention is given. The stiffness used for the springs to get the relative transverse motion within 0.1[m] are a factor 100 higher than the mooring stiffness. Therefore this relatively soft system didn't have much influence.

In this research the results presented are based on the significant waves and not on the extreme. Usually the most probable maximum (MPM) wave is taken into account during the design of an offshore structure. This is the expected single highest wave that passes during a certain period. This MPM wave is used to design a system that will be strong enough to withstand all the waves. In this research the objective is to reduce the relative motions within 0.1[m]. With this significant wave approach, the system might excite more than the given margin of 0.1[m]. However when this wave passed away, the system shall be within the limit of 0.1[m] again. During the operation there will be a critical moment were this MPM wave would cause problems. This moment might be only a small period of time and therefore it might not be necessary to design the system to be within this 0.1[m] margin through the entire operation. The system should however be build that it can handle the MPM wave forces.

The viscous roll damping has been neglected in the python script. This is based on the assumption that the designed system would have large natural frequencies so that they are far away from the wave frequency. However in the final design the springs are connected at a height of 9[m]. The roll natural frequency is therefore around 0.7 [rad/s]. At this frequency the wave spectrum has passed its peak but there is still a noticeable amount left. Including the viscous roll damping should have influence on the output values but not on the conclusions. Therefore it would have been better to include the viscous roll damping but the conclusions about the interdependence of the stiffness, damping and location of the spring/dashpot systems would have been similar.

Chapter 7

Conclusion

7.1 Conclusion

The focus of this research is to find a system to control the transverse relative motions between the SHTV and the FPSO. Until today this load/discharge operation can only take place in a sheltered area like a harbour, a fjord or a bay. If an SHTV would be able to load and discharge outside sheltered places (offshore), then a new market in the oil and gas industry can be created. The difficulty with this offshore operation is the environmental loading. The main objective is to gain insight in the interaction between the two vessels trough their connections in order to design a relative motion reduction system. The approach of this thesis is to run a 3DOF analysis in the frequency domain to understand the interdependence between sway, roll and yaw motion influenced by two transverse spring/dashpot systems. A script has been written in Python to execute the calculation of the equation of motions for 208.000 combinations of spring stiffness, damping and their location. Based on the results of the numerical model the three sub questions and finally the research question stated in chapter 1.4 can be answered:

All of the 3 DOF motions that have been investigated have influence on the transverse motion in the outer contact points to the cribbing. The sway motion is in the transverse direction and therefore it is not influenced by the location of the spring/dashpot system. The roll motion acts on both outer contact points to the cribbing in the same lateral plane. The roll component to the transverse motion is equal in both outer contact points. From the results it is learned that the roll motion is in phase with the sway motion. This means, whenever the vessel moves to the right due to sway, the vessel rolls to the right due to roll. At the outer contact points, which are located at keel level, the roll motion counters some of the sway motion. The vertical location of the springs has been varied between 9[m] and 0[m]. The results show that the best vertical location for the springs varies from 9[m] to 3[m] for medium to higher stiffnesses. To obtain the minimum required stiffness the springs should be located at 9[m].

The explanation for this is that whenever the stiffness goes up to the highest stiffnesses it reduces the motions the most if the springs are located at the resultant wave force. The yaw motion acts on both outer contact points to the cribbing in a different lateral plane. So if one outer contact point moves to the right the other moves to the left. Since the yaw component of the transverse motion in the two outer contact points are in counter phase, the yaw cannot be used to reduce the transverse motion in both of these points. Therefore an approach should be used to minimise the yaw component as much as possible but keep the yaw components to the outer contact points equal. In other words the aim should be to let the outer contact points yaw around the centre point between them with the longest arm possible to the spring/dashpot systems. During the offshore load/ discharge operation the FPSO is assumed to stay connected to its mooring system. It is advised to perform the load/discharge operation on an external turret moored FPSO in stead of an internal turret moored FPSO. The external turret moored FPSO will protrude less and so the motion reduction system is less difficult to connect to the bow. For this reason the yaw component to the transverse motion is easier to reduce during the operation with an external turret moored FPSO.

After examining every stiffness from 1000 to 32000[kN/m] in steps of 1000[kN/m], it has been found that 12000[kN/m] is the minimum amount of stiffness necessary to get both keel points within 0.1[m] significant motion. This is only possible if the springs are connected to their optimal location. In this case the front spring should be at 240[m] longitudinal and 9[m] vertical, the spring at the stern should be connected at 30[m] longitudinal and 9[m] vertical. The combination of these locations provides the yaw component to be as small as possible and the roll component to be in phase with the sway motion so it cancels some transverse motion. Since this research is based on a parametric study this is the optimal point that has been found through calculations. The absolute minimum value might be lower if an optimisation algorithm is used and the points around the found optimum are investigated.

The damping has most influence during the resonance frequencies. When the system gets through these frequencies during the installation of the springs large motions and forces will occur. Only a fraction of the critical damping is sufficient to reduce the motions and the combined spring/damper forces of the FPSO during resonance. Therefore it is strongly suggested to use structural damping in the design of the relative motion reduction system. A damper of 2000[kNs/m] at each spring location seems suitable. With this system the significant forces are expected to be around 2500[kN]. When the damping is added to the system the optimal location for the spring/damper systems change and can therefore be further optimised.

After examining multiple stiffnesses and locations of the springs, insight is gained about the influence of the spring location and stiffness on the relative motions between an FPSO and SHTV. It is found possible to get the transverse motions at keel level within the limits of the cribbing. By positioning the spring/dashpot systems in the corresponding optimal location the minimum required stiffness can be reduced. In search for the optimal point the yaw component is reduced as much as possible and the roll component is in phase with the sway motion to neutralise some transverse motion. In order to get safely through the resonance frequencies during installation of the spring system it is advised to add structural damping to the system. A fraction of the critical damping at each spring location appears to be adequate in reducing the motions and forces during resonance. The significant forces in both spring/dashpot locations are very high but workable.

7.2 Future research

To improve the numerical model and make it better applicable to reality, three steps of research are identified and discussed below.

1. The first step would be to include surge, heave and pitch in the numerical model. The influence of the roll motion on the vertical motion can be investigated. From this analysis conclusions can be made if the roll motion could really be used to counter a part of the sway motion in the contact points at the keel.
2. The second step would be to calculate and import the hydrodynamic data of the SHTV and include the sway, roll and yaw motions of the SHTV in the numerical

model. Both vessels move in 3 DOF and are influenced by the incoming waves and the connections in between. A new set of equations of motions should be derived and solved in the numerical model. This step could be taken to gain insight in the interaction through these connections.

3. The third step would be to build a model in Ansys AQWA where all 12 degrees of freedom are included. The wave reflections, wave radiation and small gap influences could be taken into account. This will be a computational demanding model and therefore it is advised to perform the previous steps first in order to fully understand the system before building a complex model

Appendix A

Vanguard specifications

EQUIPMENT SHEET

DOCKWISE VANGUARD
SEMI SUBMERSIBLE HEAVY LIFT VESSEL

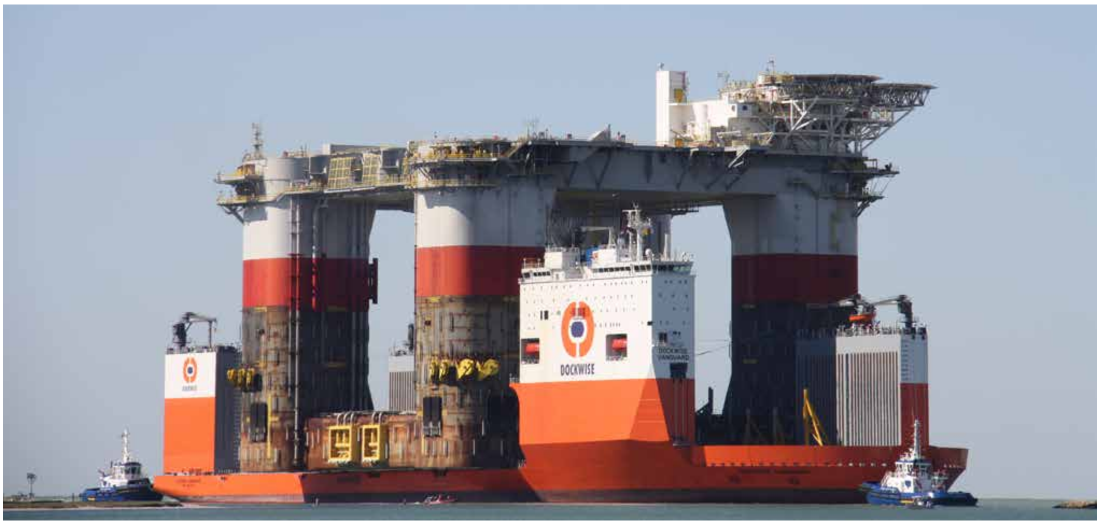

CONSTRUCTION/CLASSIFICATION

Built by	Hyundai Heavy Industries
Year of construction	2012
Classification	DNV, X1A1 Semi-Submersible Heavy Lift Vessel RP, E0, CLEAN, DK(+), BIS, PWDK
IMO number	9618783
Call sign (flag)	PBDI (Curacao)

MAIN DATA

Length overall	275.00 m
Breadth moulded/max	70.00 m / 78.75 m
Depth	15.50 m
Draft submerged at FPP/APP	31.50 / 31.50 m
Summer draft (B-100)	10.94 m
Deck Space [L x B]	275.00 x 70.00 m
Deadweight	116,175 mt
Trial speed	14.50 kn
Total installed power	28,500 kW
Main Engines	2 x 8,700 kW and 2 x 4,350 kW
Main Propulsion	2 x 12 MW CPP propellers
Azimuth thrusters	2 x 3,000 kW Retractable with CPP propellers
Bow thruster	1 x 3,000 kW with CPP

NAVIGATION EQUIPMENT

- 2 pcs DGPS
- 1 pcs Doppler speed log
- 2 pcs echo sounder
- 1 pcs navtex
- 1 pcs weatherfax
- 2 pcs ECDIS
- 2 pcs radar
- 1 pcs dual Gyro compass
- SPOS – Ship Performance Optimisation System
- OCTOPUS - Octopus Onboard System (ship motion monitoring and decision support system by Amarcon)

COMMUNICATIONS EQUIPMENT

- Fully compliant with GMDSS A-3
- 1 pcs MF/HF radio station
- 1 pcs Inmarsat Broadband
- 2 pcs Inmarsat-C
- 1 pcs SSAS
- 1 pcs AIS
- 4 pcs VHF-DSC
- 2 pcs EPIRB
- 2 pcs SART
- 3 pcs VHF handheld
- 10 pcs UHF handheld
- 1 pcs VSAT

BALLASTING

- 4 main ballast pumps 5300 m³/hr@ 50 m
- 1 ballast pump 1500 m³/hr@ 50 m
- 2 stripping pumps 400 m³/hr@ 70 m
- 2 stripping ejectors 300 m³/hr@ 20 m

Appendix B

Environmental data

B.1 Wave roses for the coast of Brazil

hydronamic

Offshore wave roses and workability

Boskalis

Offshore wave roses and workability for total wave height (sea and swell)

Coordinate: *15.0°S 36.00°W*
Depth: *4399m*
Samples: *24836 samples (1997.1.1−2013.12.31)*
Database: *WorldWaves offshore database (February 2015)*

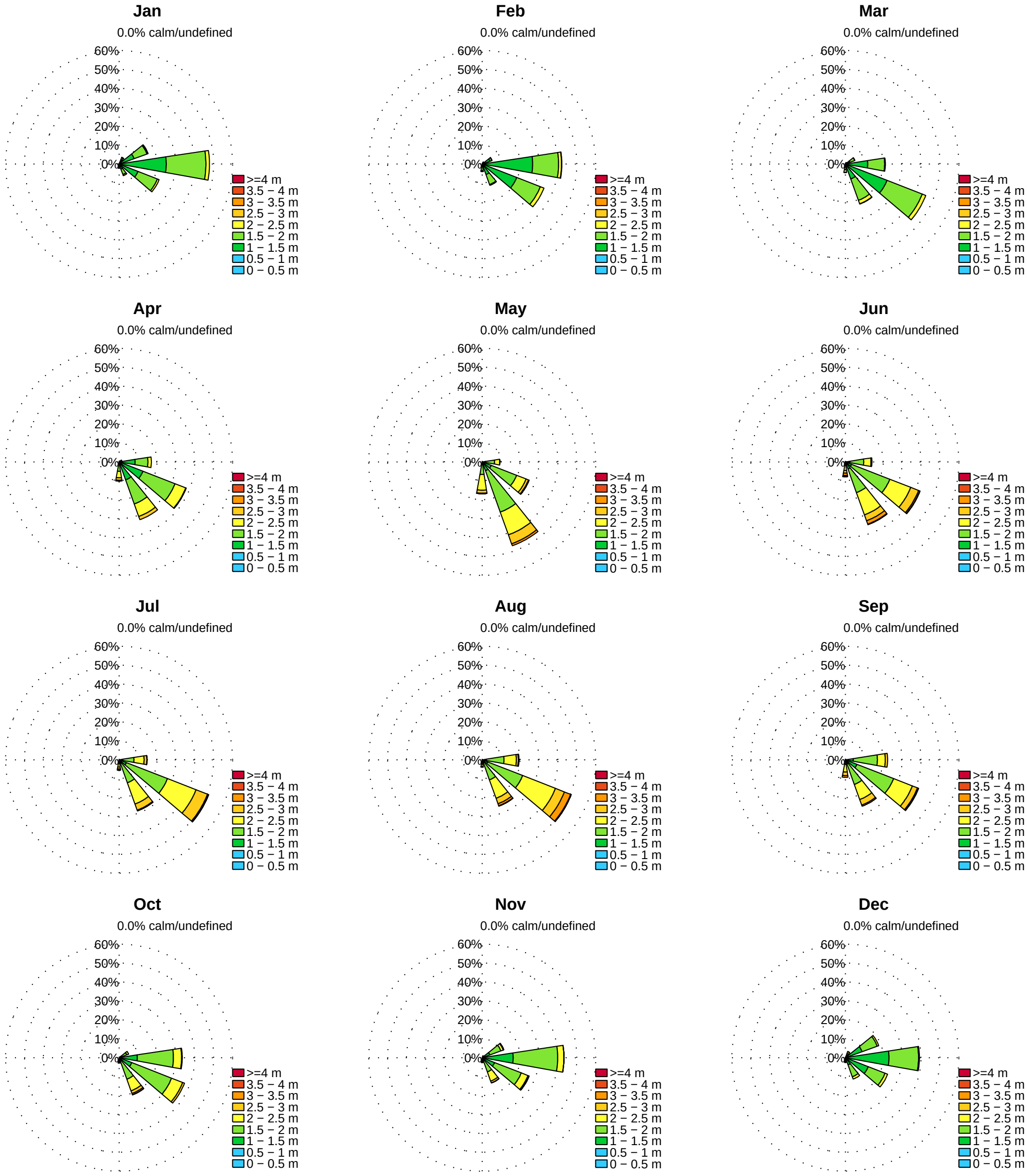

Workability [%]

	Jan	Feb	Mar	Apr.	May	Jun	Jul	Aug	Sep	Oct	Nov	Dec	year
H_s=0.50m	0	0	0	0	0	0	0	0	0	0	0	0	0
H_s=0.75m	0	0	0	0	0	0	0	0	0	0	0	0	0
H_s=1.00m	2	4	2	1	0	0	0	0	0	0	1	2	1
H_s=1.50m	50	60	50	35	13	11	9	7	15	21	31	52	29
H_s=2.00m	94	95	94	78	62	55	51	48	62	77	83	94	74
H_s=2.50m	99	100	100	96	90	85	86	84	89	96	97	100	93
H_s=3.00m	100	100	100	100	98	95	98	94	98	99	100	100	98
H_s=3.50m	100	100	100	100	100	99	100	99	100	100	100	100	100

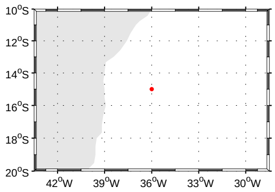

− Input time series: *g:\WERKBAARHEID\Worldwaves\data\offshore_points\2015\wave\world\extracted\Dat_files\ww15_offshore_15.0S_036.0W.dat*
− m−file: *G:\matlab\GSAL\Matlab\MetOcean_MATLAB_20150422\Plot_wave_wind_roses\plot_wave_wind_roses_2014_v2.m*
− print date: *25−Apr−2015 02:12:35*

B.2 Wave roses for the coast of West-Africa

hydronamic

Offshore wave roses and workability

Boskalis

Offshore wave roses and workability for total wave height (sea and swell)

Coordinate: *0.0°S 3.00°E*
Depth: *4420m*
Samples: *24836 samples (1997.1.1−2013.12.31)*
Database: *WorldWaves offshore database (February 2015)*

Workability [%]

	Jan	Feb	Mar	Apr.	May	Jun	Jul	Aug	Sep	Oct	Nov	Dec	year
H_s=0.50m	0	0	0	0	0	0	0	0	0	0	0	0	0
H_s=0.75m	0	0	0	0	0	0	0	0	0	0	0	0	0
H_s=1.00m	19	19	7	1	0	0	1	0	1	2	3	14	6
H_s=1.50m	92	93	82	61	41	36	36	34	42	60	73	89	61
H_s=2.00m	100	100	99	96	87	86	85	78	87	94	97	100	92
H_s=2.50m	100	100	100	100	99	99	98	95	97	99	100	100	99
H_s=3.00m	100	100	100	100	100	100	100	99	100	100	100	100	100
H_s=3.50m	100	100	100	100	100	100	100	100	100	100	100	100	100

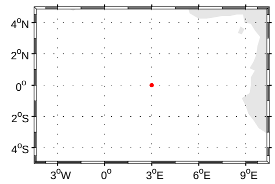

− **Input time series:** *g:\WERKBAARHEID\Worldwaves\data\offshore_points\2015\wave\world\extracted\Dat_files\ww15_offshore_00.0N_003.0E.dat*
− **m−file:** *G:\matlab\GSAL\Matlab\MetOcean_MATLAB_20150422\Plot_wave_wind_roses\plot_wave_wind_roses_2014_v2.m*
− **print date:** *24−Apr−2015 13:59:52*

B.3 Wind roses for the coast of West-Africa

hydronamic

Offshore Wind roses and Workability

Boskalis

Offshore wind roses and workability

Coordinate:	*0.0°S 3.00°E*
Depth:	*4420m*
Samples:	*24836 samples (1997.1.1−2013.12.31)*
Database:	*WorldWaves offshore database (February 2015)*

Workability [%]

	Jan	Feb	Mar	Apr.	May	Jun	Jul	Aug	Sep	Oct	Nov	Dec	year
U<1.6m/s (<=Bft.1)	22	23	20	18	8	3	3	3	3	6	9	18	11
U<3.4m/s (<=Bft.2)	40	39	38	32	15	5	5	6	5	9	15	30	20
U<5.5m/s (<=Bft.3)	86	87	85	77	55	38	40	40	35	45	61	79	61
U<8.0m/s (<=Bft.4)	100	100	100	98	96	95	96	96	96	97	99	99	98
U<10.8m/s (<=Bft.5)	100	100	100	100	100	100	100	100	100	100	100	100	100
U<13.9m/s (<=Bft.6)	100	100	100	100	100	100	100	100	100	100	100	100	100
U<17.2m/s (<=Bft.7)	100	100	100	100	100	100	100	100	100	100	100	100	100
U<20.8m/s (<=Bft.8)	100	100	100	100	100	100	100	100	100	100	100	100	100

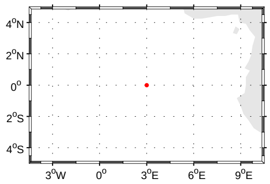

− Input time series: *g:\WERKBAARHEID\Worldwaves\data\offshore_points\2015\wave\world\Dat_files\ww15_offshore_00.0N_003.0E.dat*
− m−file: *G:\matlab\GSAL\Matlab\MetOcean_MATLAB_20150422\Plot_wave_wind_roses\plot_wave_wind_roses_2014_v2.m*
− print date: *29−Apr−2015 10:41:01*

B.4 Workability West Africa in January

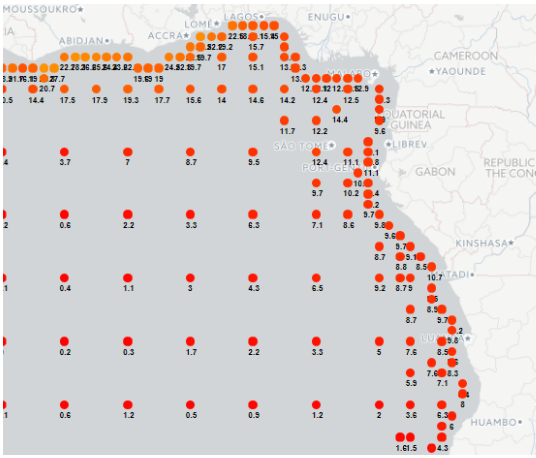

(a) $H_s = 1.0, T_p = 10$

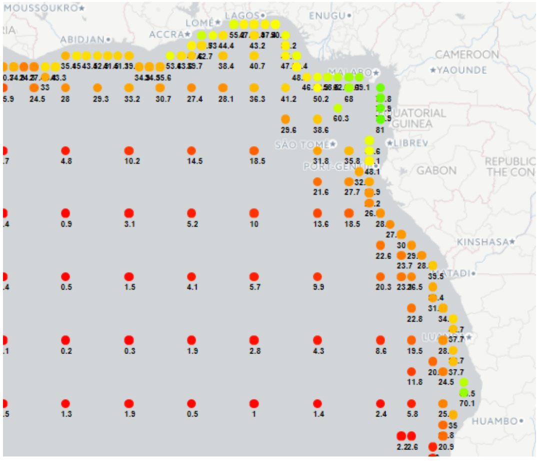

(b) $H_s = 1.0, T_p = 14$

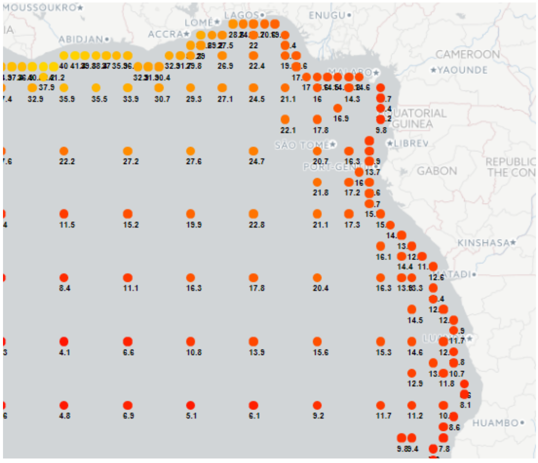

(c) $H_s = 1.25, T_p = 10$

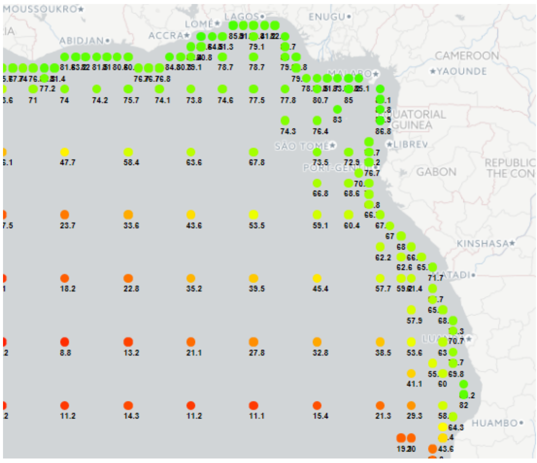

(d) $H_s = 1.25, T_p = 14$

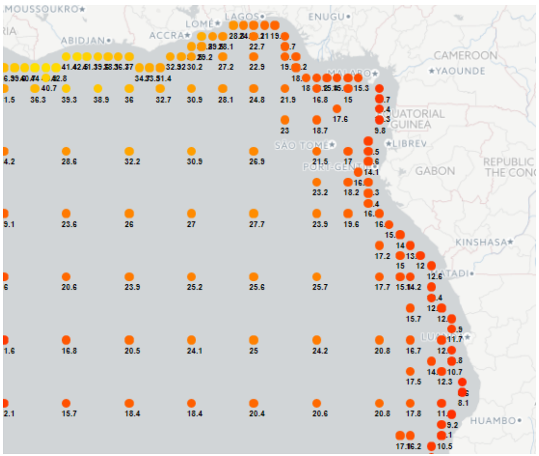

(e) $H_s = 1.5, T_p = 10$

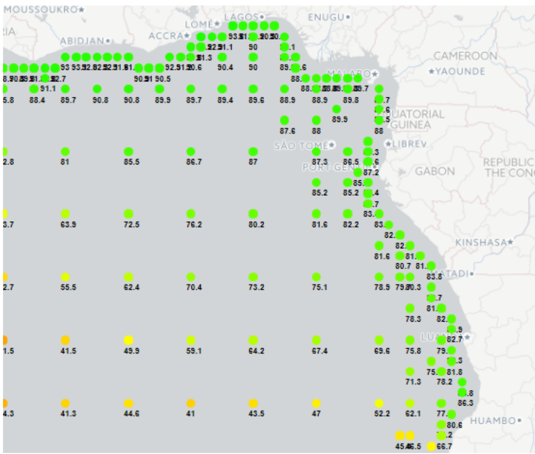

(f) $H_s = 1.5, T_p = 14$

FIGURE B.1: Workability West Africa January

Appendix C

Minimal required stiffness

C.1 Minimum stiffness for different spring heights

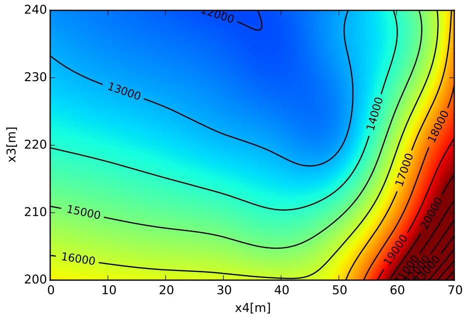

(a) $z = 9$[m]

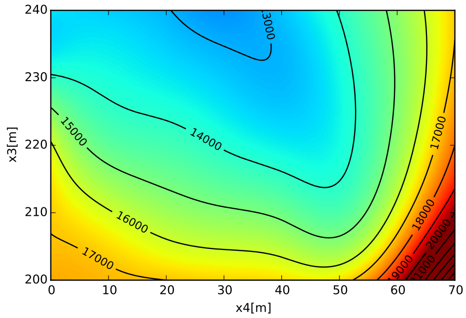

(b) $z = 8$[m]

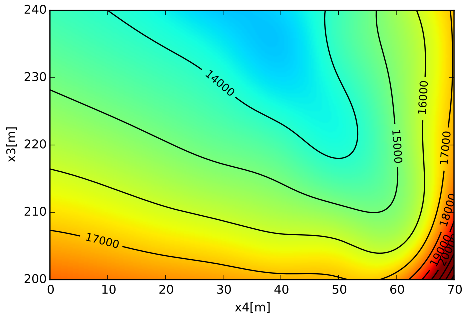

(c) $z = 7$[m]

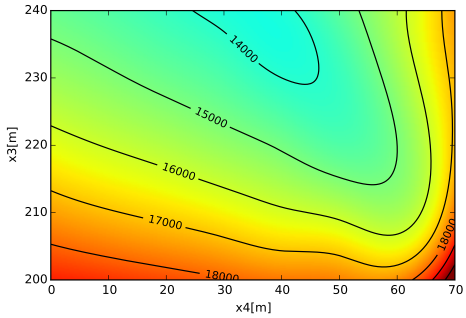

(d) $z = 6$[m]

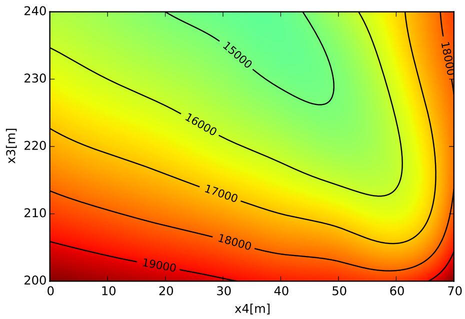

(e) $z = 5$[m]

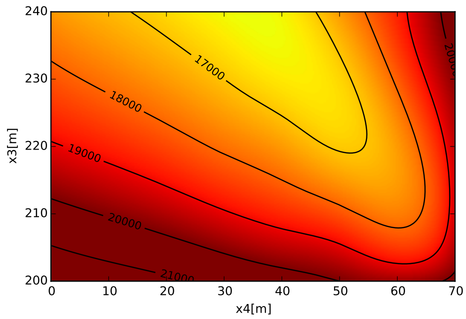

(f) $z = 4$[m]

FIGURE C.1: Minimum stiffness for different spring height in [kN/m]

C.2 Minimum stiffness including damping

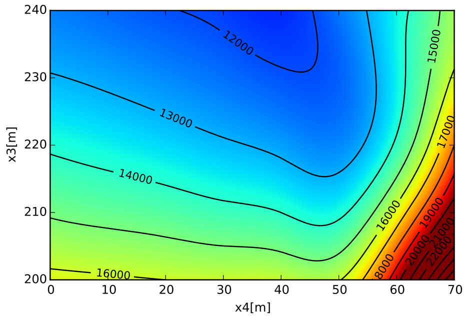

(a) $C = 1000$[kNs/m]

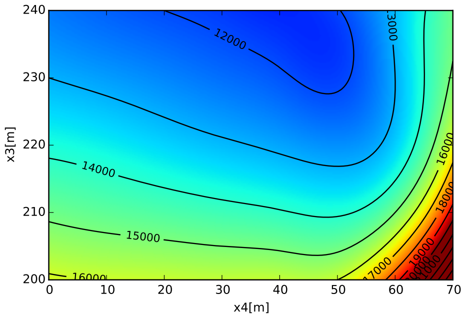

(b) $C = 2000$[kNs/m]

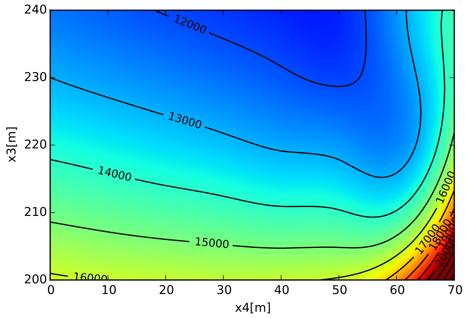

(c) $C = 3000$[kNs/m]

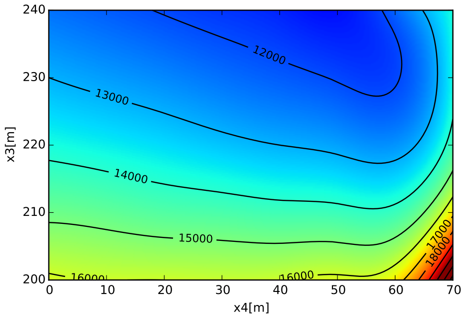

(d) $C = 4000$[kNs/m]

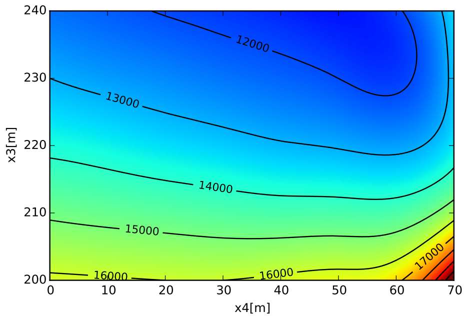

(e) $C = 5000$[kNs/m]

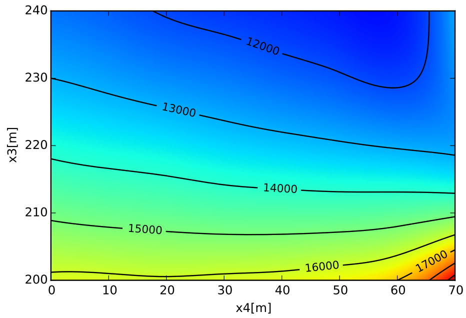

(f) $C = 6000$[kNs/m]

FIGURE C.2: Minimum stiffness including damping at z=9[m]

Appendix D

Hydrodynamic data from Octopus Seaway

MOTIONCOEFFICIENTS AND WAVE-LOADS

FORWARD SPEED = 0.00 kn
WAVE DIRECTION = +210 deg off stern

SURGE EQUATION

SQRT	ENC	.............SURGE.............			.......COUPLING TO HEAVE.......			.......COUPLING TO PITCH.......			WAVE-MOMENT	
SL/WL	FREQ	MASS	DAMPING	RESTORING	MASS	DAMPING	RESTORING	MASS	DAMPING	RESTORING	AMPL	PHASE
(-)	(r/s)	(kN*s2/m/m	(kN*s/m/m)	(kN/m/m)	(kN*s2/m/m	(kN*s/m/m)	(kN/m/m)	(kN*s2/m)	(kN*s/m)	(kN/m)	(kN/m)	(deg)
0.100	0.05	5.22E+04	1.04E+00	0.00E+00	0.00E+00	0.00E+00	0.00E+00	-9.16E+04	-8.66E+00	0.00E+00	1.13E+02	270.0
0.201	0.10	5.28E+04	3.28E+01	0.00E+00	0.00E+00	0.00E+00	0.00E+00	-9.65E+04	-2.73E+02	0.00E+00	4.53E+02	269.6
0.301	0.15	5.35E+04	1.95E+02	0.00E+00	0.00E+00	0.00E+00	0.00E+00	-1.02E+05	-1.63E+03	0.00E+00	1.02E+03	268.4
0.402	0.20	5.38E+04	5.79E+02	0.00E+00	0.00E+00	0.00E+00	0.00E+00	-1.05E+05	-4.83E+03	0.00E+00	1.79E+03	266.7
0.502	0.25	5.33E+04	1.12E+03	0.00E+00	0.00E+00	0.00E+00	0.00E+00	-1.00E+05	-9.34E+03	0.00E+00	2.64E+03	265.0
0.602	0.30	5.23E+04	1.65E+03	0.00E+00	0.00E+00	0.00E+00	0.00E+00	-9.19E+04	-1.38E+04	0.00E+00	3.45E+03	264.1
0.703	0.35	5.12E+04	2.06E+03	0.00E+00	0.00E+00	0.00E+00	0.00E+00	-8.30E+04	-1.72E+04	0.00E+00	4.05E+03	264.3
0.803	0.40	5.03E+04	2.34E+03	0.00E+00	0.00E+00	0.00E+00	0.00E+00	-7.53E+04	-1.95E+04	0.00E+00	4.24E+03	265.7
0.904	0.45	4.95E+04	2.50E+03	0.00E+00	0.00E+00	0.00E+00	0.00E+00	-6.91E+04	-2.08E+04	0.00E+00	3.85E+03	268.9
1.004	0.50	4.89E+04	2.57E+03	0.00E+00	0.00E+00	0.00E+00	0.00E+00	-6.41E+04	-2.14E+04	0.00E+00	2.80E+03	276.0
1.104	0.55	4.84E+04	2.58E+03	0.00E+00	0.00E+00	0.00E+00	0.00E+00	-6.00E+04	-2.15E+04	0.00E+00	1.29E+03	302.7
1.205	0.60	4.80E+04	2.57E+03	0.00E+00	0.00E+00	0.00E+00	0.00E+00	-5.65E+04	-2.15E+04	0.00E+00	1.38E+03	42.0
1.305	0.65	4.77E+04	2.57E+03	0.00E+00	0.00E+00	0.00E+00	0.00E+00	-5.36E+04	-2.14E+04	0.00E+00	2.90E+03	67.2
1.406	0.70	4.74E+04	2.58E+03	0.00E+00	0.00E+00	0.00E+00	0.00E+00	-5.14E+04	-2.16E+04	0.00E+00	3.62E+03	75.6
1.506	0.75	4.72E+04	2.61E+03	0.00E+00	0.00E+00	0.00E+00	0.00E+00	-5.01E+04	-2.18E+04	0.00E+00	2.98E+03	83.6
1.606	0.80	4.72E+04	2.61E+03	0.00E+00	0.00E+00	0.00E+00	0.00E+00	-4.94E+04	-2.18E+04	0.00E+00	1.21E+03	108.5
1.707	0.85	4.71E+04	2.56E+03	0.00E+00	0.00E+00	0.00E+00	0.00E+00	-4.89E+04	-2.13E+04	0.00E+00	1.41E+03	231.0
1.807	0.90	4.70E+04	2.48E+03	0.00E+00	0.00E+00	0.00E+00	0.00E+00	-4.83E+04	-2.07E+04	0.00E+00	2.59E+03	250.7
1.907	0.95	4.69E+04	2.42E+03	0.00E+00	0.00E+00	0.00E+00	0.00E+00	-4.76E+04	-2.02E+04	0.00E+00	2.06E+03	261.3
2.008	1.00	4.69E+04	2.40E+03	0.00E+00	0.00E+00	0.00E+00	0.00E+00	-4.70E+04	-2.01E+04	0.00E+00	4.47E+02	326.0
2.108	1.05	4.69E+04	2.38E+03	0.00E+00	0.00E+00	0.00E+00	0.00E+00	-4.69E+04	-1.99E+04	0.00E+00	1.54E+03	65.8
2.209	1.10	4.69E+04	2.31E+03	0.00E+00	0.00E+00	0.00E+00	0.00E+00	-4.68E+04	-1.93E+04	0.00E+00	1.48E+03	81.3
2.309	1.15	4.68E+04	2.25E+03	0.00E+00	0.00E+00	0.00E+00	0.00E+00	-4.64E+04	-1.88E+04	0.00E+00	3.97E+02	174.8
2.409	1.20	4.68E+04	2.30E+03	0.00E+00	0.00E+00	0.00E+00	0.00E+00	-4.61E+04	-1.92E+04	0.00E+00	1.26E+03	246.7
2.510	1.25	4.69E+04	2.33E+03	0.00E+00	0.00E+00	0.00E+00	0.00E+00	-4.69E+04	-1.94E+04	0.00E+00	7.50E+02	277.4
2.610	1.30	4.70E+04	2.06E+03	0.00E+00	0.00E+00	0.00E+00	0.00E+00	-4.79E+04	-1.72E+04	0.00E+00	8.16E+02	48.0
2.711	1.35	4.68E+04	1.68E+03	0.00E+00	0.00E+00	0.00E+00	0.00E+00	-4.63E+04	-1.40E+04	0.00E+00	8.77E+02	81.1
2.811	1.40	4.64E+04	1.81E+03	0.00E+00	0.00E+00	0.00E+00	0.00E+00	-4.34E+04	-1.51E+04	0.00E+00	4.98E+02	196.4
2.911	1.45	4.64E+04	2.49E+03	0.00E+00	0.00E+00	0.00E+00	0.00E+00	-4.31E+04	-2.08E+04	0.00E+00	8.29E+02	244.4
3.012	1.50	4.69E+04	2.86E+03	0.00E+00	0.00E+00	0.00E+00	0.00E+00	-4.68E+04	-2.38E+04	0.00E+00	4.95E+02	350.0
3.112	1.55	4.72E+04	2.38E+03	0.00E+00	0.00E+00	0.00E+00	0.00E+00	-4.97E+04	-1.98E+04	0.00E+00	7.73E+02	57.3
3.213	1.60	4.72E+04	1.83E+03	0.00E+00	0.00E+00	0.00E+00	0.00E+00	-4.96E+04	-1.53E+04	0.00E+00	4.38E+02	167.3
3.313	1.65	4.71E+04	1.51E+03	0.00E+00	0.00E+00	0.00E+00	0.00E+00	-4.90E+04	-1.26E+04	0.00E+00	5.32E+02	234.9
3.413	1.70	4.70E+04	1.16E+03	0.00E+00	0.00E+00	0.00E+00	0.00E+00	-4.77E+04	-9.67E+03	0.00E+00	3.96E+02	358.1
3.514	1.75	4.67E+04	1.15E+03	0.00E+00	0.00E+00	0.00E+00	0.00E+00	-4.56E+04	-9.63E+03	0.00E+00	2.59E+02	66.3
3.614	1.80	4.67E+04	1.64E+03	0.00E+00	0.00E+00	0.00E+00	0.00E+00	-4.59E+04	-1.36E+04	0.00E+00	4.05E+02	188.3
3.715	1.85	4.64E+04	1.47E+03	0.00E+00	0.00E+00	0.00E+00	0.00E+00	-4.27E+04	-1.23E+04	0.00E+00	1.58E+02	312.5
3.815	1.90	4.62E+04	2.34E+02	0.00E+00	0.00E+00	0.00E+00	0.00E+00	-4.15E+04	-1.95E+03	0.00E+00	2.59E+02	23.2
3.915	1.95	4.69E+04	-1.44E+02	0.00E+00	0.00E+00	0.00E+00	0.00E+00	-4.74E+04	1.20E+03	0.00E+00	2.64E+02	182.2
4.016	2.00	4.69E+04	-8.17E+00	0.00E+00	0.00E+00	0.00E+00	0.00E+00	-4.69E+04	6.81E+01	0.00E+00	8.27E+01	286.8
4.116	2.05	4.66E+04	-2.02E-01	0.00E+00	0.00E+00	0.00E+00	0.00E+00	-4.45E+04	1.69E+00	0.00E+00	1.61E+02	16.0
4.217	2.10	4.61E+04	2.16E-02	0.00E+00	0.00E+00	0.00E+00	0.00E+00	-4.04E+04	-1.80E-01	0.00E+00	1.69E+02	174.2
4.317	2.15	4.96E+04	2.69E-02	0.00E+00	0.00E+00	0.00E+00	0.00E+00	-7.01E+04	-2.25E-01	0.00E+00	1.99E+02	331.5
4.417	2.20	5.64E+04	2.33E-02	0.00E+00	0.00E+00	0.00E+00	0.00E+00	-1.27E+05	-1.94E-01	0.00E+00	2.22E+02	55.4
4.518	2.25	5.85E+04	1.62E-02	0.00E+00	0.00E+00	0.00E+00	0.00E+00	-1.44E+05	-1.35E-01	0.00E+00	4.85E+02	183.1
4.618	2.30	5.85E+04	1.62E-02	0.00E+00	0.00E+00	0.00E+00	0.00E+00	-1.44E+05	-1.35E-01	0.00E+00	4.84E+02	338.8
4.719	2.35	5.85E+04	1.62E-02	0.00E+00	0.00E+00	0.00E+00	0.00E+00	-1.44E+05	-1.35E-01	0.00E+00	3.05E+02	134.1
4.819	2.40	5.85E+04	1.62E-02	0.00E+00	0.00E+00	0.00E+00	0.00E+00	-1.44E+05	-1.35E-01	0.00E+00	1.33E+02	261.2
4.919	2.45	5.85E+04	1.62E-02	0.00E+00	0.00E+00	0.00E+00	0.00E+00	-1.44E+05	-1.35E-01	0.00E+00	1.98E+02	14.0
5.020	2.50	5.85E+04	1.62E-02	0.00E+00	0.00E+00	0.00E+00	0.00E+00	-1.44E+05	-1.35E-01	0.00E+00	2.91E+02	178.8

MOTIONCOEFFICIENTS AND WAVE-LOADS

FORWARD SPEED = 0.00 kn
WAVE DIRECTION = +210 deg off stern

SWAY EQUATION

SQRT	ENC	..............SWAY.............			.......COUPLING TO ROLL........			........COUPLING TO YAW........			WAVE-MOMENT	
SL/WL	FREQ	MASS	DAMPING	RESTORING	MASS	DAMPING	RESTORING	MASS	DAMPING	RESTORING	AMPL	PHASE
(-)	(r/s)	(kN*s2/m/m)	(kN*s/m/m)	(kN/m/m)	(kN*s2/m)	(kN*s/m)	(kN/m)	(kN*s2/m)	(kN*s/m)	(kN/m)	(kN/m)	(deg)
0.100	0.05	5.88E+04	5.29E-02	0.00E+00	-1.06E+05	-6.06E-01	0.00E+00	-1.69E+04	-2.91E-01	0.00E+00	7.34E+01	270.0
0.201	0.10	5.91E+04	1.94E+00	0.00E+00	-1.07E+05	-2.07E+01	0.00E+00	-1.66E+04	2.35E+00	0.00E+00	2.94E+02	270.0
0.301	0.15	5.94E+04	1.41E+01	0.00E+00	-1.10E+05	-1.48E+02	0.00E+00	-1.58E+04	1.87E+01	0.00E+00	6.59E+02	269.9
0.402	0.20	6.00E+04	5.71E+01	0.00E+00	-1.15E+05	-5.95E+02	0.00E+00	-1.47E+04	8.02E+01	0.00E+00	1.16E+03	269.7
0.502	0.25	6.06E+04	1.69E+02	0.00E+00	-1.20E+05	-1.72E+03	0.00E+00	-1.31E+04	2.52E+02	0.00E+00	1.77E+03	269.3
0.602	0.30	6.14E+04	4.03E+02	0.00E+00	-1.25E+05	-4.03E+03	0.00E+00	-1.12E+04	6.50E+02	0.00E+00	2.42E+03	268.7
0.703	0.35	6.22E+04	8.26E+02	0.00E+00	-1.30E+05	-8.03E+03	0.00E+00	-8.95E+03	1.45E+03	0.00E+00	3.02E+03	267.8
0.803	0.40	6.28E+04	1.50E+03	0.00E+00	-1.32E+05	-1.41E+04	0.00E+00	-6.75E+03	2.89E+03	0.00E+00	3.40E+03	266.5
0.904	0.45	6.31E+04	2.45E+03	0.00E+00	-1.31E+05	-2.23E+04	0.00E+00	-5.09E+03	5.21E+03	0.00E+00	3.40E+03	265.0
1.004	0.50	6.29E+04	3.65E+03	0.00E+00	-1.25E+05	-3.19E+04	0.00E+00	-4.59E+03	8.52E+03	0.00E+00	2.86E+03	263.2
1.104	0.55	6.22E+04	5.02E+03	0.00E+00	-1.15E+05	-4.19E+04	0.00E+00	-5.86E+03	1.27E+04	0.00E+00	1.77E+03	261.2
1.205	0.60	6.11E+04	6.45E+03	0.00E+00	-1.01E+05	-5.12E+04	0.00E+00	-9.22E+03	1.75E+04	0.00E+00	3.06E+02	258.0
1.305	0.65	5.97E+04	7.83E+03	0.00E+00	-8.64E+04	-5.88E+04	0.00E+00	-1.46E+04	2.22E+04	0.00E+00	1.12E+03	78.9
1.406	0.70	5.81E+04	9.07E+03	0.00E+00	-7.14E+04	-6.41E+04	0.00E+00	-2.13E+04	2.61E+04	0.00E+00	2.03E+03	77.8
1.506	0.75	5.65E+04	1.01E+04	0.00E+00	-5.76E+04	-6.70E+04	0.00E+00	-2.88E+04	2.88E+04	0.00E+00	2.04E+03	78.6
1.606	0.80	5.49E+04	1.10E+04	0.00E+00	-4.56E+04	-6.78E+04	0.00E+00	-3.60E+04	2.99E+04	0.00E+00	1.19E+03	85.0
1.707	0.85	5.34E+04	1.17E+04	0.00E+00	-3.57E+04	-6.67E+04	0.00E+00	-4.24E+04	2.92E+04	0.00E+00	2.76E+02	174.1
1.807	0.90	5.21E+04	1.22E+04	0.00E+00	-2.79E+04	-6.42E+04	0.00E+00	-4.74E+04	2.70E+04	0.00E+00	9.28E+02	243.8
1.907	0.95	5.09E+04	1.26E+04	0.00E+00	-2.20E+04	-6.07E+04	0.00E+00	-5.07E+04	2.37E+04	0.00E+00	9.74E+02	262.5
2.008	1.00	4.98E+04	1.28E+04	0.00E+00	-1.78E+04	-5.64E+04	0.00E+00	-5.23E+04	1.98E+04	0.00E+00	5.74E+02	306.6
2.108	1.05	4.89E+04	1.29E+04	0.00E+00	-1.49E+04	-5.17E+04	0.00E+00	-5.26E+04	1.58E+04	0.00E+00	5.32E+02	20.1
2.209	1.10	4.81E+04	1.30E+04	0.00E+00	-1.32E+04	-4.68E+04	0.00E+00	-5.18E+04	1.22E+04	0.00E+00	4.87E+02	75.9
2.309	1.15	4.74E+04	1.29E+04	0.00E+00	-1.24E+04	-4.18E+04	0.00E+00	-5.05E+04	9.25E+03	0.00E+00	4.87E+02	143.9
2.409	1.20	4.68E+04	1.28E+04	0.00E+00	-1.23E+04	-3.69E+04	0.00E+00	-4.89E+04	6.95E+03	0.00E+00	4.24E+02	192.9
2.510	1.25	4.63E+04	1.27E+04	0.00E+00	-1.27E+04	-3.21E+04	0.00E+00	-4.73E+04	5.29E+03	0.00E+00	2.94E+02	286.5
2.610	1.30	4.59E+04	1.25E+04	0.00E+00	-1.35E+04	-2.75E+04	0.00E+00	-4.58E+04	4.14E+03	0.00E+00	4.29E+02	343.3
2.711	1.35	4.56E+04	1.22E+04	0.00E+00	-1.47E+04	-2.31E+04	0.00E+00	-4.46E+04	3.38E+03	0.00E+00	1.90E+02	53.3
2.811	1.40	4.53E+04	1.19E+04	0.00E+00	-1.60E+04	-1.89E+04	0.00E+00	-4.37E+04	2.86E+03	0.00E+00	3.65E+02	148.7
2.911	1.45	4.50E+04	1.16E+04	0.00E+00	-1.75E+04	-1.50E+04	0.00E+00	-4.29E+04	2.48E+03	0.00E+00	1.87E+02	193.9
3.012	1.50	4.48E+04	1.13E+04	0.00E+00	-1.90E+04	-1.14E+04	0.00E+00	-4.23E+04	2.17E+03	0.00E+00	2.92E+02	321.6
3.112	1.55	4.47E+04	1.10E+04	0.00E+00	-2.07E+04	-7.99E+03	0.00E+00	-4.18E+04	1.88E+03	0.00E+00	1.71E+02	0.3
3.213	1.60	4.46E+04	1.07E+04	0.00E+00	-2.23E+04	-4.83E+03	0.00E+00	-4.13E+04	1.58E+03	0.00E+00	2.49E+02	136.9
3.313	1.65	4.45E+04	1.03E+04	0.00E+00	-2.39E+04	-1.91E+03	0.00E+00	-4.10E+04	1.27E+03	0.00E+00	1.13E+02	179.2
3.413	1.70	4.44E+04	9.99E+03	0.00E+00	-2.55E+04	7.93E+02	0.00E+00	-4.07E+04	9.18E+02	0.00E+00	2.27E+02	314.6
3.514	1.75	4.43E+04	9.65E+03	0.00E+00	-2.71E+04	3.30E+03	0.00E+00	-4.04E+04	5.41E+02	0.00E+00	3.60E+01	43.5
3.614	1.80	4.43E+04	9.32E+03	0.00E+00	-2.86E+04	5.63E+03	0.00E+00	-4.02E+04	1.38E+02	0.00E+00	1.97E+02	136.8
3.715	1.85	4.43E+04	8.98E+03	0.00E+00	-3.01E+04	7.80E+03	0.00E+00	-4.00E+04	-2.89E+02	0.00E+00	8.86E+01	298.7
3.815	1.90	4.43E+04	8.66E+03	0.00E+00	-3.15E+04	9.85E+03	0.00E+00	-3.97E+04	-7.32E+02	0.00E+00	1.14E+02	319.9
3.915	1.95	4.43E+04	8.33E+03	0.00E+00	-3.29E+04	1.18E+04	0.00E+00	-3.95E+04	-1.19E+03	0.00E+00	1.33E+02	119.6
4.016	2.00	4.43E+04	8.02E+03	0.00E+00	-3.43E+04	1.37E+04	0.00E+00	-3.93E+04	-1.65E+03	0.00E+00	2.21E+01	254.3
4.116	2.05	4.44E+04	7.70E+03	0.00E+00	-3.56E+04	1.57E+04	0.00E+00	-3.91E+04	-2.11E+03	0.00E+00	8.34E+01	291.8
4.217	2.10	4.44E+04	7.39E+03	0.00E+00	-3.69E+04	1.78E+04	0.00E+00	-3.88E+04	-2.57E+03	0.00E+00	8.82E+01	106.9
4.317	2.15	4.44E+04	7.08E+03	0.00E+00	-3.82E+04	2.06E+04	0.00E+00	-3.86E+04	-2.99E+03	0.00E+00	3.03E+01	303.6
4.417	2.20	4.44E+04	6.70E+03	0.00E+00	-4.02E+04	2.63E+04	0.00E+00	-3.84E+04	-3.25E+03	0.00E+00	3.62E+01	262.0
4.518	2.25	4.46E+04	6.55E+03	0.00E+00	-4.04E+04	1.69E+04	0.00E+00	-3.86E+04	-7.22E+03	0.00E+00	5.86E+01	91.7
4.618	2.30	4.47E+04	6.26E+03	0.00E+00	-4.14E+04	1.92E+04	0.00E+00	-3.57E+04	8.48E+03	0.00E+00	4.84E+01	285.7
4.719	2.35	4.47E+04	6.03E+03	0.00E+00	-4.27E+04	2.62E+04	0.00E+00	-3.73E+04	-2.18E+03	0.00E+00	2.29E+01	152.0
4.819	2.40	4.47E+04	5.72E+03	0.00E+00	-4.53E+04	3.54E+04	0.00E+00	-3.73E+04	-4.69E+03	0.00E+00	3.00E+01	37.7
4.919	2.45	4.46E+04	5.01E+03	0.00E+00	-5.59E+04	6.44E+04	0.00E+00	-3.73E+04	-5.24E+03	0.00E+00	2.64E+01	244.9
5.020	2.50	4.53E+04	5.70E+03	0.00E+00	-5.25E+04	-6.20E+04	0.00E+00	-3.41E+04	1.78E+03	0.00E+00	1.73E+01	120.4

MOTIONCOEFFICIENTS AND WAVE-LOADS FORWARD SPEED = 0.00 kn
~~~~~~ ~~~~~~~~~~~~~~~ ~~~~~~~~~~~ WAVE DIRECTION = +210 deg off stern

HEAVE EQUATION
~~~~~~ ~~~~~~~~

SQRT	ENC	.......COUPLING TO SURGE.......			.............HEAVE.............			.......COUPLING TO PITCH.......			WAVE-MOMENT	
SL/WL	FREQ	MASS	DAMPING	RESTORING	MASS	DAMPING	RESTORING	MASS	DAMPING	RESTORING	AMPL	PHASE
(-)	(r/s)	(kN*s2/m/m	(kN*s/m/m)	(kN/m/m)	(kN*s2/m/m	(kN*s/m/m)	(kN/m/m)	(kN*s2/m)	(kN*s/m)	(kN/m)	(kN/m)	(deg)
0.100	0.05	0.00E+00	0.00E+00	0.00E+00	5.09E+05	1.35E+04	7.63E+04	1.18E+06	3.41E+04	1.85E+05	7.63E+04	360.0
0.201	0.10	0.00E+00	0.00E+00	0.00E+00	3.81E+05	2.51E+04	7.63E+04	8.58E+05	6.39E+04	1.85E+05	7.59E+04	359.9
0.301	0.15	0.00E+00	0.00E+00	0.00E+00	3.08E+05	3.46E+04	7.63E+04	6.74E+05	8.89E+04	1.85E+05	7.23E+04	1.5
0.402	0.20	0.00E+00	0.00E+00	0.00E+00	2.60E+05	4.20E+04	7.63E+04	5.50E+05	1.09E+05	1.85E+05	6.53E+04	6.5
0.502	0.25	0.00E+00	0.00E+00	0.00E+00	2.26E+05	4.77E+04	7.63E+04	4.63E+05	1.26E+05	1.85E+05	6.01E+04	9.9
0.602	0.30	0.00E+00	0.00E+00	0.00E+00	2.01E+05	5.18E+04	7.63E+04	3.99E+05	1.40E+05	1.85E+05	5.40E+04	13.7
0.703	0.35	0.00E+00	0.00E+00	0.00E+00	1.82E+05	5.47E+04	7.63E+04	3.50E+05	1.51E+05	1.85E+05	4.65E+04	18.1
0.803	0.40	0.00E+00	0.00E+00	0.00E+00	1.68E+05	5.65E+04	7.63E+04	3.12E+05	1.61E+05	1.85E+05	3.76E+04	22.9
0.904	0.45	0.00E+00	0.00E+00	0.00E+00	1.56E+05	5.74E+04	7.63E+04	2.83E+05	1.69E+05	1.85E+05	2.77E+04	28.0
1.004	0.50	0.00E+00	0.00E+00	0.00E+00	1.48E+05	5.76E+04	7.63E+04	2.59E+05	1.76E+05	1.85E+05	1.70E+04	32.4
1.104	0.55	0.00E+00	0.00E+00	0.00E+00	1.41E+05	5.71E+04	7.63E+04	2.39E+05	1.83E+05	1.85E+05	7.25E+03	33.5
1.205	0.60	0.00E+00	0.00E+00	0.00E+00	1.36E+05	5.60E+04	7.63E+04	2.23E+05	1.89E+05	1.85E+05	9.57E+02	225.0
1.305	0.65	0.00E+00	0.00E+00	0.00E+00	1.33E+05	5.45E+04	7.63E+04	2.09E+05	1.94E+05	1.85E+05	6.35E+03	213.6
1.406	0.70	0.00E+00	0.00E+00	0.00E+00	1.30E+05	5.25E+04	7.63E+04	1.97E+05	1.99E+05	1.85E+05	8.31E+03	206.8
1.506	0.75	0.00E+00	0.00E+00	0.00E+00	1.28E+05	5.03E+04	7.63E+04	1.86E+05	2.04E+05	1.85E+05	6.66E+03	197.7
1.606	0.80	0.00E+00	0.00E+00	0.00E+00	1.27E+05	4.78E+04	7.63E+04	1.76E+05	2.09E+05	1.85E+05	3.04E+03	176.9
1.707	0.85	0.00E+00	0.00E+00	0.00E+00	1.27E+05	4.52E+04	7.63E+04	1.68E+05	2.13E+05	1.85E+05	1.78E+03	49.5
1.807	0.90	0.00E+00	0.00E+00	0.00E+00	1.27E+05	4.24E+04	7.63E+04	1.59E+05	2.16E+05	1.85E+05	3.58E+03	18.9
1.907	0.95	0.00E+00	0.00E+00	0.00E+00	1.27E+05	3.97E+04	7.63E+04	1.52E+05	2.20E+05	1.85E+05	2.87E+03	0.6
2.008	1.00	0.00E+00	0.00E+00	0.00E+00	1.28E+05	3.69E+04	7.63E+04	1.45E+05	2.22E+05	1.85E+05	9.66E+02	306.4
2.108	1.05	0.00E+00	0.00E+00	0.00E+00	1.29E+05	3.42E+04	7.63E+04	1.38E+05	2.25E+05	1.85E+05	1.58E+03	204.2
2.209	1.10	0.00E+00	0.00E+00	0.00E+00	1.30E+05	3.15E+04	7.63E+04	1.32E+05	2.26E+05	1.85E+05	1.63E+03	176.6
2.309	1.15	0.00E+00	0.00E+00	0.00E+00	1.31E+05	2.90E+04	7.63E+04	1.27E+05	2.27E+05	1.85E+05	6.21E+02	116.7
2.409	1.20	0.00E+00	0.00E+00	0.00E+00	1.33E+05	2.66E+04	7.63E+04	1.22E+05	2.28E+05	1.85E+05	8.95E+02	14.7
2.510	1.25	0.00E+00	0.00E+00	0.00E+00	1.34E+05	2.43E+04	7.63E+04	1.17E+05	2.28E+05	1.85E+05	6.99E+02	332.3
2.610	1.30	0.00E+00	0.00E+00	0.00E+00	1.35E+05	2.22E+04	7.63E+04	1.13E+05	2.27E+05	1.85E+05	4.54E+02	210.1
2.711	1.35	0.00E+00	0.00E+00	0.00E+00	1.37E+05	2.02E+04	7.63E+04	1.09E+05	2.26E+05	1.85E+05	7.11E+02	162.7
2.811	1.40	0.00E+00	0.00E+00	0.00E+00	1.38E+05	1.84E+04	7.63E+04	1.06E+05	2.25E+05	1.85E+05	2.03E+02	67.9
2.911	1.45	0.00E+00	0.00E+00	0.00E+00	1.40E+05	1.67E+04	7.63E+04	1.03E+05	2.23E+05	1.85E+05	4.89E+02	345.0
3.012	1.50	0.00E+00	0.00E+00	0.00E+00	1.41E+05	1.52E+04	7.63E+04	1.01E+05	2.21E+05	1.85E+05	1.08E+02	255.6
3.112	1.55	0.00E+00	0.00E+00	0.00E+00	1.42E+05	1.38E+04	7.63E+04	9.86E+04	2.18E+05	1.85E+05	3.31E+02	163.0
3.213	1.60	0.00E+00	0.00E+00	0.00E+00	1.43E+05	1.26E+04	7.63E+04	9.68E+04	2.15E+05	1.85E+05	4.41E+01	30.5
3.313	1.65	0.00E+00	0.00E+00	0.00E+00	1.44E+05	1.14E+04	7.63E+04	9.53E+04	2.12E+05	1.85E+05	4.47E+02	254.5
3.413	1.70	0.00E+00	0.00E+00	0.00E+00	1.45E+05	1.04E+04	7.63E+04	9.41E+04	2.09E+05	1.85E+05	5.49E+02	84.1
3.514	1.75	0.00E+00	0.00E+00	0.00E+00	1.46E+05	9.43E+03	7.63E+04	9.32E+04	2.05E+05	1.85E+05	5.12E+02	240.4
3.614	1.80	0.00E+00	0.00E+00	0.00E+00	1.47E+05	8.57E+03	7.63E+04	9.25E+04	2.01E+05	1.85E+05	7.74E+01	91.1
3.715	1.85	0.00E+00	0.00E+00	0.00E+00	1.48E+05	7.79E+03	7.63E+04	9.20E+04	1.98E+05	1.85E+05	1.29E+02	147.3
3.815	1.90	0.00E+00	0.00E+00	0.00E+00	1.49E+05	7.08E+03	7.63E+04	9.17E+04	1.94E+05	1.85E+05	2.84E+02	231.4
3.915	1.95	0.00E+00	0.00E+00	0.00E+00	1.50E+05	6.44E+03	7.63E+04	9.16E+04	1.90E+05	1.85E+05	2.67E+02	124.6
4.016	2.00	0.00E+00	0.00E+00	0.00E+00	1.51E+05	5.84E+03	7.63E+04	9.16E+04	1.86E+05	1.85E+05	1.04E+02	357.0
4.116	2.05	0.00E+00	0.00E+00	0.00E+00	1.51E+05	5.30E+03	7.63E+04	9.18E+04	1.82E+05	1.85E+05	1.51E+02	289.4
4.217	2.10	0.00E+00	0.00E+00	0.00E+00	1.52E+05	4.78E+03	7.63E+04	9.20E+04	1.79E+05	1.85E+05	2.11E+02	202.7
4.317	2.15	0.00E+00	0.00E+00	0.00E+00	1.52E+05	4.33E+03	7.63E+04	9.24E+04	1.75E+05	1.85E+05	1.00E+02	9.4
4.417	2.20	0.00E+00	0.00E+00	0.00E+00	1.53E+05	4.00E+03	7.63E+04	9.28E+04	1.72E+05	1.85E+05	1.72E+02	111.3
4.518	2.25	0.00E+00	0.00E+00	0.00E+00	1.54E+05	3.96E+03	7.63E+04	9.35E+04	1.71E+05	1.85E+05	3.66E+01	359.8
4.618	2.30	0.00E+00	0.00E+00	0.00E+00	1.55E+05	4.70E+03	7.63E+04	9.45E+04	1.66E+05	1.85E+05	9.77E+01	282.8
4.719	2.35	0.00E+00	0.00E+00	0.00E+00	1.54E+05	5.21E+03	7.63E+04	9.06E+04	1.46E+05	1.85E+05	5.79E+01	131.3
4.819	2.40	0.00E+00	0.00E+00	0.00E+00	1.55E+05	4.02E+03	7.63E+04	8.80E+04	1.28E+05	1.85E+05	4.52E+01	358.4
4.919	2.45	0.00E+00	0.00E+00	0.00E+00	1.55E+05	3.33E+03	7.63E+04	9.59E+04	1.53E+05	1.85E+05	7.95E+01	242.7
5.020	2.50	0.00E+00	0.00E+00	0.00E+00	1.56E+05	3.38E+03	7.63E+04	9.68E+04	1.42E+05	1.85E+05	8.55E+01	224.9

MOTIONCOEFFICIENTS AND WAVE-LOADS

FORWARD SPEED = 0.00 kn
WAVE DIRECTION = +210 deg off stern

ROLL EQUATION

SQRT	ENC	.......COUPLING TO SWAY........			.............ROLL.............			........COUPLING TO YAW........			WAVE-MOMENT	
SL/WL	FREQ	MASS	DAMPING	RESTORING	MASS	DAMPING	RESTORING	MASS	DAMPING	RESTORING	AMPL	PHASE
(-)	(r/s)	(kN*s2/m)	(kN*s/m)	(kN/m)	(kN*s2*m/m	(kN*s*m/m)	(kN*m/m)	(kN*s2*m/m	(kN*s*m/m)	(kN*m/m)	(kN*m/m)	(deg)
0.100	0.05	-1.06E+05	-6.06E-01	0.00E+00	1.16E+07	4.37E+02	4.85E+06	6.73E+05	1.48E+00	0.00E+00	7.54E+02	89.9
0.201	0.10	-1.07E+05	-2.07E+01	0.00E+00	1.17E+07	3.85E+03	4.85E+06	6.80E+05	6.99E+01	0.00E+00	3.01E+03	89.7
0.301	0.15	-1.10E+05	-1.48E+02	0.00E+00	1.17E+07	1.49E+04	4.85E+06	6.92E+05	4.99E+02	0.00E+00	6.72E+03	89.4
0.402	0.20	-1.15E+05	-5.95E+02	0.00E+00	1.17E+07	4.21E+04	4.85E+06	7.09E+05	2.00E+03	0.00E+00	1.18E+04	88.7
0.502	0.25	-1.20E+05	-1.72E+03	0.00E+00	1.18E+07	1.02E+05	4.85E+06	7.31E+05	5.83E+03	0.00E+00	1.80E+04	87.8
0.602	0.30	-1.25E+05	-4.03E+03	0.00E+00	1.18E+07	2.34E+05	4.85E+06	7.55E+05	1.37E+04	0.00E+00	2.48E+04	86.4
0.703	0.35	-1.30E+05	-8.03E+03	0.00E+00	1.19E+07	5.94E+05	4.85E+06	7.78E+05	2.76E+04	0.00E+00	3.13E+04	84.7
0.803	0.40	-1.32E+05	-1.41E+04	0.00E+00	1.19E+07	1.25E+06	4.85E+06	7.96E+05	4.93E+04	0.00E+00	3.64E+04	82.4
0.904	0.45	-1.31E+05	-2.23E+04	0.00E+00	1.18E+07	7.89E+05	4.85E+06	8.04E+05	7.96E+04	0.00E+00	3.84E+04	79.6
1.004	0.50	-1.25E+05	-3.19E+04	0.00E+00	1.18E+07	6.14E+05	4.85E+06	7.98E+05	1.18E+05	0.00E+00	3.59E+04	76.4
1.104	0.55	-1.15E+05	-4.19E+04	0.00E+00	1.17E+07	5.59E+05	4.85E+06	7.77E+05	1.62E+05	0.00E+00	2.80E+04	72.6
1.205	0.60	-1.01E+05	-5.12E+04	0.00E+00	1.15E+07	5.38E+05	4.85E+06	7.42E+05	2.09E+05	0.00E+00	1.52E+04	67.0
1.305	0.65	-8.64E+04	-5.88E+04	0.00E+00	1.14E+07	5.82E+05	4.85E+06	6.95E+05	2.56E+05	0.00E+00	1.46E+03	313.1
1.406	0.70	-7.14E+04	-6.41E+04	0.00E+00	1.12E+07	6.48E+05	4.85E+06	6.39E+05	2.98E+05	0.00E+00	1.59E+04	249.7
1.506	0.75	-5.76E+04	-6.70E+04	0.00E+00	1.11E+07	6.73E+05	4.85E+06	5.78E+05	3.33E+05	0.00E+00	2.60E+04	243.7
1.606	0.80	-4.56E+04	-6.78E+04	0.00E+00	1.10E+07	6.66E+05	4.85E+06	5.19E+05	3.59E+05	0.00E+00	2.71E+04	238.1
1.707	0.85	-3.57E+04	-6.67E+04	0.00E+00	1.10E+07	6.37E+05	4.85E+06	4.64E+05	3.73E+05	0.00E+00	1.80E+04	229.5
1.807	0.90	-2.79E+04	-6.42E+04	0.00E+00	1.09E+07	5.76E+05	4.85E+06	4.18E+05	3.78E+05	0.00E+00	3.45E+03	165.5
1.907	0.95	-2.20E+04	-6.07E+04	0.00E+00	1.09E+07	5.72E+05	4.85E+06	3.83E+05	3.75E+05	0.00E+00	1.49E+04	60.9
2.008	1.00	-1.78E+04	-5.64E+04	0.00E+00	1.09E+07	6.95E+05	4.85E+06	3.58E+05	3.67E+05	0.00E+00	2.08E+04	48.9
2.108	1.05	-1.49E+04	-5.17E+04	0.00E+00	1.09E+07	6.81E+05	4.85E+06	3.43E+05	3.59E+05	0.00E+00	1.36E+04	35.7
2.209	1.10	-1.32E+04	-4.68E+04	0.00E+00	1.09E+07	4.41E+05	4.85E+06	3.34E+05	3.53E+05	0.00E+00	3.53E+03	285.6
2.309	1.15	-1.24E+04	-4.18E+04	0.00E+00	1.09E+07	4.18E+05	4.85E+06	3.29E+05	3.50E+05	0.00E+00	1.21E+04	228.1
2.409	1.20	-1.23E+04	-3.69E+04	0.00E+00	1.09E+07	3.83E+05	4.85E+06	3.26E+05	3.51E+05	0.00E+00	9.63E+03	214.3
2.510	1.25	-1.27E+04	-3.21E+04	0.00E+00	1.09E+07	2.95E+05	4.85E+06	3.23E+05	3.56E+05	0.00E+00	1.77E+03	100.4
2.610	1.30	-1.35E+04	-2.75E+04	0.00E+00	1.09E+07	2.74E+05	4.85E+06	3.18E+05	3.63E+05	0.00E+00	6.70E+03	41.8
2.711	1.35	-1.47E+04	-2.31E+04	0.00E+00	1.09E+07	2.58E+05	4.85E+06	3.13E+05	3.72E+05	0.00E+00	2.50E+03	30.0
2.811	1.40	-1.60E+04	-1.89E+04	0.00E+00	1.09E+07	2.04E+05	4.85E+06	3.06E+05	3.80E+05	0.00E+00	3.79E+03	217.9
2.911	1.45	-1.75E+04	-1.50E+04	0.00E+00	1.09E+07	2.18E+05	4.85E+06	2.99E+05	3.89E+05	0.00E+00	2.84E+03	219.2
3.012	1.50	-1.90E+04	-1.14E+04	0.00E+00	1.10E+07	1.79E+05	4.85E+06	2.91E+05	3.97E+05	0.00E+00	2.29E+03	20.7
3.112	1.55	-2.07E+04	-7.99E+03	0.00E+00	1.10E+07	1.80E+05	4.85E+06	2.83E+05	4.03E+05	0.00E+00	2.39E+03	36.4
3.213	1.60	-2.23E+04	-4.83E+03	0.00E+00	1.10E+07	1.62E+05	4.85E+06	2.75E+05	4.09E+05	0.00E+00	1.74E+03	180.7
3.313	1.65	-2.39E+04	-1.91E+03	0.00E+00	1.10E+07	1.59E+05	4.85E+06	2.67E+05	4.13E+05	0.00E+00	1.59E+03	210.4
3.413	1.70	-2.55E+04	7.93E+02	0.00E+00	1.10E+07	1.54E+05	4.85E+06	2.59E+05	4.15E+05	0.00E+00	1.56E+03	356.6
3.514	1.75	-2.71E+04	3.30E+03	0.00E+00	1.10E+07	1.51E+05	4.85E+06	2.52E+05	4.17E+05	0.00E+00	8.81E+02	43.7
3.614	1.80	-2.86E+04	5.63E+03	0.00E+00	1.10E+07	1.53E+05	4.85E+06	2.45E+05	4.18E+05	0.00E+00	1.25E+03	177.2
3.715	1.85	-3.01E+04	7.80E+03	0.00E+00	1.10E+07	1.53E+05	4.85E+06	2.39E+05	4.17E+05	0.00E+00	7.00E+02	283.0
3.815	1.90	-3.15E+04	9.85E+03	0.00E+00	1.10E+07	1.56E+05	4.85E+06	2.34E+05	4.16E+05	0.00E+00	6.97E+02	7.2
3.915	1.95	-3.29E+04	1.18E+04	0.00E+00	1.10E+07	1.62E+05	4.85E+06	2.28E+05	4.14E+05	0.00E+00	8.91E+02	128.2
4.016	2.00	-3.43E+04	1.37E+04	0.00E+00	1.10E+07	1.67E+05	4.85E+06	2.24E+05	4.12E+05	0.00E+00	4.52E+02	277.8
4.116	2.05	-3.56E+04	1.57E+04	0.00E+00	1.10E+07	1.75E+05	4.85E+06	2.20E+05	4.08E+05	0.00E+00	5.00E+02	315.1
4.217	2.10	-3.69E+04	1.78E+04	0.00E+00	1.10E+07	1.87E+05	4.85E+06	2.16E+05	4.05E+05	0.00E+00	7.19E+02	116.8
4.317	2.15	-3.82E+04	2.06E+04	0.00E+00	1.10E+07	2.05E+05	4.85E+06	2.13E+05	4.00E+05	0.00E+00	3.57E+02	291.2
4.417	2.20	-4.02E+04	2.63E+04	0.00E+00	1.10E+07	2.50E+05	4.85E+06	2.11E+05	3.90E+05	0.00E+00	1.78E+02	267.6
4.518	2.25	-4.04E+04	1.69E+04	0.00E+00	1.10E+07	1.52E+05	4.85E+06	1.53E+05	4.78E+05	0.00E+00	5.60E+02	99.1
4.618	2.30	-4.14E+04	1.92E+04	0.00E+00	1.11E+07	1.63E+05	4.85E+06	2.01E+05	1.14E+05	0.00E+00	3.82E+02	273.8
4.719	2.35	-4.27E+04	2.62E+04	0.00E+00	1.10E+07	2.42E+05	4.85E+06	2.07E+05	3.20E+05	0.00E+00	2.07E+02	109.0
4.819	2.40	-4.53E+04	3.54E+04	0.00E+00	1.10E+07	3.34E+05	4.85E+06	2.04E+05	3.60E+05	0.00E+00	1.71E+02	355.3
4.919	2.45	-5.59E+04	6.44E+04	0.00E+00	1.10E+07	6.29E+05	4.85E+06	2.15E+05	3.40E+05	0.00E+00	2.70E+02	209.1
5.020	2.50	-5.25E+04	-6.20E+04	0.00E+00	1.09E+07	-5.26E+05	4.85E+06	3.38E+05	-3.67E+05	0.00E+00	3.04E+02	60.5

MOTIONCOEFFICIENTS AND WAVE-LOADS
~~~~~~ ~~~~~~ ~~~~~~~~~~ ~~~~~~~~~~~~

FORWARD SPEED = 0.00 kn
WAVE DIRECTION = +210 deg off stern

PITCH EQUATION
~~~~~~ ~~~~~~~~

SQRT	ENC	.......COUPLING TO SURGE.......			.......COUPLING TO HEAVE.......			.............PITCH.............			WAVE-MOMENT	
SL/WL	FREQ	MASS	DAMPING	RESTORING	MASS	DAMPING	RESTORING	MASS	DAMPING	RESTORING	AMPL	PHASE
(-)	(r/s)	(kN*s2/m)	(kN*s/m)	(kN/m)	(kN*s2/m)	(kN*s/m)	(kN/m)	(kN*s2*m/m	(kN*s*m/m)	(kN*m/m)	(kN*m/m)	(deg)
0.100	0.05	-9.16E+04	-8.66E+00	0.00E+00	1.18E+06	3.41E+04	1.85E+05	1.53E+09	3.91E+07	2.54E+08	1.92E+05	343.1
0.201	0.10	-9.65E+04	-2.73E+02	0.00E+00	8.58E+05	6.39E+04	1.85E+05	1.16E+09	7.33E+07	2.54E+08	2.88E+05	309.5
0.301	0.15	-1.02E+05	-1.63E+03	0.00E+00	6.74E+05	8.89E+04	1.85E+05	9.52E+08	1.02E+08	2.54E+08	5.13E+05	291.4
0.402	0.20	-1.05E+05	-4.83E+03	0.00E+00	5.50E+05	1.09E+05	1.85E+05	8.10E+08	1.24E+08	2.54E+08	8.08E+05	287.5
0.502	0.25	-1.00E+05	-9.34E+03	0.00E+00	4.63E+05	1.26E+05	1.85E+05	7.09E+08	1.42E+08	2.54E+08	1.16E+06	286.2
0.602	0.30	-9.19E+04	-1.38E+04	0.00E+00	3.99E+05	1.40E+05	1.85E+05	6.33E+08	1.56E+08	2.54E+08	1.53E+06	287.0
0.703	0.35	-8.30E+04	-1.72E+04	0.00E+00	3.50E+05	1.51E+05	1.85E+05	5.76E+08	1.66E+08	2.54E+08	1.87E+06	289.1
0.803	0.40	-7.53E+04	-1.95E+04	0.00E+00	3.12E+05	1.61E+05	1.85E+05	5.33E+08	1.72E+08	2.54E+08	2.11E+06	292.0
0.904	0.45	-6.91E+04	-2.08E+04	0.00E+00	2.83E+05	1.69E+05	1.85E+05	4.98E+08	1.77E+08	2.54E+08	2.21E+06	295.5
1.004	0.50	-6.41E+04	-2.14E+04	0.00E+00	2.59E+05	1.76E+05	1.85E+05	4.71E+08	1.79E+08	2.54E+08	2.12E+06	297.9
1.104	0.55	-6.00E+04	-2.15E+04	0.00E+00	2.39E+05	1.83E+05	1.85E+05	4.50E+08	1.79E+08	2.54E+08	1.81E+06	299.4
1.205	0.60	-5.65E+04	-2.15E+04	0.00E+00	2.23E+05	1.89E+05	1.85E+05	4.34E+08	1.78E+08	2.54E+08	1.30E+06	297.8
1.305	0.65	-5.36E+04	-2.14E+04	0.00E+00	2.09E+05	1.94E+05	1.85E+05	4.21E+08	1.75E+08	2.54E+08	6.96E+05	291.6
1.406	0.70	-5.14E+04	-2.16E+04	0.00E+00	1.97E+05	1.99E+05	1.85E+05	4.12E+08	1.71E+08	2.54E+08	1.32E+05	236.9
1.506	0.75	-5.01E+04	-2.18E+04	0.00E+00	1.86E+05	2.04E+05	1.85E+05	4.05E+08	1.67E+08	2.54E+08	4.08E+05	125.8
1.606	0.80	-4.94E+04	-2.18E+04	0.00E+00	1.76E+05	2.09E+05	1.85E+05	4.00E+08	1.61E+08	2.54E+08	5.79E+05	113.3
1.707	0.85	-4.89E+04	-2.13E+04	0.00E+00	1.68E+05	2.13E+05	1.85E+05	3.96E+08	1.55E+08	2.54E+08	4.34E+05	97.5
1.807	0.90	-4.83E+04	-2.07E+04	0.00E+00	1.59E+05	2.16E+05	1.85E+05	3.94E+08	1.48E+08	2.54E+08	1.53E+05	57.9
1.907	0.95	-4.76E+04	-2.02E+04	0.00E+00	1.52E+05	2.20E+05	1.85E+05	3.94E+08	1.42E+08	2.54E+08	2.02E+05	301.6
2.008	1.00	-4.70E+04	-2.01E+04	0.00E+00	1.45E+05	2.22E+05	1.85E+05	3.94E+08	1.35E+08	2.54E+08	2.70E+05	276.0
2.108	1.05	-4.69E+04	-1.99E+04	0.00E+00	1.38E+05	2.25E+05	1.85E+05	3.95E+08	1.28E+08	2.54E+08	1.50E+05	247.0
2.209	1.10	-4.68E+04	-1.93E+04	0.00E+00	1.32E+05	2.26E+05	1.85E+05	3.97E+08	1.21E+08	2.54E+08	9.46E+04	135.1
2.309	1.15	-4.64E+04	-1.88E+04	0.00E+00	1.27E+05	2.27E+05	1.85E+05	3.99E+08	1.14E+08	2.54E+08	1.51E+05	89.8
2.409	1.20	-4.61E+04	-1.92E+04	0.00E+00	1.22E+05	2.28E+05	1.85E+05	4.01E+08	1.08E+08	2.54E+08	7.30E+04	49.2
2.510	1.25	-4.69E+04	-1.94E+04	0.00E+00	1.17E+05	2.28E+05	1.85E+05	4.04E+08	1.01E+08	2.54E+08	7.61E+04	283.4
2.610	1.30	-4.79E+04	-1.72E+04	0.00E+00	1.13E+05	2.27E+05	1.85E+05	4.07E+08	9.51E+07	2.54E+08	8.72E+04	243.0
2.711	1.35	-4.63E+04	-1.40E+04	0.00E+00	1.09E+05	2.26E+05	1.85E+05	4.10E+08	8.94E+07	2.54E+08	3.36E+04	134.8
2.811	1.40	-4.34E+04	-1.51E+04	0.00E+00	1.06E+05	2.25E+05	1.85E+05	4.13E+08	8.40E+07	2.54E+08	6.60E+04	68.9
2.911	1.45	-4.31E+04	-2.08E+04	0.00E+00	1.03E+05	2.23E+05	1.85E+05	4.16E+08	7.90E+07	2.54E+08	1.90E+04	341.7
3.012	1.50	-4.68E+04	-2.38E+04	0.00E+00	1.01E+05	2.21E+05	1.85E+05	4.19E+08	7.42E+07	2.54E+08	4.60E+04	246.6
3.112	1.55	-4.97E+04	-1.98E+04	0.00E+00	9.86E+04	2.18E+05	1.85E+05	4.22E+08	6.97E+07	2.54E+08	1.05E+04	163.1
3.213	1.60	-4.96E+04	-1.53E+04	0.00E+00	9.68E+04	2.15E+05	1.85E+05	4.25E+08	6.55E+07	2.54E+08	2.95E+04	61.3
3.313	1.65	-4.90E+04	-1.26E+04	0.00E+00	9.53E+04	2.12E+05	1.85E+05	4.28E+08	6.16E+07	2.54E+08	4.01E+04	236.7
3.413	1.70	-4.77E+04	-9.67E+03	0.00E+00	9.41E+04	2.09E+05	1.85E+05	4.30E+08	5.79E+07	2.54E+08	1.14E+04	177.0
3.514	1.75	-4.56E+04	-9.63E+03	0.00E+00	9.32E+04	2.05E+05	1.85E+05	4.33E+08	5.45E+07	2.54E+08	7.87E+03	14.9
3.614	1.80	-4.59E+04	-1.36E+04	0.00E+00	9.25E+04	2.01E+05	1.85E+05	4.35E+08	5.14E+07	2.54E+08	2.74E+04	185.3
3.715	1.85	-4.27E+04	-1.23E+04	0.00E+00	9.20E+04	1.98E+05	1.85E+05	4.37E+08	4.84E+07	2.54E+08	1.95E+04	74.2
3.815	1.90	-4.15E+04	-1.95E+03	0.00E+00	9.17E+04	1.94E+05	1.85E+05	4.40E+08	4.56E+07	2.54E+08	2.58E+04	184.7
3.915	1.95	-4.74E+04	1.20E+03	0.00E+00	9.16E+04	1.90E+05	1.85E+05	4.42E+08	4.30E+07	2.54E+08	1.34E+04	82.0
4.016	2.00	-4.69E+04	6.81E+01	0.00E+00	9.16E+04	1.86E+05	1.85E+05	4.44E+08	4.06E+07	2.54E+08	1.78E+04	28.1
4.116	2.05	-4.45E+04	1.69E+00	0.00E+00	9.18E+04	1.82E+05	1.85E+05	4.46E+08	3.83E+07	2.54E+08	8.65E+03	261.8
4.217	2.10	-4.04E+04	-1.80E-01	0.00E+00	9.20E+04	1.79E+05	1.85E+05	4.48E+08	3.62E+07	2.54E+08	8.37E+03	69.9
4.317	2.15	-7.01E+04	-2.25E-01	0.00E+00	9.24E+04	1.75E+05	1.85E+05	4.50E+08	3.42E+07	2.54E+08	1.55E+04	127.2
4.417	2.20	-1.27E+05	-1.94E-01	0.00E+00	9.28E+04	1.72E+05	1.85E+05	4.52E+08	3.23E+07	2.54E+08	1.13E+04	193.7
4.518	2.25	-1.44E+05	-1.35E-01	0.00E+00	9.35E+04	1.71E+05	1.85E+05	4.54E+08	3.07E+07	2.54E+08	1.71E+04	19.0
4.618	2.30	-1.44E+05	-1.35E-01	0.00E+00	9.45E+04	1.66E+05	1.85E+05	4.56E+08	3.05E+07	2.54E+08	6.86E+03	211.6
4.719	2.35	-1.44E+05	-1.35E-01	0.00E+00	9.06E+04	1.46E+05	1.85E+05	4.57E+08	3.20E+07	2.54E+08	4.94E+03	200.3
4.819	2.40	-1.44E+05	-1.35E-01	0.00E+00	8.80E+04	1.28E+05	1.85E+05	4.58E+08	2.97E+07	2.54E+08	9.86E+03	13.2
4.919	2.45	-1.44E+05	-1.35E-01	0.00E+00	9.59E+04	1.53E+05	1.85E+05	4.59E+08	2.65E+07	2.54E+08	6.63E+03	257.9
5.020	2.50	-1.44E+05	-1.35E-01	0.00E+00	9.68E+04	1.42E+05	1.85E+05	4.60E+08	2.57E+07	2.54E+08	6.03E+03	79.4

MOTIONCOEFFICIENTS AND WAVE-LOADS
~~~~~~ ~~~~~~ ~~~~~~~~~ ~~~~~~~~~~~

FORWARD SPEED = 0.00 kn
WAVE DIRECTION = +210 deg off stern

YAW EQUATION
~~~~~~ ~~~~~~

SQRT	ENC	.......COUPLING TO SWAY........			.......COUPLING TO ROLL........			.............YAW.............			WAVE-MOMENT	
SL/WL	FREQ	MASS	DAMPING	RESTORING	MASS	DAMPING	RESTORING	MASS	DAMPING	RESTORING	AMPL	PHASE
(-)	(r/s)	(kN*s2/m)	(kN*s/m)	(kN/m)	(kN*s2*m/m	(kN*s*m/m)	(kN*m/m)	(kN*s2*m/m	(kN*s*m/m)	(kN*m/m)	(kN*m/m)	(deg)
0.100	0.05	-1.69E+04	-2.91E-01	0.00E+00	6.73E+05	1.48E+00	0.00E+00	2.25E+08	1.72E+02	0.00E+00	5.41E+01	14.3
0.201	0.10	-1.66E+04	2.35E+00	0.00E+00	6.80E+05	6.99E+01	0.00E+00	2.26E+08	5.15E+03	0.00E+00	8.41E+02	3.5
0.301	0.15	-1.58E+04	1.87E+01	0.00E+00	6.92E+05	4.99E+02	0.00E+00	2.27E+08	3.73E+04	0.00E+00	4.24E+03	1.3
0.402	0.20	-1.47E+04	8.02E+01	0.00E+00	7.09E+05	2.00E+03	0.00E+00	2.28E+08	1.51E+05	0.00E+00	1.33E+04	0.3
0.502	0.25	-1.31E+04	2.52E+02	0.00E+00	7.31E+05	5.83E+03	0.00E+00	2.30E+08	4.46E+05	0.00E+00	3.20E+04	359.5
0.602	0.30	-1.12E+04	6.50E+02	0.00E+00	7.55E+05	1.37E+04	0.00E+00	2.33E+08	1.07E+06	0.00E+00	6.44E+04	358.7
0.703	0.35	-8.95E+03	1.45E+03	0.00E+00	7.78E+05	2.76E+04	0.00E+00	2.35E+08	2.20E+06	0.00E+00	1.13E+05	357.6
0.803	0.40	-6.75E+03	2.89E+03	0.00E+00	7.96E+05	4.93E+04	0.00E+00	2.37E+08	4.01E+06	0.00E+00	1.76E+05	356.3
0.904	0.45	-5.09E+03	5.21E+03	0.00E+00	8.04E+05	7.96E+04	0.00E+00	2.38E+08	6.61E+06	0.00E+00	2.44E+05	354.7
1.004	0.50	-4.59E+03	8.52E+03	0.00E+00	7.98E+05	1.18E+05	0.00E+00	2.39E+08	1.00E+07	0.00E+00	3.01E+05	353.0
1.104	0.55	-5.86E+03	1.27E+04	0.00E+00	7.77E+05	1.62E+05	0.00E+00	2.37E+08	1.40E+07	0.00E+00	3.23E+05	351.2
1.205	0.60	-9.22E+03	1.75E+04	0.00E+00	7.42E+05	2.09E+05	0.00E+00	2.35E+08	1.84E+07	0.00E+00	2.88E+05	349.5
1.305	0.65	-1.46E+04	2.22E+04	0.00E+00	6.95E+05	2.56E+05	0.00E+00	2.32E+08	2.29E+07	0.00E+00	1.89E+05	348.6
1.406	0.70	-2.13E+04	2.61E+04	0.00E+00	6.39E+05	2.98E+05	0.00E+00	2.28E+08	2.72E+07	0.00E+00	4.55E+04	355.3
1.506	0.75	-2.88E+04	2.88E+04	0.00E+00	5.78E+05	3.33E+05	0.00E+00	2.23E+08	3.12E+07	0.00E+00	9.52E+04	158.4
1.606	0.80	-3.60E+04	2.99E+04	0.00E+00	5.19E+05	3.59E+05	0.00E+00	2.19E+08	3.47E+07	0.00E+00	1.71E+05	161.5
1.707	0.85	-4.24E+04	2.92E+04	0.00E+00	4.64E+05	3.73E+05	0.00E+00	2.14E+08	3.79E+07	0.00E+00	1.49E+05	166.4
1.807	0.90	-4.74E+04	2.70E+04	0.00E+00	4.18E+05	3.78E+05	0.00E+00	2.10E+08	4.05E+07	0.00E+00	6.04E+04	193.7
1.907	0.95	-5.07E+04	2.37E+04	0.00E+00	3.83E+05	3.75E+05	0.00E+00	2.06E+08	4.27E+07	0.00E+00	6.42E+04	303.9
2.008	1.00	-5.23E+04	1.98E+04	0.00E+00	3.58E+05	3.67E+05	0.00E+00	2.02E+08	4.45E+07	0.00E+00	8.83E+04	332.1
2.108	1.05	-5.26E+04	1.58E+04	0.00E+00	3.43E+05	3.59E+05	0.00E+00	1.98E+08	4.59E+07	0.00E+00	5.54E+04	15.8
2.209	1.10	-5.18E+04	1.22E+04	0.00E+00	3.34E+05	3.53E+05	0.00E+00	1.95E+08	4.68E+07	0.00E+00	5.65E+04	91.7
2.309	1.15	-5.05E+04	9.25E+03	0.00E+00	3.29E+05	3.50E+05	0.00E+00	1.92E+08	4.73E+07	0.00E+00	4.89E+04	138.3
2.409	1.20	-4.89E+04	6.95E+03	0.00E+00	3.26E+05	3.51E+05	0.00E+00	1.90E+08	4.75E+07	0.00E+00	4.13E+04	224.9
2.510	1.25	-4.73E+04	5.29E+03	0.00E+00	3.23E+05	3.56E+05	0.00E+00	1.87E+08	4.74E+07	0.00E+00	4.87E+04	273.5
2.610	1.30	-4.58E+04	4.14E+03	0.00E+00	3.18E+05	3.63E+05	0.00E+00	1.85E+08	4.70E+07	0.00E+00	2.43E+04	358.3
2.711	1.35	-4.46E+04	3.38E+03	0.00E+00	3.13E+05	3.72E+05	0.00E+00	1.84E+08	4.65E+07	0.00E+00	4.47E+04	71.1
2.811	1.40	-4.37E+04	2.86E+03	0.00E+00	3.06E+05	3.80E+05	0.00E+00	1.82E+08	4.57E+07	0.00E+00	1.96E+04	126.0
2.911	1.45	-4.29E+04	2.48E+03	0.00E+00	2.99E+05	3.89E+05	0.00E+00	1.81E+08	4.49E+07	0.00E+00	3.70E+04	239.8
3.012	1.50	-4.23E+04	2.17E+03	0.00E+00	2.91E+05	3.97E+05	0.00E+00	1.80E+08	4.40E+07	0.00E+00	1.93E+04	278.9
3.112	1.55	-4.18E+04	1.88E+03	0.00E+00	2.83E+05	4.03E+05	0.00E+00	1.79E+08	4.29E+07	0.00E+00	3.06E+04	54.0
3.213	1.60	-4.13E+04	1.58E+03	0.00E+00	2.75E+05	4.09E+05	0.00E+00	1.79E+08	4.19E+07	0.00E+00	1.53E+04	90.7
3.313	1.65	-4.10E+04	1.27E+03	0.00E+00	2.67E+05	4.13E+05	0.00E+00	1.78E+08	4.08E+07	0.00E+00	2.73E+04	230.1
3.413	1.70	-4.07E+04	9.18E+02	0.00E+00	2.59E+05	4.15E+05	0.00E+00	1.78E+08	3.97E+07	0.00E+00	7.04E+03	279.7
3.514	1.75	-4.04E+04	5.41E+02	0.00E+00	2.52E+05	4.17E+05	0.00E+00	1.77E+08	3.86E+07	0.00E+00	2.46E+04	49.1
3.614	1.80	-4.02E+04	1.38E+02	0.00E+00	2.45E+05	4.18E+05	0.00E+00	1.77E+08	3.74E+07	0.00E+00	6.17E+03	202.0
3.715	1.85	-4.00E+04	-2.89E+02	0.00E+00	2.39E+05	4.17E+05	0.00E+00	1.77E+08	3.63E+07	0.00E+00	1.80E+04	229.3
3.815	1.90	-3.97E+04	-7.32E+02	0.00E+00	2.34E+05	4.16E+05	0.00E+00	1.77E+08	3.52E+07	0.00E+00	1.40E+04	34.5
3.915	1.95	-3.95E+04	-1.19E+03	0.00E+00	2.28E+05	4.14E+05	0.00E+00	1.77E+08	3.41E+07	0.00E+00	5.04E+03	56.6
4.016	2.00	-3.93E+04	-1.65E+03	0.00E+00	2.24E+05	4.12E+05	0.00E+00	1.77E+08	3.31E+07	0.00E+00	1.38E+04	208.6
4.116	2.05	-3.91E+04	-2.11E+03	0.00E+00	2.20E+05	4.08E+05	0.00E+00	1.77E+08	3.20E+07	0.00E+00	8.18E+03	23.5
4.217	2.10	-3.88E+04	-2.57E+03	0.00E+00	2.16E+05	4.05E+05	0.00E+00	1.77E+08	3.10E+07	0.00E+00	2.86E+03	356.0
4.317	2.15	-3.86E+04	-2.99E+03	0.00E+00	2.13E+05	4.00E+05	0.00E+00	1.77E+08	2.99E+07	0.00E+00	8.82E+03	192.6
4.417	2.20	-3.84E+04	-3.25E+03	0.00E+00	2.11E+05	3.90E+05	0.00E+00	1.77E+08	2.88E+07	0.00E+00	7.73E+03	20.4
4.518	2.25	-3.86E+04	-7.22E+03	0.00E+00	1.53E+05	4.78E+05	0.00E+00	1.77E+08	2.76E+07	0.00E+00	2.90E+03	231.6
4.618	2.30	-3.57E+04	8.48E+03	0.00E+00	2.01E+05	1.14E+05	0.00E+00	1.77E+08	2.65E+07	0.00E+00	4.04E+03	153.0
4.719	2.35	-3.73E+04	-2.18E+03	0.00E+00	2.07E+05	3.20E+05	0.00E+00	1.77E+08	2.62E+07	0.00E+00	5.48E+03	352.2
4.819	2.40	-3.73E+04	-4.69E+03	0.00E+00	2.04E+05	3.60E+05	0.00E+00	1.77E+08	2.54E+07	0.00E+00	4.17E+03	192.9
4.919	2.45	-3.73E+04	-5.24E+03	0.00E+00	2.15E+05	3.40E+05	0.00E+00	1.77E+08	2.40E+07	0.00E+00	3.05E+03	61.0
5.020	2.50	-3.41E+04	1.78E+03	0.00E+00	3.38E+05	-3.67E+05	0.00E+00	1.78E+08	2.36E+07	0.00E+00	2.75E+03	275.1

Appendix E

Hydrodynamic from data Ansys AQWA

ADDED MASS-VARIATION WITHWAVE PERIOD/FREQUENCY

PERIOD (SECS)	FREQ (RAD/S)	M 11	M 22	M 33	M 44	M 55	M 66	M 13	M 15	M 24	M 26	M 35	M 46
125.70	0.05	1.13E+03	1.62E+04	2.58E+05	3.77E+06	4.57E+08	5.16E+07	5.94E+02	5.12E+05	-1.02E+05	-1.74E+04	6.38E+05	5.83E+05
62.83	0.10	1.15E+03	1.64E+04	2.63E+05	3.78E+06	4.63E+08	5.19E+07	5.94E+02	5.22E+05	-1.03E+05	-1.72E+04	6.53E+05	5.86E+05
41.89	0.15	1.19E+03	1.66E+04	2.68E+05	3.80E+06	4.76E+08	5.24E+07	5.94E+02	5.42E+05	-1.05E+05	-1.69E+04	6.71E+05	5.91E+05
31.42	0.20	1.24E+03	1.71E+04	2.57E+05	3.82E+06	4.96E+08	5.31E+07	6.03E+02	5.75E+05	-1.09E+05	-1.64E+04	6.48E+05	5.99E+05
25.13	0.25	1.32E+03	1.77E+04	2.36E+05	3.87E+06	5.21E+08	5.41E+07	6.25E+02	6.18E+05	-1.14E+05	-1.57E+04	5.98E+05	6.11E+05
20.94	0.30	1.38E+03	1.85E+04	2.11E+05	3.92E+06	5.43E+08	5.55E+07	6.58E+02	6.53E+05	-1.20E+05	-1.46E+04	5.35E+05	6.28E+05
17.95	0.35	1.40E+03	1.95E+04	1.84E+05	3.98E+06	5.46E+08	5.76E+07	6.91E+02	6.57E+05	-1.27E+05	-1.31E+04	4.66E+05	6.51E+05
15.71	0.40	1.34E+03	2.04E+04	1.58E+05	4.03E+06	5.25E+08	6.05E+07	7.02E+02	6.18E+05	-1.34E+05	-1.10E+04	3.99E+05	6.84E+05
13.96	0.45	1.22E+03	2.10E+04	1.36E+05	4.04E+06	4.84E+08	6.40E+07	6.75E+02	5.44E+05	-1.36E+05	-8.31E+03	3.40E+05	7.24E+05
12.57	0.50	1.10E+03	2.10E+04	1.19E+05	3.99E+06	4.32E+08	6.72E+07	6.17E+02	4.55E+05	-1.33E+05	-5.66E+03	2.95E+05	7.64E+05
11.42	0.55	9.95E+02	2.04E+04	1.07E+05	3.88E+06	3.77E+08	6.87E+07	5.66E+02	3.71E+05	-1.23E+05	-3.92E+03	2.66E+05	7.84E+05
10.47	0.60	9.41E+02	1.94E+04	1.00E+05	3.74E+06	3.30E+08	6.75E+07	5.48E+02	3.13E+05	-1.10E+05	-3.63E+03	2.47E+05	7.69E+05
9.67	0.65	9.08E+02	1.80E+04	9.51E+04	3.61E+06	2.96E+08	6.42E+07	5.54E+02	2.81E+05	-9.52E+04	-4.74E+03	2.32E+05	7.28E+05
8.98	0.70	8.56E+02	1.64E+04	9.13E+04	3.48E+06	2.74E+08	6.02E+07	5.59E+02	2.62E+05	-8.04E+04	-7.11E+03	2.19E+05	6.93E+05
8.38	0.75	7.80E+02	1.48E+04	8.84E+04	3.37E+06	2.59E+08	5.62E+07	5.48E+02	2.41E+05	-6.60E+04	-1.10E+04	2.08E+05	6.69E+05
7.85	0.80	7.04E+02	1.32E+04	8.64E+04	3.28E+06	2.47E+08	5.20E+07	5.32E+02	2.19E+05	-5.31E+04	-1.65E+04	1.96E+05	6.29E+05
7.39	0.85	6.43E+02	1.18E+04	8.53E+04	3.22E+06	2.38E+08	4.79E+07	5.24E+02	2.00E+05	-4.24E+04	-2.26E+04	1.86E+05	5.64E+05
6.98	0.90	5.92E+02	1.05E+04	8.47E+04	3.17E+06	2.31E+08	4.40E+07	5.21E+02	1.85E+05	-3.38E+04	-2.85E+04	1.75E+05	5.00E+05
6.61	0.95	5.45E+02	9.30E+03	8.46E+04	3.15E+06	2.27E+08	4.05E+07	5.18E+02	1.72E+05	-2.71E+04	-3.40E+04	1.65E+05	4.50E+05
6.28	1.00	5.04E+02	8.27E+03	8.49E+04	3.13E+06	2.23E+08	3.73E+07	5.16E+02	1.62E+05	-2.22E+04	-3.88E+04	1.55E+05	3.98E+05
5.98	1.05	4.68E+02	7.39E+03	8.56E+04	3.12E+06	2.22E+08	3.44E+07	5.15E+02	1.53E+05	-1.87E+04	-4.26E+04	1.47E+05	3.52E+05
5.71	1.10	4.38E+02	6.63E+03	8.63E+04	3.12E+06	2.21E+08	3.18E+07	5.16E+02	1.46E+05	-1.65E+04	-4.54E+04	1.40E+05	3.20E+05
5.46	1.15	4.10E+02	5.96E+03	8.71E+04	3.12E+06	2.20E+08	2.95E+07	5.17E+02	1.40E+05	-1.54E+04	-4.74E+04	1.33E+05	2.91E+05
5.24	1.20	3.87E+02	5.40E+03	8.78E+04	3.13E+06	2.20E+08	2.74E+07	5.17E+02	1.35E+05	-1.52E+04	-4.86E+04	1.25E+05	2.70E+05
5.03	1.25	3.65E+02	4.91E+03	8.86E+04	3.14E+06	2.19E+08	2.56E+07	5.14E+02	1.30E+05	-1.57E+04	-4.93E+04	1.18E+05	2.54E+05
4.83	1.30	3.47E+02	4.47E+03	8.94E+04	3.16E+06	2.19E+08	2.39E+07	5.14E+02	1.26E+05	-1.66E+04	-4.96E+04	1.11E+05	2.41E+05
4.65	1.35	3.31E+02	4.09E+03	9.04E+04	3.17E+06	2.20E+08	2.24E+07	5.11E+02	1.23E+05	-1.70E+04	-4.95E+04	1.05E+05	2.30E+05
4.49	1.40	3.17E+02	3.78E+03	9.14E+04	3.17E+06	2.21E+08	2.10E+07	5.10E+02	1.20E+05	-1.72E+04	-4.92E+04	1.00E+05	2.20E+05
4.33	1.45	3.06E+02	3.53E+03	9.25E+04	3.18E+06	2.22E+08	1.99E+07	5.11E+02	1.19E+05	-1.78E+04	-4.86E+04	9.59E+04	2.11E+05
4.19	1.50	2.96E+02	3.33E+03	9.37E+04	3.20E+06	2.24E+08	1.89E+07	5.09E+02	1.19E+05	-1.90E+04	-4.79E+04	9.25E+04	2.04E+05
4.05	1.55	2.88E+02	3.17E+03	9.49E+04	3.21E+06	2.26E+08	1.81E+07	5.09E+02	1.19E+05	-2.03E+04	-4.71E+04	9.02E+04	1.97E+05
3.93	1.60	2.81E+02	3.04E+03	9.61E+04	3.22E+06	2.28E+08	1.74E+07	5.07E+02	1.19E+05	-2.19E+04	-4.63E+04	8.78E+04	1.91E+05
3.81	1.65	2.75E+02	2.93E+03	9.73E+04	3.23E+06	2.30E+08	1.68E+07	5.07E+02	1.20E+05	-2.35E+04	-4.56E+04	8.61E+04	1.87E+05
3.70	1.70	2.70E+02	2.86E+03	9.84E+04	3.24E+06	2.32E+08	1.63E+07	5.04E+02	1.21E+05	-2.51E+04	-4.48E+04	8.44E+04	1.83E+05
3.59	1.75	2.67E+02	2.82E+03	9.95E+04	3.24E+06	2.34E+08	1.59E+07	5.01E+02	1.23E+05	-2.67E+04	-4.40E+04	8.24E+04	1.79E+05
3.49	1.80	2.64E+02	2.79E+03	1.00E+05	3.26E+06	2.36E+08	1.56E+07	4.97E+02	1.24E+05	-2.83E+04	-4.33E+04	8.06E+04	1.75E+05
3.40	1.85	2.62E+02	2.77E+03	1.01E+05	3.27E+06	2.38E+08	1.54E+07	4.93E+02	1.25E+05	-2.99E+04	-4.24E+04	7.88E+04	1.71E+05
3.31	1.90	2.62E+02	2.77E+03	1.02E+05	3.27E+06	2.40E+08	1.52E+07	4.88E+02	1.27E+05	-3.14E+04	-4.16E+04	7.72E+04	1.68E+05
3.22	1.95	2.61E+02	2.78E+03	1.03E+05	3.28E+06	2.41E+08	1.50E+07	4.81E+02	1.29E+05	-3.29E+04	-4.08E+04	7.54E+04	1.66E+05
3.14	2.00	2.62E+02	2.80E+03	1.03E+05	3.29E+06	2.42E+08	1.49E+07	4.76E+02	1.30E+05	-3.42E+04	-4.01E+04	7.46E+04	1.64E+05
3.06	2.05	2.62E+02	2.84E+03	1.03E+05	3.29E+06	2.43E+08	1.49E+07	4.69E+02	1.32E+05	-3.55E+04	-3.94E+04	7.24E+04	1.61E+05
2.99	2.10	2.63E+02	2.87E+03	1.03E+05	3.29E+06	2.44E+08	1.49E+07	4.63E+02	1.34E+05	-3.67E+04	-3.87E+04	7.16E+04	1.60E+05
2.92	2.15	2.64E+02	2.92E+03	1.04E+05	3.29E+06	2.44E+08	1.49E+07	4.57E+02	1.35E+05	-3.78E+04	-3.82E+04	7.10E+04	1.58E+05
2.86	2.20	2.66E+02	2.96E+03	1.04E+05	3.30E+06	2.45E+08	1.49E+07	4.52E+02	1.37E+05	-3.88E+04	-3.76E+04	7.08E+04	1.57E+05
2.79	2.25	2.68E+02	3.01E+03	1.04E+05	3.30E+06	2.45E+08	1.49E+07	4.48E+02	1.38E+05	-3.99E+04	-3.72E+04	7.08E+04	1.56E+05
2.73	2.30	2.70E+02	3.06E+03	1.04E+05	3.30E+06	2.46E+08	1.50E+07	4.45E+02	1.40E+05	-4.08E+04	-3.67E+04	7.15E+04	1.56E+05
2.67	2.35	2.72E+02	3.11E+03	1.04E+05	3.30E+06	2.47E+08	1.51E+07	4.43E+02	1.41E+05	-4.16E+04	-3.63E+04	7.27E+04	1.56E+05
2.62	2.40	2.74E+02	3.16E+03	1.05E+05	3.30E+06	2.48E+08	1.52E+07	4.42E+02	1.43E+05	-4.23E+04	-3.60E+04	7.44E+04	1.56E+05
2.56	2.45	2.76E+02	3.21E+03	1.05E+05	3.30E+06	2.49E+08	1.53E+07	4.43E+02	1.45E+05	-4.30E+04	-3.56E+04	7.68E+04	1.56E+05
2.51	2.50	2.79E+02	3.27E+03	1.05E+05	3.31E+06	2.50E+08	1.54E+07	4.45E+02	1.46E+05	-4.36E+04	-3.53E+04	7.97E+04	1.56E+05

DAMPING-VARIATION WITH WAVE PERIOD/FREQUENCY

PERIOD (SECS)	FREQ (RAD/S)	C 11	C 22	C 33	C 44	C 55	C 66	C 13	C 15	C 24	C 26	C 35	C 46
125.70	0.05	3.65E-03	6.75E-03	8.68E+02	7.25E-01	7.25E+03	5.39E-03	-1.50E-02	2.22E+00	-6.93E-02	-1.50E-03	2.26E+03	1.57E-02
62.83	0.10	6.44E-02	1.22E-01	2.78E+03	1.29E+01	4.37E+04	4.37E-01	-1.89E-01	3.92E+01	-1.24E+00	-2.54E-02	7.26E+03	2.73E-01
41.89	0.15	7.34E-01	1.44E+00	8.02E+03	1.50E+02	3.34E+05	1.85E+01	-1.14E+00	4.46E+02	-1.45E+01	-2.68E-01	2.11E+04	3.06E+00
31.42	0.20	5.05E+00	1.06E+01	1.68E+04	1.08E+03	2.00E+06	4.12E+02	-3.51E+00	3.05E+03	-1.06E+02	-1.58E+00	4.48E+04	2.25E+01
25.13	0.25	2.07E+01	4.90E+01	2.69E+04	4.84E+03	7.78E+06	4.59E+03	-6.01E+00	1.24E+04	-4.82E+02	-4.50E+00	7.26E+04	1.16E+02
20.94	0.30	5.85E+01	1.66E+02	3.67E+04	1.59E+04	2.13E+07	3.18E+04	-4.77E+00	3.48E+04	-1.61E+03	-8.52E-01	1.01E+05	5.07E+02
17.95	0.35	1.23E+02	4.48E+02	4.53E+04	4.13E+04	4.41E+07	1.56E+05	5.97E+00	7.27E+04	-4.26E+03	5.50E+01	1.27E+05	1.96E+03
15.71	0.40	2.02E+02	1.00E+03	5.16E+04	8.90E+04	7.29E+07	5.85E+05	2.96E+01	1.20E+05	-9.34E+03	3.07E+02	1.48E+05	6.59E+03
13.96	0.45	2.77E+02	1.91E+03	5.50E+04	1.62E+05	1.02E+08	1.73E+06	5.97E+01	1.66E+05	-1.73E+04	1.06E+03	1.62E+05	1.90E+04
12.57	0.50	3.31E+02	3.13E+03	5.57E+04	2.53E+05	1.27E+08	4.14E+06	8.02E+01	1.99E+05	-2.77E+04	2.68E+03	1.69E+05	4.60E+04
11.42	0.55	3.61E+02	4.53E+03	5.46E+04	3.44E+05	1.43E+08	8.02E+06	8.06E+01	2.16E+05	-3.88E+04	5.37E+03	1.73E+05	9.13E+04
10.47	0.60	3.86E+02	5.96E+03	5.31E+04	4.18E+05	1.49E+08	1.28E+07	6.94E+01	2.18E+05	-4.89E+04	8.94E+03	1.77E+05	1.47E+05
9.67	0.65	4.28E+02	7.33E+03	5.15E+04	4.67E+05	1.48E+08	1.73E+07	6.47E+01	2.16E+05	-5.73E+04	1.31E+04	1.82E+05	1.96E+05
8.98	0.70	4.84E+02	8.60E+03	4.97E+04	4.95E+05	1.44E+08	2.13E+07	7.37E+01	2.20E+05	-6.37E+04	1.77E+04	1.88E+05	2.35E+05
8.38	0.75	5.34E+02	9.68E+03	4.77E+04	5.06E+05	1.40E+08	2.49E+07	8.53E+01	2.26E+05	-6.78E+04	2.25E+04	1.94E+05	2.81E+05
7.85	0.80	5.65E+02	1.05E+04	4.53E+04	4.97E+05	1.37E+08	2.81E+07	8.83E+01	2.30E+05	-6.95E+04	2.69E+04	2.01E+05	3.40E+05
7.39	0.85	5.85E+02	1.12E+04	4.28E+04	4.72E+05	1.32E+08	3.08E+07	8.62E+01	2.31E+05	-6.92E+04	2.99E+04	2.07E+05	3.91E+05
6.98	0.90	6.03E+02	1.17E+04	4.02E+04	4.38E+05	1.27E+08	3.30E+07	8.61E+01	2.30E+05	-6.74E+04	3.18E+04	2.12E+05	4.20E+05
6.61	0.95	6.17E+02	1.20E+04	3.76E+04	4.04E+05	1.21E+08	3.48E+07	8.70E+01	2.29E+05	-6.43E+04	3.25E+04	2.17E+05	4.42E+05
6.28	1.00	6.25E+02	1.23E+04	3.50E+04	3.67E+05	1.15E+08	3.63E+07	8.69E+01	2.26E+05	-6.03E+04	3.20E+04	2.21E+05	4.60E+05
5.98	1.05	6.29E+02	1.24E+04	3.26E+04	3.30E+05	1.10E+08	3.74E+07	8.70E+01	2.22E+05	-5.59E+04	3.04E+04	2.24E+05	4.63E+05
5.71	1.10	6.32E+02	1.25E+04	3.04E+04	2.95E+05	1.05E+08	3.82E+07	8.84E+01	2.19E+05	-5.10E+04	2.82E+04	2.27E+05	4.61E+05
5.46	1.15	6.32E+02	1.24E+04	2.82E+04	2.62E+05	9.99E+07	3.88E+07	9.23E+01	2.15E+05	-4.60E+04	2.55E+04	2.29E+05	4.58E+05
5.24	1.20	6.30E+02	1.23E+04	2.61E+04	2.30E+05	9.50E+07	3.92E+07	9.68E+01	2.10E+05	-4.09E+04	2.26E+04	2.32E+05	4.50E+05
5.03	1.25	6.26E+02	1.22E+04	2.40E+04	2.01E+05	9.00E+07	3.94E+07	1.04E+02	2.05E+05	-3.62E+04	1.97E+04	2.33E+05	4.43E+05
4.83	1.30	6.20E+02	1.21E+04	2.19E+04	1.78E+05	8.47E+07	3.94E+07	1.10E+02	1.99E+05	-3.21E+04	1.69E+04	2.33E+05	4.36E+05
4.65	1.35	6.12E+02	1.18E+04	1.99E+04	1.67E+05	7.95E+07	3.93E+07	1.14E+02	1.92E+05	-2.86E+04	1.41E+04	2.33E+05	4.31E+05
4.49	1.40	6.03E+02	1.16E+04	1.80E+04	1.55E+05	7.45E+07	3.89E+07	1.21E+02	1.85E+05	-2.45E+04	1.14E+04	2.31E+05	4.25E+05
4.33	1.45	5.94E+02	1.13E+04	1.63E+04	1.43E+05	6.97E+07	3.84E+07	1.28E+02	1.77E+05	-2.00E+04	8.88E+03	2.29E+05	4.19E+05
4.19	1.50	5.83E+02	1.10E+04	1.47E+04	1.32E+05	6.52E+07	3.78E+07	1.32E+02	1.70E+05	-1.59E+04	6.66E+03	2.26E+05	4.13E+05
4.05	1.55	5.71E+02	1.07E+04	1.32E+04	1.22E+05	6.10E+07	3.71E+07	1.40E+02	1.64E+05	-1.19E+04	4.70E+03	2.23E+05	4.07E+05
3.93	1.60	5.59E+02	1.04E+04	1.19E+04	1.16E+05	5.73E+07	3.64E+07	1.46E+02	1.57E+05	-8.58E+03	2.99E+03	2.21E+05	4.01E+05
3.81	1.65	5.46E+02	1.00E+04	1.09E+04	1.10E+05	5.39E+07	3.55E+07	1.56E+02	1.51E+05	-4.90E+03	1.33E+03	2.19E+05	3.96E+05
3.70	1.70	5.32E+02	9.70E+03	1.02E+04	1.04E+05	5.12E+07	3.47E+07	1.64E+02	1.45E+05	-2.63E+03	-1.58E+02	2.17E+05	3.91E+05
3.59	1.75	5.18E+02	9.37E+03	9.73E+03	9.67E+04	4.90E+07	3.38E+07	1.72E+02	1.40E+05	-5.11E+02	-1.47E+03	2.14E+05	3.86E+05
3.49	1.80	5.03E+02	9.04E+03	9.45E+03	9.08E+04	4.71E+07	3.28E+07	1.81E+02	1.34E+05	2.01E+03	-2.76E+03	2.11E+05	3.83E+05
3.40	1.85	4.89E+02	8.72E+03	9.44E+03	8.91E+04	4.58E+07	3.19E+07	1.88E+02	1.29E+05	3.14E+03	-3.77E+03	2.08E+05	3.78E+05
3.31	1.90	4.75E+02	8.40E+03	9.55E+03	9.18E+04	4.47E+07	3.09E+07	1.92E+02	1.25E+05	3.98E+03	-4.52E+03	2.03E+05	3.73E+05
3.22	1.95	4.61E+02	8.09E+03	9.68E+03	9.66E+04	4.38E+07	3.00E+07	1.95E+02	1.21E+05	4.58E+03	-4.98E+03	1.98E+05	3.68E+05
3.14	2.00	4.47E+02	7.79E+03	9.76E+03	1.02E+05	4.29E+07	2.90E+07	1.96E+02	1.16E+05	5.05E+03	-5.39E+03	1.93E+05	3.63E+05
3.06	2.05	4.34E+02	7.51E+03	9.75E+03	1.06E+05	4.18E+07	2.81E+07	1.95E+02	1.12E+05	5.37E+03	-5.63E+03	1.87E+05	3.56E+05
2.99	2.10	4.22E+02	7.22E+03	9.52E+03	1.08E+05	4.04E+07	2.73E+07	1.92E+02	1.08E+05	5.69E+03	-5.83E+03	1.80E+05	3.52E+05
2.92	2.15	4.09E+02	6.96E+03	9.07E+03	1.08E+05	3.86E+07	2.64E+07	1.87E+02	1.04E+05	5.97E+03	-5.94E+03	1.73E+05	3.46E+05
2.86	2.20	3.97E+02	6.70E+03	8.41E+03	1.06E+05	3.65E+07	2.56E+07	1.81E+02	1.00E+05	6.18E+03	-6.14E+03	1.65E+05	3.40E+05
2.79	2.25	3.85E+02	6.46E+03	7.57E+03	1.03E+05	3.40E+07	2.48E+07	1.72E+02	9.65E+04	6.25E+03	-6.22E+03	1.57E+05	3.34E+05
2.73	2.30	3.74E+02	6.22E+03	6.56E+03	9.80E+04	3.13E+07	2.40E+07	1.62E+02	9.26E+04	6.20E+03	-6.37E+03	1.48E+05	3.28E+05
2.67	2.35	3.62E+02	5.98E+03	5.45E+03	9.20E+04	2.84E+07	2.32E+07	1.52E+02	8.86E+04	6.08E+03	-6.45E+03	1.39E+05	3.23E+05
2.62	2.40	3.51E+02	5.76E+03	4.29E+03	8.47E+04	2.54E+07	2.25E+07	1.40E+02	8.48E+04	5.91E+03	-6.55E+03	1.31E+05	3.16E+05
2.56	2.45	3.40E+02	5.55E+03	3.09E+03	7.66E+04	2.24E+07	2.18E+07	1.29E+02	8.10E+04	5.72E+03	-6.67E+03	1.22E+05	3.09E+05
2.51	2.50	3.30E+02	5.35E+03	1.85E+03	6.82E+04	1.93E+07	2.12E+07	1.17E+02	7.73E+04	5.53E+03	-6.79E+03	1.13E+05	3.03E+05

FROUDE KRYLOV + DIFFRACTION FORCES-VARIATION WITH WAVE PERIOD/FREQUENCY

DIRECTION	-150												
PERIOD	FREQ	X		Y		Z		RX		RY		RZ	
(SECS)	(RAD/S)	(DEGREES	PHASE	AMP	PHASE	AMP	PHASE	AMP	PHASE	AMP	PHASE	AMP	PHASE
125.66	0.05	1.88E+02	90.44	1.48E+02	90.01	7.57E+04	0.04	1.55E+03	-89.68	2.29E+05	31.23	2.12E+02	-12.17
62.83	0.10	4.29E+02	90.77	3.40E+02	90.01	7.33E+04	-0.06	3.54E+03	-89.63	3.29E+05	54.72	1.10E+03	-5.07
41.89	0.15	8.04E+02	90.89	6.47E+02	90.03	6.91E+04	-0.68	6.68E+03	-89.4	5.28E+05	70.28	4.03E+03	-2.35
31.42	0.20	1.34E+03	90.84	1.11E+03	90.08	6.33E+04	-2.43	1.13E+04	-88.96	8.34E+05	78.92	1.21E+04	-1.01
25.13	0.25	1.94E+03	90.5	1.67E+03	90.2	5.66E+04	-5.6	1.69E+04	-88.28	1.18E+06	83.14	2.86E+04	-0.26
20.94	0.30	2.48E+03	89.3	2.25E+03	90.46	4.92E+04	-10.32	2.27E+04	-87.28	1.48E+06	84.67	5.66E+04	0.27
17.95	0.35	2.84E+03	86.27	2.76E+03	90.89	4.16E+04	-16.42	2.78E+04	-85.88	1.69E+06	83.63	9.75E+04	0.74
15.71	0.40	2.97E+03	80.49	3.06E+03	91.47	3.35E+04	-23.77	3.11E+04	-84.03	1.77E+06	79.7	1.49E+05	1.29
13.96	0.45	2.86E+03	71.49	2.98E+03	92.04	2.50E+04	-32.85	3.13E+04	-81.73	1.74E+06	72.87	2.04E+05	1.98
12.57	0.50	2.52E+03	59.04	2.46E+03	92.26	1.64E+04	-45.84	2.75E+04	-78.97	1.61E+06	63.65	2.47E+05	2.75
11.42	0.55	1.96E+03	41.24	1.50E+03	91.34	9.04E+03	-68.83	1.98E+04	-75.34	1.38E+06	52.42	2.58E+05	3.18
10.47	0.60	1.32E+03	9.87	3.14E+02	79.48	4.64E+03	-121.05	9.16E+03	-67.86	1.05E+06	38.23	2.23E+05	2.36
9.67	0.65	1.07E+03	-46.27	7.77E+02	-82.23	4.98E+03	172.59	2.89E+03	74.85	6.64E+05	16.32	1.42E+05	-2.3
8.98	0.70	1.38E+03	-95.04	1.38E+03	-89.92	6.04E+03	137.84	1.20E+04	100.77	3.66E+05	-28.56	4.30E+04	-35.1
8.38	0.75	1.67E+03	-126.08	1.36E+03	-101.75	5.52E+03	110.74	1.65E+04	105.5	3.43E+05	-95.19	6.64E+04	-149.4
7.85	0.80	1.61E+03	-154.11	9.50E+02	-128.96	3.88E+03	74.83	1.48E+04	109.74	4.07E+05	-135.46	1.00E+05	-170.65
7.39	0.85	1.26E+03	169.1	6.91E+02	179.65	2.83E+03	16.09	7.47E+03	119.35	3.60E+05	-168.02	8.26E+04	160.45
6.98	0.90	1.01E+03	114.82	5.59E+02	126.58	2.98E+03	-40.41	3.24E+03	-107.48	2.54E+05	145.48	7.40E+04	104.92
6.61	0.95	1.02E+03	58.79	5.38E+02	47.37	2.82E+03	-85.59	1.03E+04	-80.28	2.23E+05	82.95	8.08E+04	67.47
6.28	1.00	1.00E+03	7.93	9.08E+02	1.56	2.32E+03	-137.5	1.12E+04	-75.26	2.19E+05	30.73	4.30E+04	28.06
5.98	1.05	9.40E+02	-45.46	8.30E+02	-19.01	1.97E+03	164.38	5.30E+03	-72.37	1.87E+05	-24.52	5.54E+04	-83.51
5.71	1.10	8.22E+02	-99.68	2.27E+02	-81.36	1.66E+03	100.87	2.75E+03	104.14	1.70E+05	-84.21	8.58E+04	-108.44
5.46	1.15	6.57E+02	-166.99	6.40E+02	173.35	1.64E+03	35.16	6.54E+03	101.05	1.38E+05	-144.02	4.10E+04	-135.12
5.24	1.20	7.07E+02	122.14	6.13E+02	151.34	1.43E+03	-20.38	4.29E+03	79.04	1.24E+05	140.72	4.58E+04	91.84
5.03	1.25	6.52E+02	64.23	2.51E+02	56.3	1.01E+03	-97.36	2.77E+03	-7.33	1.26E+05	79.95	5.91E+04	65.91
4.83	1.30	5.09E+02	-12.47	4.75E+02	-9.13	1.15E+03	-174.01	2.54E+03	-65.65	8.78E+04	9.92	2.42E+04	-23.52
4.65	1.35	5.41E+02	-88.71	2.46E+02	-81.15	9.06E+02	123.61	2.96E+03	-164.42	9.41E+04	-75.43	4.92E+04	-92.42
4.49	1.40	4.67E+02	-162.71	4.17E+02	-165.63	7.91E+02	32.54	3.47E+03	163.45	7.87E+04	-141.57	2.15E+04	-162.46
4.33	1.45	4.40E+02	116.79	2.00E+02	129.2	7.60E+02	-42.41	1.02E+03	38.56	6.91E+04	129.77	4.37E+04	103.64
4.19	1.50	3.87E+02	31.23	3.72E+02	22.56	6.37E+02	-126.42	3.33E+03	-14.41	6.46E+04	49.4	2.06E+04	43.95
4.05	1.55	3.86E+02	-53.55	2.05E+02	-37.25	5.85E+02	146.37	1.15E+03	-74.35	5.58E+04	-38.8	3.74E+04	-68.43
3.93	1.60	3.22E+02	-142.4	3.12E+02	-152.19	5.23E+02	54.34	2.33E+03	172.08	5.07E+04	-125.73	1.98E+04	-134.96
3.81	1.65	3.34E+02	122.38	1.89E+02	132.18	4.57E+02	-34.21	1.30E+03	96.11	4.68E+04	136.88	3.21E+04	116.2
3.70	1.70	2.90E+02	29.49	2.79E+02	28.61	4.33E+02	-137.2	1.76E+03	3.87	4.05E+04	46.8	1.77E+04	26.39
3.59	1.75	2.92E+02	-69.59	1.77E+02	-72.35	3.80E+02	130.57	1.25E+03	-111.37	3.92E+04	-57.71	2.84E+04	-65.84
3.49	1.80	2.76E+02	-170.34	2.45E+02	-158.37	3.69E+02	22.21	1.35E+03	-174.34	3.41E+04	-154.48	1.87E+04	176.69
3.40	1.85	2.61E+02	90.49	1.99E+02	79.99	3.37E+02	-77.89	1.30E+03	45.3	3.34E+04	98.88	2.17E+04	102.25
3.31	1.90	2.60E+02	-16.85	1.78E+02	-0.07	3.16E+02	174.57	8.28E+02	-26.47	3.08E+04	-7.38	2.21E+04	-25.82
3.22	1.95	2.27E+02	-121.11	2.10E+02	-120.37	3.16E+02	66.43	1.14E+03	-151.37	2.78E+04	-114.57	1.40E+04	-120.09
3.14	2.00	2.26E+02	129.9	1.43E+02	126.74	2.70E+02	-43.56	8.92E+02	86.51	2.77E+04	134.91	1.93E+04	134.46
3.06	2.05	2.02E+02	15.88	1.49E+02	30.58	2.69E+02	-154.02	6.70E+02	-12.36	2.39E+04	19.48	1.63E+04	3.66
2.99	2.10	1.78E+02	-97.69	1.58E+02	-96.82	2.32E+02	87.72	1.02E+03	-130.16	2.21E+04	-93.76	1.12E+04	-98.81
2.92	2.15	1.66E+02	145.88	1.11E+02	138.16	2.13E+02	-30.48	7.89E+02	91.6	1.99E+04	146.95	1.41E+04	149.13
2.86	2.20	1.50E+02	21.68	9.81E+01	35.07	1.80E+02	-151.87	6.27E+02	-11.16	1.84E+04	24.47	1.33E+04	11.13
2.79	2.25	1.26E+02	-102.57	1.13E+02	-93.18	1.67E+02	86.19	7.30E+02	-132.48	1.56E+04	-103.31	8.56E+03	-116.39
2.73	2.30	1.10E+02	132.5	9.34E+01	125.41	1.48E+02	-45.73	7.45E+02	90.94	1.33E+04	131.47	7.76E+03	137.16
2.67	2.35	9.90E+01	1.71	5.93E+01	-3.99	1.22E+02	-178.87	5.78E+02	-47.66	1.23E+04	1.26	9.18E+03	1.38
2.62	2.40	8.48E+01	-136.64	5.32E+01	-121.81	1.03E+02	49.86	4.29E+02	-168.29	1.11E+04	-136.82	8.08E+03	-148.05
2.56	2.45	6.86E+01	82.89	5.54E+01	99.37	9.03E+01	-87.98	4.88E+02	64.06	9.23E+03	82.03	5.73E+03	65.15
2.51	2.50	5.74E+01	-60.38	5.29E+01	-53.23	7.99E+01	127.04	5.20E+02	-84.42	7.73E+03	-60.82	3.79E+03	-69.96

Bibliography

[1] Otc 2012: Dockwise vanguard wins spotlight on new technology award. *www.offshoreenergytoday.com*, may 2012.

[2] Leo H. Holthuijsen. Waves in oceanic and coastal waters. 2007.

[3] E.A. Hellinga, T. Terpstra, and H.C. Leerdam. Offshore dry-docking of fpsos; a response to industry needs. *Dockwise Shipping B.V.*, oktober 2013.

[4] Giorgio Biscardini, David Branson, Adrian Del Maestro, and Reid Morrison. 2017 oil and gas trends adjusting business models to a period of recovery. *https://www.strategyand.pwc.com/trend/2017-oil-and-gas-trends*, 2017.

[5] O.A.J. Peters and R.H.M. Huijsmans. Assessing hydrodynamic behavior during offshore loading and discharge in the heavy marine transport. *Delft University of Technology*, June 2011.

[6] J.W. van Beelen. Development of relative horizontal motion reduction systems. *TU Delft & Dockwise*, September 2016.

[7] P.C. Lee. Investigation of a method for controlling the relative horizontal motions between an htv and its cargo. *TU Delft & Dockwise*, Augustus 2012.

[8] J.M.J. Journe and W.W. Massie. Offshore hydromechanics. *Delft University of Technology*, Januari 2001.

[9] E. Kurt Albaugh, Bob Mahlstedt, David Davis, Chris Barton, and Heather Hambling. 2016 worldwide survey of floating production, storage and offloading (fpso) units. *Offshore magazine*, august 2016.

[10] J.M.J. Journe. Theoretical manual of seaway. *Delft University of Technology*, February 2001.

[11] Design of ocean systems, lecture 14 mooring dynamics(3). *MIT*, page 14, April 2011.

[12] A.V. Metrikine. Dynamics,slender structures and introduction to continuum mechanics. *Delft University of Technology*.

[13] J.M.J. Spijkers, A.W.C.M. Vrouwenvelder, and E.C. Klaver. Structural dynamics ct4140 - part 1- structural vibrations. *Delft University of Technology*.

[14] A.V. Metrikine and A.W.C.M. Vrouwenvelder. Dynamics of structures - ct4140 - part 2 - wave dynamics. *Delft University of Technology*.

[15] Walther H. Michel. Sea spectra revisited. *Marine Technology*, 36(04):211–227, winter 1999.